

LIFETIMES AND FATES OF TOXIC CHEMICALS
IN CALIFORNIA'S ATMOSPHERE

Final Report
Contract Number A5-104-32
California Air Resources Board
August 1987

Co-Principal Investigators

Arthur M. Winer
Roger Atkinson

Research Staff

Janet Arey
Sara M. Aschmann
Mark A. Goodman
Ernesto C. Tuazon

Statewide Air Pollution Research Center
University of California, Riverside
Riverside, CA 92521

ABSTRACT

The atmospheric chemistry of sixteen organic compounds, all directly relevant to the California Air Resources Board's responsibilities for assessing and regulating toxic air contaminants, has been experimentally investigated using the Statewide Air Pollution Research Center's environmental chamber facilities. Specifically, we determined the kinetics and/or the products of the gas-phase reactions of hydroxyl (OH) radicals, ozone (O_3), and nitrate (NO_3) radicals with ethylene oxide, vinyl chloride, 1,1-dichloroethene, cis- and trans-1,2-dichloroethene, trichloroethene, tetrachloroethene, acrolein, allyl chloride, benzyl chloride, o-, m- and p-cresol, naphthalene, 1,4-benzodioxan and 2,3-dihydrobenzofuran.

These kinetic data were used to calculate corresponding atmospheric lifetimes for each compound, for the three possible reaction pathways. Except for the three cresol isomers and 2,3-dihydrobenzofuran, which also react rapidly with NO_3 radicals, the dominant reaction pathway for the compounds studied is by reaction with the OH radical. None of the compounds investigated react sufficiently fast with O_3 under atmospheric conditions for this process to represent a significant atmospheric removal pathway. Based on their atmospheric lifetimes of ~5 min to 10 hrs, the cresols, 1,4-benzodioxan and 2,3-dihydrobenzofuran are expected to have a local range of influence. Vinyl chloride, 1,1-dichloroethene, acrolein, allyl chloride and naphthalene, with lifetimes between ~1 and ~5 days, will be regionally distributed while benzyl chloride cis- and trans-dichloroethene, trichloroethene and ethylene oxide, with lifetimes from ~1 week to ~1 yr, can be globally distributed, as well as having more local effects.

Where feasible, product studies were conducted, principally using in situ Fourier transform infrared spectroscopy and gas chromatography, to determine the atmospheric reaction products produced from the parent compounds investigated. These product studies provided valuable mechanistic data, especially for the reactions of the chloroethenes, allyl chloride and acrolein with the OH radical.

The OH radical rate constant data obtained in this program were combined with available literature data in order to further develop appropriate structure-reactivity relationships. Such relationships permit cost-effective estimation of the atmospheric lifetimes for additional organic compounds whose low volatility or chemical complexity make direct experimental investigation difficult or impossible.

TABLE OF CONTENTS

	<u>Page</u>
Abstract	ii
Acknowledgments	v
List of Figures	vii
List of Tables	xii
Glossary of Terms, Abbreviations and Symbols	xv
I. PROJECT SUMMARY	I-1
A. Introduction and Statement of the Problem	I-1
B. Objectives	I-2
C. Methods of Approach	I-2
D. Summary of Results and Conclusions	I-3
II. INTRODUCTION	II-1
III. METHODS OF PROCEDURE	III-1
1. Determination of OH Radical Reaction Rate Constants	III-1
2. Determination of Rate Constants for Reaction of O ₃ with Organics	III-5
3. Determination of NO ₃ Radical Reaction Rate Constants for Organics	III-6
4. Determination of the N ₂ O ₅ Reaction Rate Constant for Naphthalene	III-7
5. Investigation of Products of OH Radical Reactions with Organics	III-8
IV. EXPERIMENTAL RESULTS AND DISCUSSION	IV-1
A. Ethylene Oxide	IV-1
B. Vinyl Chloride, 1,1-Dichloroethene, <u>cis</u> - and <u>trans</u> -1,2-Dichloroethene, Trichloroethene and Tetrachloroethene	IV-2
1. Kinetics of NO ₃ Radical Reactions	IV-3
2. Kinetics of Cl ³ Atom Reactions	IV-5
3. Kinetics of the OH Radical Reactions with the Dichloroethenes	IV-15
4. Product Studies of the OH Radical Reactions	IV-23
C. Allyl Chloride	IV-38
1. Kinetics of the Ozone Reaction	IV-39
2. Kinetics of the NO ₃ Radical Reaction	IV-41
3. Determination of the Rate Constant for OH Radical Reaction	IV-41
4. Product Study of the OH Radical Reaction	IV-44

TABLE OF CONTENTS

	<u>Page</u>
D. Acrolein	IV-51
1. Kinetics of the NO ₃ Radical Reaction	IV-51
2. Products of the OH Radical Reaction	IV-52
E. 1,4-Benzodioxan and 2,3-Dihydrobenzofuran	IV-59
1. Kinetics of the Reactions with O ₃	IV-59
2. Kinetics of the Reactions with NO ₃ Radicals	IV-60
3. Kinetics of OH Radical Reactions with 1,4-Benzodioxan and 2,3-Dihydrobenzofuran	IV-61
4. Products of the OH Radical Reactions with 1,4-Benzodioxan and 2,3-Dihydrobenzofuran	IV-68
F. Naphthalene	IV-76
G. Benzyl Chloride	IV-80
1. Kinetics of the O ₃ Reaction	IV-80
2. Kinetics of the NO ₃ Radical Reaction	IV-81
3. Kinetics of the OH Radical Reaction	IV-81
4. Products of the OH Radical Reaction	IV-83
H. ortho-Cresol and the meta and para Isomers	IV-85
1. Products of the NO ₃ Radical Reaction	IV-87
I. Other Compounds Studied	IV-90
1. Kinetics of the Reaction of O ₃ with 2,3-Benzofuran	IV-91
2. Kinetics of the Reactions of NO ₃ Radicals with Ethylbenzene, Tetralin, Acetylene, Propyne and Crotonaldehyde	IV-92
3. Kinetics of the Reactions of OH Radicals with <u>cis-</u> and <u>trans-</u> 1,3-Dichloropropene and 3-Chloro-2-chloromethyl-1-propene	IV-92
V. ENVIRONMENTAL IMPLICATIONS	V-1
VI. ESTIMATION OF GAS-PHASE HYDROXYL RADICAL RATE CONSTANTS FOR ORGANIC COMPOUNDS	VI-1
A. H-Atom Abstraction from C-H and O-H Bonds	VI-2
B. OH Radical Addition to >C=C< and -C≡C- Bonds	VI-7
C. OH Radical Addition to Aromatic Rings	VI-9
D. OH Radical Reaction with -NH ₂ , >NH, >N-, -SH and -S- Containing Compounds	VI-14
E. Phosphorus-Containing Organics	VI-18
F. Conclusions	VI-19
VII. REFERENCES	VII-1
VIII. PUBLISHED SCIENTIFIC PAPERS RESULTING WHOLLY OR IN PART FROM THIS PROGRAM	VIII-1

ACKNOWLEDGMENTS

Stimulating discussions and valuable exchanges of technical information, for which we express our appreciation, took place at various times during this program with members of the California Air Resources Board research staff, including John Holmes, Jack Suder, William Loscutoff, Tom Parker, Ralph Propper, Douglas Lawson and Eric Fujita. We gratefully acknowledge William Long for assistance in carrying out this research, and Christy LaClaire for typing this report.

This report was submitted in fulfillment of Contract No. A5-104-32 by the Statewide Air Pollution Research Center, University of California, Riverside, under the partial sponsorship of the California Air Resources Board. Work was completed as of July 31, 1987.

The statements and conclusions in this report are those of the contractor and not necessarily those of the California Air Resources Board. The mention of commercial products, their source or their use in connection with material reported herein is not to be construed as either an actual or implied endorsement of such products.

LIST OF FIGURES

<u>Figure Number</u>	<u>Title</u>	<u>Page</u>
III-1	SAPRC 5800-liter evacuable Teflon-coated environmental chamber	III-2
III-2	SAPRC 6400-liter all-Teflon chamber	III-3
IV-1	Plots of equation (IX) for the reaction of NO ₃ radicals with vinyl chloride and <u>trans</u> -1,2-dichloroethene, with ethene as the reference organic	IV-6
IV-2	Plots of equation (IX) for reactions of NO ₃ radicals with trichloroethene and <u>cis</u> -1,2-dichloroethene, with ethene as the reference organic	IV-7
IV-3	Plots of equation (X) for the reaction of Cl atoms with vinyl chloride, <u>trans</u> -1,2-dichloroethene, trichloroethene and tetrachloroethene, with ethene as the reference organic	IV-10
IV-4	Plots of equation (X) for the reaction of Cl atoms with 1,1-dichloroethene, <u>cis</u> -1,2-dichloroethene and ethane, with ethene as the reference organic	IV-11
IV-5	Plots of the amounts of <u>cis</u> - and <u>trans</u> -1,2-dichloroethene formed (corrected for secondary reactions with Cl atoms; see text) against the amounts of <u>trans</u> - or <u>cis</u> -1,2-dichloroethene, respectively, consumed in Cl ₂ -1,2-dichloroethene-ethene-air irradiations	IV-13
IV-6	Plots of equation (XI) for 1,1-dichloroethene in the absence of ethane (Δ) and in the presence of 7×10^{14} molecule cm ⁻³ (○) and 1.5×10^{15} molecule cm ⁻³ (●) of ethane	IV-17
IV-7	Plots of equation (XI) for <u>cis</u> -1,2-dichloroethene in the absence of ethane (●, displaced vertically by 0.04 units for clarity) and in the presence of 7×10^{14} molecule cm ⁻³ of ethane (○)	IV-18
IV-8	Plots of equation (XI) for <u>trans</u> -1,2-dichloroethene in the absence of ethane (●, displaced vertically by 0.04 units for clarity) and presence of 7×10^{14} molecule cm ⁻³ of ethane (○)	IV-19

LIST OF FIGURES
(continued)

<u>Figure Number</u>	<u>Title</u>	<u>Page</u>
IV-9	FT-IR absorption spectra obtained from a $C_2H_5ONO-NO-1,1$ -dichloroethene-air irradiation; concentrations in parentheses are in units of 10^{13} molecule cm^{-3} . (A) 1,1-dichloroethene; (B) initial mixture of 1,1-dichloroethene (23.6), ethyl nitrite (24.0) and nitric oxide (24.0); (C) mixture of products and reactants after 27 min of irradiation; (D) derived from (C) to show only the products arising from the reaction of 1,1-dichloroethene with the OH radical (see text for a discussion of the overlapped unknown band at $\sim 965\text{ cm}^{-1}$)	IV-25
IV-10	FT-IR absorption spectra obtained from a $CH_3ONO-NO$ -trichloroethene-air irradiation; concentrations in parentheses are in units of 10^{13} molecule cm^{-3} . (A) trichloroethene; (B) initial mixture of trichloroethene (24.5), methyl nitrite (24.0) and nitric oxide (12.0); (C) mixture of products and reactants after 12 min of irradiation; (D) derived from (C) to show only the products arising from the reaction of trichloroethene with the OH radical (the absorption band at 1139 cm^{-1} is due to an unknown product)	IV-26
IV-11	FT-IR absorption spectra obtained from a $CH_3ONO-NO$ -tetrachloroethene-air irradiation; concentrations in parentheses are in units of 10^{13} molecule cm^{-3} . (A) tetrachloroethene; (B) initial mixture of tetrachloroethene (23.2), methyl nitrite (24.0) and nitric oxide (12.0); (C) mixture of products and reactants after 38 min of irradiation; (D) derived from (C-B) to show only the consumption of tetrachloroethene and the formation of products from its OH radical reaction	IV-27
IV-12	Plots of the amounts of $HCHO$ (●) and $HC(O)Cl$ (○) formed (corrected for loss by reaction with the OH radical, see text) against the amount of vinyl chloride consumed in a $C_2H_5ONO-NO$ -vinyl chloride-air irradiation in the presence of 7×10^{14} molecule cm^{-3} of ethane.	IV-28
IV-13	Plot of the amounts of $HCHO$ (●) and $COCl_2$ (○, Δ) formed (those for $HCHO$ corrected for loss by reaction with the OH radical, see text) against the amount of 1,1-dichloroethene consumed in $C_2H_5ONO-NO-1,1$ -dichloroethene-air (●,○) and $CH_3ONO-NO-1,1$ -dichloroethene- CH_3OCH_3 -air (Δ) irradiations in the presence of 7×10^{14} molecule cm^{-3} of ethane. The solid line is derived from a least-squares analysis of all of the data shown	IV-29

LIST OF FIGURES
(continued)

<u>Figure Number</u>	<u>Title</u>	<u>Page</u>
IV-14	Plot of the O_3 decay rate against the allyl chloride concentration at 296 ± 2 K.	IV-40
IV-15	Plot of equation (VII) for the reaction of NO_3 radicals with allyl chloride, with ethene as the reference organic	IV-42
IV-16	Plot of the equation (III) for the reaction of OH radicals with allyl chloride, with propene as the reference organic (O - data obtained in the absence of added ethane, Δ - data obtained in the presence of 1.9×10^{15} molecule cm^{-3} of added ethane)	IV-43
IV-17	FT-IR spectra from the allyl chloride + OH reaction. (A) $CH_2=CHCH_2Cl$; (B) initial mixture of $CH_2=CHCH_2Cl$ (4.9×10^{14}), C_2H_5ONO (2.4×10^{14}) and NO (1.9×10^{14}) [concentrations in units of molecule cm^{-3}]; (C) product spectrum after 9 min of irradiation.	IV-46
IV-18	FT-IR spectra of products from allyl chloride. (A) Derived from Figure IV-17C by subtraction of absorptions by the reactants HNO_3 , $HONO$, CH_3CHO , PAN, and $HCHO$; (B) spectrum A minus $HC(O)Cl$ absorptions; (C) residual spectrum of the unknown product(s) (after subtraction of CH_2ClCHO absorptions from spectrum B).	IV-47
IV-19	FT-IR absorption spectra of (A) acrolein and (B) the C_2H_5ONO - NO -acrolein-air reactant mixture	IV-54
IV-20	FT-IR absorption spectra of (A) the reactant mixture after 18 min irradiation, with the initial reactant spectrum (Figure IV-19B) subtracted and (B) after subtraction of absorptions due to CO and $HCHO$	IV-55
IV-21	Plot of equation (VII) for the reaction of NO_3 radicals with 2,3-dihydrobenzofuran, with <u>trans</u> -2-butene as the reference alkene. The initial NO_2 concentrations were: Δ - 5×10^{13} molecule cm^{-3} , \square - 1.2×10^{14} molecule cm^{-3} , and \circ - 2.4×10^{14} molecule cm^{-3}	IV-62
IV-22	Plot of equation (III) for the gas-phase reaction of OH radicals with 1,4-benzodioxan and 2,3-dihydrobenzofuran, with propene as the reference organic	IV-64

LIST OF FIGURES
(continued)

<u>Figure Number</u>	<u>Title</u>	<u>Page</u>
IV-23	Total ion current (TIC) trace for the GC/MS analysis of the dichloromethane extract of a ~4000-liter PUF plug chamber sample from the OH radical reaction of 1,4-benzodioxan. Peak #1 is unreacted 1,4-benzodioxan. The product peaks are tentatively identified from their mass spectra as: peak #2, hydroxy-; peak #3, nitro-; and peak #4, hydroxy-nitro-derivatives of 2,4-benzodioxan	IV-70
IV-24	TIC trace for the GC/MS analysis of the dichloromethane extract of a ~4000-liter PUF plug chamber sample from the OH radical reaction of 2,3-dihydrobenzofuran. Peak #1 is unreacted 2,3-dihydrobenzofuran. The product peaks, numbers 2, 3, 4 and 5, have been tentatively identified from their mass spectra as: peaks 2 and 3, nitro-isomers of 2,3-dihydrobenzofuran; peaks 4 and 5, hydroxynitro-isomers of dihydrobenzofuran	IV-71
IV-25	Infrared spectra of (A) 1,4-benzodioxan and (B) 2,3-dihydrobenzofuran.	IV-73
IV-26	Product spectra from (A) 1,4-benzodioxan-CH ₃ ONO-NO-air mixture after 10 min of irradiation; (B) same mixture after 43 min of irradiation; (C) irradiated 1,4-benzodioxan-Cl ₂ -NO-air mixture	IV-74
IV-27	Product spectra from: (A) 2,3-dihydrobenzofuran-CH ₃ ONO-NO-air mixture after 17 min of irradiation; (B) same mixture after 62 min of irradiation; (C) irradiated 2,3-dihydrobenzofuran-Cl ₂ -NO-air mixture	IV-75
IV-28	Plot of the N ₂ O ₅ decay rates against the average naphthalene concentrations (\bullet - $[\text{NO}_2]_{\text{av}}/[\text{N}_2\text{O}_5]_{\text{initial}} < 1$; \circ - $[\text{NO}_2]_{\text{av}}/[\text{N}_2\text{O}_5]_{\text{initial}} > 1$)	IV-79
IV-29	Plot of equation (III) for the reaction of OH radicals with benzyl chloride, with dimethyl ether as the reference compound. (\circ - in the absence of ethane; Δ - in the presence of 4.8×10^{14} molecule cm ⁻³ of ethane)	IV-82
IV-30	Infrared spectra of (A) benzyl chloride; (B) initial benzyl chloride-CH ₃ ONO-NO-air mixture, and (C) mixture after 57 min of irradiation	IV-84
IV-31	Residual spectra of products from (A) benzyl chloride-CH ₃ ONO-NO-air mixture after 17 min of irradiation; (B) same mixture after 57 min of irradiation; (C) irradiated benzyl chloride-Cl ₂ -NO-air mixture	IV-86

LIST OF FIGURES
(continued)

<u>Figure Number</u>	<u>Title</u>	<u>Page</u>
IV-32	Infrared spectra of the cresol isomers	IV-88
IV-33	Product spectra from the mixture of N_2O_5 with (A) o-cresol, (B) m-cresol, and (C) p-cresol. Asterisks identify the bands of an o-cresol product which condensed at a faster rate than other components	IV-89
IV-34	Plot of equation (VII) for the reaction of NO_3 radicals with crotonaldehyde, with propene as the reference organic	IV-93
IV-35	Plots of equation (III) for the reaction of OH radicals with <u>cis</u> - and <u>trans</u> -1,3-dichloropropene, with <u>n</u> -octane as the reference organic, in the presence of ethane	IV-94
IV-36	Plot of equation (III) for the reaction of OH radicals with 3-chloro-2-chloromethyl-1-propene, with isoprene (2-methyl-1,3-butadiene) as the reference organic, in the presence of ethane	IV-95
VI-1	Plot of calculated versus experimentally measured room temperature rate constants for gas-phase reaction of the OH radical with alkanes, haloalkanes, alkenes, alkynes, haloalkenes, oxygen-containing organics and aromatic compounds (total ~270 compounds). The solid line indicates perfect agreement; the dashed lines disagreement by a factor of 2	VI-15
VI-2	Plots of calculated versus experimentally measured room temperature rate constants for the gas phase reaction of the OH radical with S- and N-containing aliphatic compounds. The solid line indicates perfect agreement; the dashed lines disagreement by a factor of 2	VI-17

LIST OF TABLES

<u>Table Number</u>	<u>Title</u>	<u>Page</u>
I-1	Calculated Atmospheric Lifetimes of Compounds Investigated for Reaction with OH and NO ₃ Radicals and O ₃	I-4
I-2	Ranges of Influence of Parent Compounds Based on Atmospheric Lifetimes	I-5
II-1	Chemical Compounds Studied	II-3
IV-1	Experimental Conditions and Results for the Behavior of Ethylene Oxide in the Presence of Water Vapor	IV-2
IV-2	Rate Constant Ratios k_{11}/k_{12} and Rate Constants k_{11} for the Gas-Phase Reactions of the NO ₃ Radical with the Chloroethenes at 298 ± 2 K	IV-8
IV-3	Rate Constant Ratios k_{13}/k_{14} and Rate Constants k_{13} for the Gas-Phase Reactions of Cl Atoms with Ethane and the Chloroethenes at 298 ± 2 K and ~735 Torr Total Pressure of Air	IV-12
IV-4	Slopes of the Plots of Equation (XI) Obtained at 298 ± 2 K and Atmospheric Pressure from Irradiated CH ₃ ONO-NO-Chloroethene-CH ₃ OCH ₃ -Air Mixtures in the Absence and Presence of C ₂ H ₆	IV-20
IV-5	Room Temperature Rate Constants for the Gas-Phase Reactions of NO ₃ and OH Radicals and O ₃ with the Chloroethenes, and the Calculated Atmospheric Lifetimes Due to These Reactions	IV-22
IV-6	Product Yields, Corrected for Reaction with the OH Radical, Determined from RONO-NO-Chloroethene-Air Irradiations in the Presence and Absence of Cl Atom Scavengers	IV-31
IV-7	Ethoxy Radical Intermediates Formed from the Chloroethenes and their Predicted Modes of Reaction	IV-35
IV-8	Experimental Data for the Gas-Phase Reaction of O ₃ with Allyl Chloride at 296 ± 2 K	IV-39
IV-9	Calculated Atmospheric Lifetimes of Allyl Chloride Due to Reaction with NO ₃ and OH Radicals and O ₃	IV-45
IV-10	Time-Concentration Data for an Irradiated C ₂ H ₅ ONO-NO-Allyl Chloride-Air Mixture	IV-48

LIST OF TABLES
(continued)

<u>Table Number</u>	<u>Title</u>	<u>Page</u>
IV-11	Calculated Atmospheric Lifetimes of Acrolein Due to Reaction with OH and NO ₃ Radicals and O ₃	IV-52
IV-12	Time-Concentration Data for an Irradiated CH ₂ =CHCHO/C ₂ H ₅ ONO/NO Mixture	IV-56
IV-13	Experimental Data for the Reactions of O ₃ with 1,4-Benzodioxan and 2,3-Dihydrobenzofuran at 297 ± 2 K	IV-60
IV-14	Rate Constant Ratios for the Gas-Phase Reactions of 1,4-Benzodioxan and 2,3-Dihydrobenzofuran with NO ₃ Radicals at 298 ± 2 K	IV-63
IV-15	Rate Constant Ratios and Rate Constants for the Reactions of OH Radicals with 1,4-Benzodioxan and 2,3-Dihydrobenzofuran	IV-65
IV-16	Calculated Atmospheric Lifetimes of 1,4-Benzodioxan and 2,3-Dihydrobenzofuran Due to Reaction with OH and NO ₃ Radicals and O ₃	IV-65
IV-17	Rate Constants k for the Gas-Phase Reaction of NO ₃ Radicals with a Series of Aromatic Compounds at Room Temperature	IV-67
IV-18	Experimental Conditions Employed and N ₂ O ₅ Decay Rates Observed for the Gas-Phase Reaction of N ₂ O ₅ with Naphthalene at 298 ± 2 K	IV-78
IV-19	Experimental Data for the Gas-Phase Reaction of O ₃ with 2,3-Benzofuran at 297 ± 2 K	IV-91
IV-20	Rate Constant Ratios and Rate Constants for Gas-Phase Reactions of the NO ₃ Radical with a Series of Organics at 298 ± 2 K	IV-96
V-1	Room Temperature Rate Constants for the Gas-Phase Reactions of OH and NO ₃ Radicals and O ₃ with the Compounds Investigated in this Study	V-2
V-2	Calculated Atmospheric Lifetimes of Compounds Investigated for Reaction with OH and NO ₃ Radicals and O ₃	V-4
V-3	Ranges of Influence of Parent Compounds Based on Atmospheric Lifetimes	V-5

LIST OF TABLES
(continued)

<u>Table Number</u>	<u>Title</u>	<u>Page</u>
VI-1	Temperature Dependent Parameters, in the Form $k = AT^2 e^{-E/T}$, for CH_3- , $-\text{CH}_2-$, $>\text{CH}-$ and $-\text{OH}$ Group Rate Constants	VI-3
VI-2	Substituent Factors $F(X)$ at 298 K	VI-5
VI-3	Room Temperature Group Rate Constants for OH Radical Addition to $>\text{C}=\text{C}<$, $-\text{C}\equiv\text{C}-$, $>\text{C}=\text{C}=\text{C}<$ and $>\text{C}=\text{C}-\text{C}=\text{C}<$ Structural Units	VI-8
VI-4	Substituent Factors $C(X)$ at 298 K	VI-9
VI-5	Estimated Electrophilic Substituent Constants σ_m^+ and σ_p^+ for $\text{C}_6\text{H}_5-\text{xCl}_x$ Groups	VI-11
VI-6	Substituent Factors $F(X)$ for H-Atom Abstraction from C-H Bonds and Group Rate Constants at 298 K for OH Radical Reaction with Thiols, Sulfides, Disulfides, Amines and Related Organics	VI-16
VI-7	Comparison of Experimental and Calculated Room Temperature Rate Constants for Reactions of OH Radicals with P-Containing Organics	VI-19

GLOSSARY OF TERMS, ABBREVIATIONS AND SYMBOLS

ARB	California Air Resources Board
cm	Centimeter
ft	Feet
FT-IR	Fourier-transform infrared absorption spectroscopy
GC	Gas chromatography
GC-MS	Gas chromatography-mass spectrometry
HNO ₃	Nitric acid
hr	Hour
K	Degrees Kelvin
k _i	Reaction rate constant
KW	Kilowatt
min	Minute
m	Meter
nm	Nanometer
NO ₃	Nitrate radical
N ₂ O ₅	Dinitrogen Pentoxide
O ₃	Ozone
OH	Hydroxyl radical
ppb	Part per billion
ppt	Part per trillion
SAPRC	Statewide Air Pollution Research Center
UCR	University of California, Riverside

I. PROJECT SUMMARY

A. Introduction and Statement of the Problem

Concern over the occurrence and effects of airborne toxic and hazardous chemicals has emerged over the past ten years as a dominant air pollution issue on a regional, statewide and national basis. During this time, recognition has grown that a wide range of sources may be responsible for emissions of significant quantities of potentially hazardous compounds. Among these sources are toxic waste disposal sites and landfills, releases from industrial or commercial processes, and emissions resulting from the application of pesticides and herbicides during agricultural operations.

Under California Assembly Bill 1807, the Tanner Bill, the California Air Resources Board (ARB) has been given major responsibility for critically assessing the presence and impacts of airborne toxic chemicals in California's atmospheres. The overall objective of this assessment is to provide a reliable and comprehensive data base for the purposes of risk assessment analyses and possible standard setting or other regulatory actions.

Important elements of the data base which must be developed for each compound under consideration as a potential toxic air contaminant include (a) the atmospheric degradation pathways of the compound, (b) its corresponding atmospheric lifetime, and (c) the products formed from the parent compound, and their fates. From such information, exposure assessments can be developed and the radius of impact of a toxic or hazardous volatile compound can be characterized as being local, regional or global in scope.

Although atmospheric lifetimes have been estimated (since they cannot be directly measured) for a large number of relatively simple organics, few data were available for the specific compounds of interest to the ARB which were investigated in this study. Moreover, there are at present no reliable predictive techniques for many of the large number of other potentially toxic or hazardous compounds emitted into the atmosphere from a wide range of sources.

B. Objectives

The specific objectives of this program were:

- To experimentally determine the rates of reaction of selected potentially hazardous or toxic organic compounds (and of certain compounds which can serve as models for important classes of volatile toxic chemicals) with key atmospheric reactive species such as hydroxyl (OH) radicals, ozone (O_3) and nitrate (NO_3) radicals. The specific compounds investigated included: ethylene oxide, vinyl chloride, 1,1-dichloroethene, cis- and trans-1,2-dichloroethene, trichloroethene, tetrachloroethene, acrolein, allyl chloride, benzyl chloride, o-, m-, and p-cresol, naphthalene, 1,4-benzodioxan and 2,3-dihydrobenzofuran, with the latter two compounds acting as "model" compounds for the dibenzo-p-dioxins and dibenzofurans and their chlorinated and brominated homologs.

- To calculate the atmospheric lifetimes of these selected toxic or model compounds using the rate constant data obtained in this program in combination with the known or assumed atmospheric concentrations of these reactive species (i.e., OH and NO_3 radicals and O_3).

- To experimentally determine, where feasible, the products formed from the reactions of the above compounds with key atmospheric species, thereby permitting a preliminary assessment of whether such atmospheric transformations result in the formation of more toxic, or less toxic, products.

- To utilize the rate data obtained in this program, along with appropriate literature data, to further develop structure-reactivity relationships which may be applied to more complex organic compounds than has previously been possible.

C. Methods of Approach

In this project, experiments involving OH and NO_3 radical reactions were conducted primarily in the SAPRC 5800-liter evacuable, Teflon-coated environmental chamber, with irradiation provided by a 24 KW Xenon arc, or in a 6400-liter all-Teflon chamber with blacklamp irradiation. Experiments concerning O_3 reactions were carried out in ~175-liter FEP Teflon reaction bags.

In the kinetic experiments, the disappearance of organic reactants was monitored by gas chromatography and/or long pathlength Fourier

transform (FT-IR) absorption spectroscopy prior to and during the irradiations. In addition, the reaction products and the reaction mechanisms of OH-radical initiated reactions with organics were studied in the 5800-liter evacuable chamber using either in situ longpath FT-IR spectroscopy or off-line GC or GC-MS analysis of grab samples from the chamber.

All of the experimental techniques employed were proven methods which have been validated at SAPRC over the past decade. Detailed information concerning these and other experimental methods used in this program are provided in Section III of this report, as well as in Section IV for the individual compounds studied.

D. Summary of Results and Conclusions

The atmospheric lifetimes against chemical reaction with OH radicals, ozone and NO_3 radicals were calculated for 16 compounds of atmospheric importance, either because they have been determined to be hazardous or toxic, or because they can serve as model compounds for important classes of hazardous substances. The calculated atmospheric lifetimes for these three gas-phase atmospheric removal processes are given in Table I-1.

The data in Table I-1 show that, except for a few cases, the dominant of these reaction pathways for the compounds studied is by daytime reaction with the OH radical. The exceptions to this are the three cresol isomers and 2,3-dihydrobenzofuran, which also react rapidly with NO_3 radicals. These compounds can therefore undergo substantial atmospheric degradation at night by reaction with NO_3 radicals, as well as with OH radicals during daylight hours. It is important to note, however, that dibenzofuran, and its chlorinated and brominated analogues, for which 2,3-dihydrobenzofuran served as a model compound, will not react with NO_3 radicals because of structural effects which are discussed in Section IV. However, the data obtained for 2,3-dihydrobenzofuran allows the atmospheric lifetimes for the dibenzofurans to be estimated, and thus it served as an appropriate model compound for this purpose.

As can be seen from Table I-1, none of the compounds investigated react sufficiently rapidly with O_3 under atmospheric conditions for this process to represent a significant atmospheric removal pathway. Similarly, although naphthalene reacts with N_2O_5 , its calculated atmospheric lifetime due to this reaction of ~80 days means that this reaction pathway

Table I-1. Calculated Atmospheric Lifetimes of Compounds Investigated for Reaction with OH and NO₃ Radicals and O₃

Organic Compound	Atmospheric Lifetimes ^a		
	OH	NO ₃	O ₃
Ethylene Oxide	330 days		
Vinyl Chloride	3.5 days	200 days	66 days
1,1-Dichloroethene	2.9 days	70 days	12 yr
<u>cis</u> -1,2-Dichloroethene	9.6 days	1.7 yr	>9 yr
<u>trans</u> -1,2-Dichloroethene	13 days	2.2 yr	110 days
Trichloroethene	9.6 days	300 days	>1.5 yr
Tetrachloroethene	140 days	3.8 yr	>2 x 10 ³ yr
Acrolein	1.2 days	80 days	60 days
Allyl Chloride	1.4 days	160 days	10 days
Benzyl Chloride	8.3 days	>160 days	>1.1 yr
o-Cresol	6.9 hr	3.5 min	64 days
m-Cresol	4.9 hr	4.6 min	87 days
p-Cresol	6.3 hr	3.3 min	35 days
Naphthalene	1.1 days	b	>80 days
1,4-Benzodioxan	11 hr	166 days	>3.8 yr
2,3-Dihydrobenzofuran	7.5 hr	11 hr	>165 days

^aFor concentrations of: O₃, 24-hr average of 7×10^{11} molecule cm⁻³; OH, 12-hr daytime average of 1×10^6 molecule cm⁻³; NO₃, 12-hr nighttime average of 2.4×10^8 molecule cm⁻³.

^bReaction with 2×10^{10} molecule cm⁻³ of N₂O₅ during nighttime hours leads to a calculated lifetime of ~80 days.

will be of negligible importance as a naphthalene loss process, compared to the OH radical reaction.

From the data in Table I-1 it is possible to group the compounds studied into three categories, corresponding to very short atmospheric lifetimes (a few minutes to one day), moderately long lifetimes (a few days), and long-lived species with lifetimes ranging from about one week to many years. Such a grouping is shown in Table I-2, with corresponding

designations of local, regional and global ranges of transport. (Clearly any compound which can undergo global transport may also have local and regional impacts, and similarly any regionally distributed pollutant may also cause local effects.)

An important qualification for the grouping given in Table I-2 concerns the possible role of the products of the atmospheric reactions of compounds which have short or moderate lifetimes since such products may in turn have regional or global impacts. Thus, in the case of some of the chloroethenes which have moderate lifetimes, certain of their atmospheric transformation products (e.g., phosgene) may be longer lived and of significant biological concern.

With regard to the class of longer-lived organics, potential health effects due to toxicity are not the only impacts to be considered. Thus, these compounds may undergo dry or wet deposition in remote, supposedly pristine, ecosystems and, in the case of certain of the chloroethenes (for example, tetrachloroethene), may reach the stratosphere with consequent effects on the stratospheric ozone layer.

Table I-2. Ranges of Influence of Parent Compounds Based on Atmospheric Lifetimes

Atmospheric Lifetime	Range of Influence	Organic Compounds
Short (<1 day)	Local	Cresols 1,4-Benzodioxan 2,3-Dihydrobenzofuran
Moderate (~1-7 days)	Regional	Vinyl Chloride 1,1-Dichloroethene Acrolein Allyl chloride Naphthalene
Long (~1 week-1 yr)	Global	Benzyl chloride <u>cis</u> -1,2-Dichloroethene <u>trans</u> -1,2-Dichloroethene Trichloroethene Tetrachloroethene Ethylene oxide

The experimental data obtained in this and related research programs at SAPRC, as well as from the literature, were employed to further develop a structure-reactivity technique for the calculation of rate constants for the reaction of OH radicals with organic compounds under atmospheric conditions. Since OH radical reaction is the dominant removal pathway for most volatile organics, this technique, based on data for some 300 compounds, offers the potential for estimating the atmospheric lifetimes of additional organic compounds whose low volatility or chemical complexity make experimental investigation difficult or impossible.

II. INTRODUCTION

Background to Present Study

In recent years there has been growing concern by both the general public and health, regulatory and legislative officials about the use, storage and transport of hazardous and toxic chemicals. The potential problems associated with the widespread manufacture and use of toxic chemical compounds was brought to worldwide attention by the accidental release of methyl isocyanate in Bhopal, India, with a resultant loss of more than 2000 lives. Similar instances of inadvertent chemical releases, but on a much smaller scale, occur frequently in California due to the large amounts of chemicals transported by railroads and on the state highways. In addition, segments of the public are exposed to a variety of toxic and hazardous chemical compounds which are emitted from hazardous waste disposal sites and landfills, from the application of pesticides and herbicides during agricultural operations, and from releases which occur in the course of industrial or commercial processes.

Present assessments of the environmental and health impacts of airborne toxic and hazardous chemicals, including pesticides, herbicides, and a wide range of volatile organic compounds, are cast almost exclusively in terms of the effects of the parent compound. In general, no consideration is given to the possible effects due to products formed from parent compounds by atmospheric reactions. Such atmospheric transformations can lead to products which are either more, or less, toxic than the parent compound. Without a thorough knowledge of these atmospheric processes, reliable and cost-effective risk assessments for releases (accidental or not) of toxic and hazardous chemicals cannot be made in the case of many volatile and reactive organic compounds.

Detailed characterization of the atmospheric degradation pathways of chemical compounds emitted into the atmosphere can provide a basis for dealing with both chronic and acute exposure situations. One example of chronic exposure is the release of pesticides and herbicides during agricultural operations and their dispersal, with concurrent chemical and physical transformations, to downwind areas where they and their products may impact residential populations as well as farm workers. A second example of chronic exposure is the emission of toxic and hazardous

chemicals from waste disposal sites and landfills adjacent to residential areas (SCAQMD 1985).

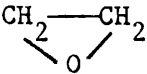
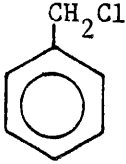
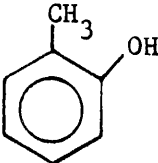
Examples of acute exposures include the recent tragedy in Bhopal, India, spills of chemicals during their transport over California's highways and railroads, and releases due to fires or industrial accidents.

For both chronic and acute exposures, the protection of public health and property requires a knowledge of the time-concentration history and chemical composition of the dispersing plume as it is transported downwind. Such a detailed understanding of the products formed from airborne toxic compounds, and their persistence in ambient air, requires that both atmospheric lifetimes and reaction products be known. At present the atmospheric lifetimes of a large number of relatively simple organics have either been measured or can be reliably calculated (Atkinson and Carter 1984, Atkinson 1986). However, for the vast majority of chemical compounds, the situation concerning the reaction products formed under atmospheric conditions is characterized by an almost complete lack of knowledge of the kind needed to develop realistic risk assessment and emergency preparedness models.

In this research program, we experimentally investigated the loss processes and the products formed from the simulated atmospheric reactions of a series of organic chemicals of interest to the ARB. The chemicals studied are shown in Table II-1. Most of these chemicals are on, or have been on, the ARB list of potential Toxic Air Contaminants. Thus, vinyl chloride, 1,1-dichloroethene, trichloroethene, tetrachloroethene, acrolein, allyl chloride, benzyl chloride, cresols and ethylene oxide are specifically on the ARB list of potential Toxic Air Contaminants, and naphthalene is the simplest of the polycyclic aromatic hydrocarbons (PAH). In addition, 1,4-benzodioxan and 2,3-dihydrobenzofuran are model compounds, of relatively high volatility, for the less volatile dibenzo-p-dioxins and the dibenzofurans, respectively.

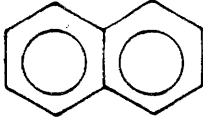
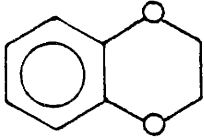
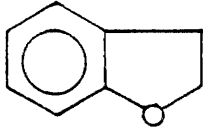
In this experimental program, for a given compound we first investigated the potentially important atmospheric gas-phase chemical removal processes to determine the dominant atmospheric reaction pathway(s). As presently understood, for chemicals present in the gas phase, these removal processes involve the following:

Table II-1. Chemical Compounds Studied

Organic	Structure
Ethylene oxide	
Vinyl chloride	$\text{CH}_2=\text{CHCl}$
<u>cis</u> -1,2-Dichloroethene	$\text{CHCl}=\text{CHCl}$
<u>trans</u> -1,2-Dichloroethene	$\text{CHCl}=\text{CHCl}$
1,1-Dichloroethene	$\text{CH}_2=\text{CCl}_2$
Trichloroethene	$\text{CHCl}=\text{CCl}_2$
Tetrachloroethene	$\text{CCl}_2=\text{CCl}_2$
Acrolein	$\text{CH}_2=\text{CHCHO}$
Allyl chloride	$\text{CH}_2=\text{CHCH}_2\text{Cl}$
Benzyl chloride	
o-Cresol	

(continued)

Table II-1 (continued) - 2

Organic	Structure
Naphthalene	
1,4-Benzodioxan	
2,3-Dihydrobenzofuran	

- Photolysis during daylight hours.
- Reaction with hydroxyl (OH) radicals during daylight hours.
- Reaction with ozone (O₃), typically during both daytime and nighttime.
- Reaction with hydroperoxyl (HO₂) radicals, typically during late daytime and early nighttime hours.
- Reaction with the gaseous nitrate (NO₃) radical during nighttime hours.
- Reaction with dinitrogen pentoxide (N₂O₅) during nighttime hours.
- Reaction with nitrogen dioxide (NO₂) during, typically, both daytime and nighttime hours.
- Reaction with gaseous nitric acid (HNO₃) and other acids.

The lifetime τ of a chemical with respect to reaction with a species X is given by

$$\tau = (k_x[X])^{-1} \quad (I)$$

where $[X]$ is the atmospheric concentration of the reactive species X and k_x is the rate constant for reaction with species X . The overall lifetime in the atmosphere due to chemical reaction is then given by

$$(\text{overall lifetime})^{-1} = \{k_{\text{OH}}[\text{OH}] + k_{\text{O}_3}[\text{O}_3] + k_{\text{NO}_3}[\text{NO}_3] + \dots\} \quad (\text{II})$$

Once the dominant atmospheric removal pathway(s) had been determined, the products of this reaction, or reactions, were then studied under atmospheric conditions.

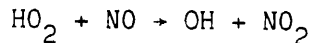
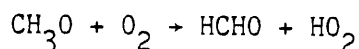
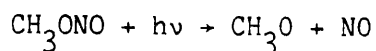
As discussed in the sections below, chlorine atoms were produced from the OH radical reactions with most of the chloroalkenes. In order to determine accurately the OH radical reaction rate constants, further experiments were necessary to avoid, or minimize, the occurrence of secondary reactions involving Cl atoms. These experiments included a study to determine the rate constants for the reaction of Cl atoms with the chloroethenes at room temperature and atmospheric pressure. The experimental methods employed in these studies, and the resulting data, are discussed in detail in the following sections. In addition to these experimental studies, we continued to develop a structure-reactivity relationship to take into account recent experimental data for OH radical reaction rate constants and our most recent structure-reactivity relationship for the estimation of OH radical reaction rate constants for organic compounds is presented in Section VI.

III. METHODS OF PROCEDURE

The potentially important atmospheric removal pathways investigated during this program for the organic compounds shown in Table II-1 were by gas-phase reaction with OH and NO₃ radicals, N₂O₅, and O₃. The experimental techniques used to investigate the kinetics and products of these gas-phase reactions are described below.

1. Determination of OH Radical Reaction Rate Constants

Hydroxyl radical reaction rate constants were determined at room temperature using the relative rate technique developed and extensively tested at SAPRC (Atkinson et al. 1981, 1982a). Hydroxyl radicals were generated by the photolysis, at wavelengths ≥ 290 nm, of methyl nitrite (CH₃ONO) in air at part-per-million (ppm) concentrations:



In order to minimize the formation of O₃ and of NO₃ radicals during these irradiations, NO was also added to the reaction mixtures, which had typical initial concentrations of: CH₃ONO, (1.2-3.6) x 10¹⁴ molecule cm⁻³; NO, (1.2-2.4) x 10¹⁴ molecule cm⁻³ and (2.4-12) x 10¹³ molecule cm⁻³ each of the reference organic and the reactant. Synthetic air (80% N₂ + 20% O₂) or dry purified air (Doyle et al. 1977) were used as the diluent gas, depending on the chamber used.

Irradiations were carried out in the SAPRC 5800-liter evacuable, Teflon-coated environmental chamber, with irradiation being provided by a 24 KW Xenon arc (Winer et al. 1980), or in ~6400-liter and ~2500-liter all-Teflon chambers with blacklight irradiation. The 5800-liter evacuable and ~6400-liter all-Teflon chambers are shown schematically in Figures III-1 and III-2, respectively. The organic reactants were quantitatively monitored by gas chromatography and/or by long pathlength Fourier transform (FT-IR) absorption spectroscopy prior to and during the irradiations.

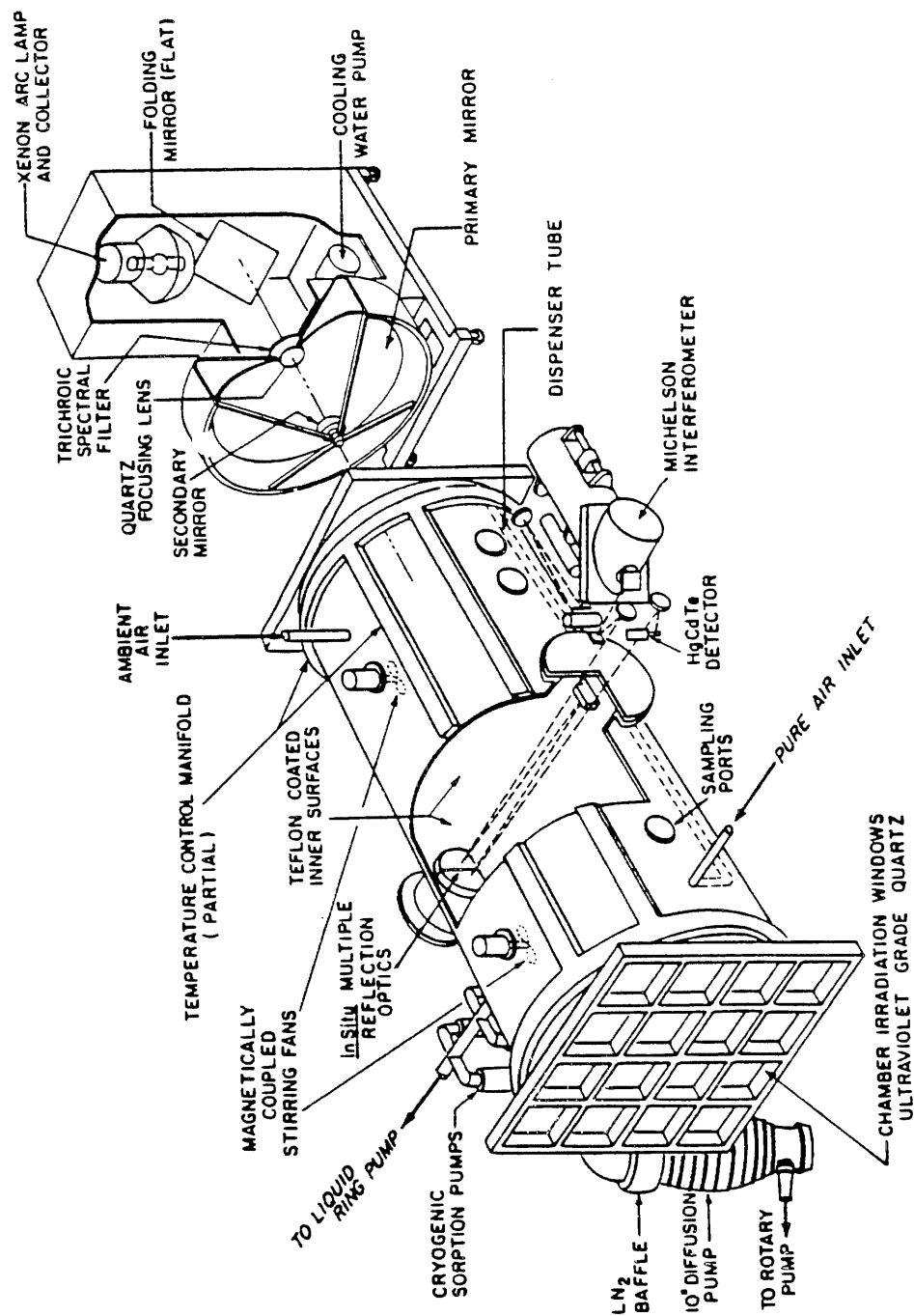


Figure III-1. SAPRC 5800-liter evacuable Teflon-coated environmental chamber.

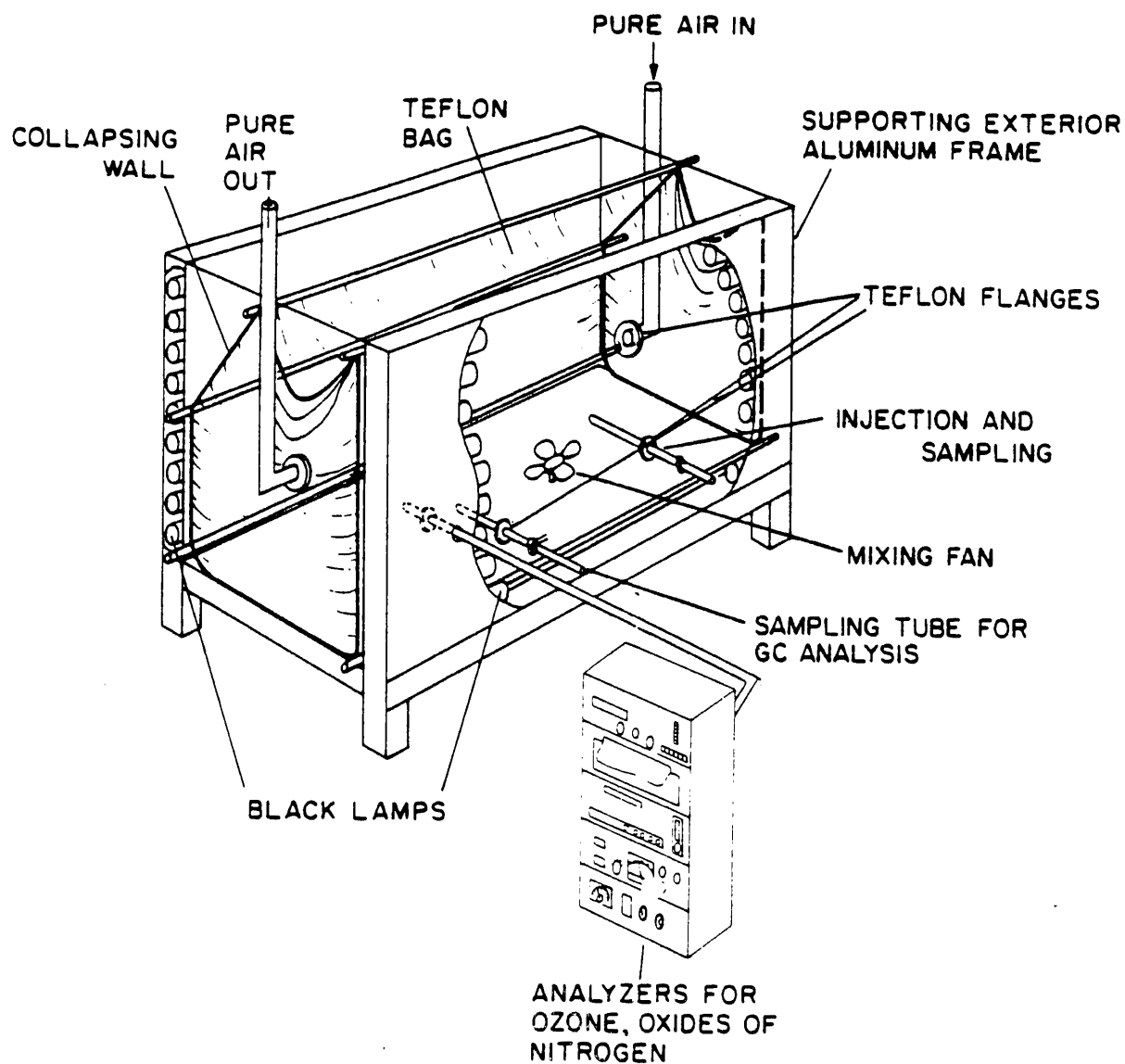
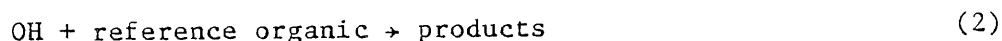
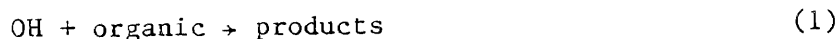


Figure III-2. SAPRC 6400-liter all-Teflon chamber.

In these reactant mixtures, the OH radicals react with both the reference organic and the reactant organic.



For organics which do not photolyze or react to any significant extent with other reactive species, the following expression can be derived (Atkinson et al. 1982a):

$$\ln \left\{ \frac{[\text{organic}]_{t_0}}{[\text{organic}]_t} \right\} = \frac{k_1}{k_2} \ln \left\{ \frac{[\text{reference organic}]_{t_0}}{[\text{reference organic}]_t} \right\} \quad (\text{III})$$

where $[\text{organic}]_{t_0}$ and $[\text{reference organic}]_{t_0}$ are the concentrations of the reactant and the reference organic, respectively, at time t_0 , $[\text{organic}]_t$ and $[\text{reference organic}]_t$ are the corresponding concentrations at time t , and k_1 and k_2 are the rate constants for reactions (1) and (2), respectively. Hence, plots of $\ln([\text{organic}]_{t_0}/[\text{organic}]_t)$ against $\ln([\text{reference organic}]_{t_0}/[\text{reference organic}]_t)$ should have a slope of k_1/k_2 and zero intercept.

For organics which can also photolyze, a more complex expression is derived,

$$\frac{1}{(t-t_0)} \ln \left\{ \frac{[\text{organic}]_{t_0}}{[\text{organic}]_t} \right\} = k_3 + \frac{k_1}{k_2(t-t_0)} \ln \left\{ \frac{[\text{reference organic}]_{t_0}}{[\text{reference organic}]_t} \right\} \quad (\text{IV})$$

where k_3 is the rate constant for photolysis of the reactant organic:



In this case, a plot of the left hand side of this equation against $(t-t_0)^{-1} \ln([\text{reference organic}]_{t_0}/[\text{reference organic}]_t)$ yields a straight line of slope k_1/k_2 and intercept k_3 . In either case, knowing the rate

constant k_2 for the reference organic, the rate constant, k_1 , of interest can be derived.

2. Determination of Rate Constants for Reaction of O_3 with Organics

Ozone reaction rate constants were determined at room temperature using the experimental technique developed and widely tested at SAPRC under U. S. Environmental Protection Agency funding (Atkinson et al. 1982b). This technique is based upon monitoring the increased rates of O_3 decay in the presence of known concentrations of a reactive organic. Under these conditions, the reactions removing O_3 are:



and, hence,

$$-d[O_3]/dt = (k_4 + k_5[\text{organic}])[O_3] \quad (V)$$

Under the experimental conditions employed in this program, the reactant concentrations were always greatly in excess of the initial O_3 concentrations (i.e., $[\text{organic}]/O_3]_{\text{initial}} \geq 10$). Hence, equation (V) may be rearranged to yield

$$-d\ln[O_3]/dt = k_4 + k_5[\text{organic}] \quad (VI)$$

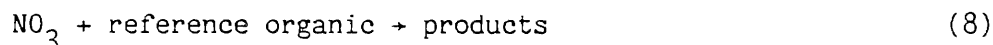
From the ozone decay rates, $-d\ln[O_3]/dt$, at various organic concentrations and with a knowledge of the background O_3 decay rate, k_4 , the rate constants k_5 were obtained.

Experiments were carried out in ~175-liter FEP Teflon reaction bags which were initially divided into two subchambers by metal barriers. Ozone, at concentrations so as to obtain ~1 ppm (2.4×10^{13} molecule cm^{-3}) in the entire reaction bag, was injected in pure air diluent into one subchamber. A known amount of the organic in pure air diluent was injected into the other subchamber. The reactions were initiated by removing the barriers and rapidly mixing the contents of the reaction bag by pushing down on alternative sides of the bag for ~1 min. After mixing of the reactants, ozone concentrations were monitored as a function of

time by a chemiluminescence analyzer and the organic concentrations in the entire bag were quantitatively analyzed by gas chromatography with flame ionization detection.

3. Determination of NO₃ Radical Reaction Rate Constants for Organics

The relative rate technique used and described by Atkinson et al. (1984a,b) was employed to determine room temperature NO₃ radical reaction rate constants. In this technique, the relative decay rates of the reactant organic and a reference organic, whose NO₃ radical rate constant is reliably known, were monitored in the presence of NO₃ radicals. The latter were generated by the thermal decomposition of N₂O₅.



Under these conditions, the equation

$$\ln \left\{ \frac{[\text{organic}]_{t_o}}{[\text{organic}]_t} \right\} - D_t = \frac{k_7}{k_8} \left[\ln \left\{ \frac{[\text{reference organic}]_{t_o}}{[\text{reference organic}]_t} \right\} - D_t \right] \quad (\text{VII})$$

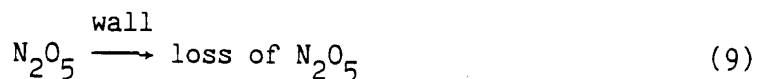
holds, where [organic]_{t_o} and [reference organic]_{t_o} are the concentrations of the reactant organic and reference organic, respectively, at time t_o, [organic]_t and [reference organic]_t are the corresponding concentrations at time t, D_t is any amount of dilution at time t caused by the additions of N₂O₅ to the chamber and k₇ and k₈ are the rate constants for reactions (7) and (8), respectively. Hence plots of [ln{[organic]_{t_o}/[organic]_t} - D_t] against [ln{[reference organic]_{t_o}/[reference organic]_t} - D_t] should yield straight line plots of slope k₇/k₈ and zero intercept.

These experiments were carried out either in the 5800-liter evacuable Teflon-coated chamber, with analyses being carried out by gas chromatography and/or FT-IR spectroscopy, or in the ~6400-liter all-Teflon chamber with analyses by gas chromatography. The amounts of dilution, D_t, were

zero for the experiments involving FT-IR analyses, and ~0.003 per addition of N_2O_5 for the experiments with GC analyses.

4. Determination of the N_2O_5 Reaction Rate Constant for Naphthalene

We have shown previously (Pitts et al. 1985) that the gaseous PAH react with N_2O_5 , and not with the NO_3 radical, under the experimental conditions encountered in environmental chambers. Our previous work only determined an approximate N_2O_5 reaction rate constant for naphthalene from a computer fit of a single reaction of N_2O_5 with naphthalene. In the present study, the rate constant for the reaction of N_2O_5 with naphthalene was determined by monitoring the enhanced decay rate of N_2O_5 in the presence of known concentrations of naphthalene. In the absence of secondary reactions, the reactions removing N_2O_5 are:



Under these conditions, and assuming exponential decays of N_2O_5 , then

$$-d \ln [N_2O_5]/dt = k_9 + k_{10}[\text{naphthalene}] \quad (\text{VIII})$$

Hence a plot of the N_2O_5 decay rate against the naphthalene concentration should be a straight line with a slope of k_{10} .

Experiments were carried out in the 5800-liter evacuable, Teflon-coated, environmental chamber equipped with an in situ multiple reflection optical system interfaced to an FT-IR absorption spectrometer (Winer et al. 1980). Naphthalene was introduced into the chamber by flowing N_2 (>99.998% stated purity) at a measured flow rate through a Pyrex tube filled with crystalline naphthalene, and was monitored by FT-IR absorption spectroscopy at 785 cm^{-1} with a spectral resolution of 1 cm^{-1} and a pathlength of 62.9 m. The infrared absorption coefficient was determined by adding incremental amounts of naphthalene to the chamber, with the Pyrex tube containing the naphthalene being weighed before and after each addition of naphthalene.

Known pressures of N_2O_5 in calibrated Pyrex bulbs were introduced into the chamber by flushing the contents of the bulbs with a stream of

N_2 , with simultaneous rapid mixing by a fan rated at 300 liter s^{-1} . N_2O_5 was monitored at 1246.3 cm^{-1} and its concentrations were determined using the absorption coefficient of Graham and Johnston (1978). N_2O_5 decay rates were obtained in the presence and absence of naphthalene, with synthetic air (80% N_2 + 20% O_2) being used as the diluent gas. The initial reactant concentrations in the experiments where naphthalene was present were: naphthalene, $(1.1-15) \times 10^{13} \text{ molecule cm}^{-3}$; and N_2O_5 , $(1.4-6.1) \times 10^{13} \text{ molecule cm}^{-3}$. NO_2 , at concentrations of up to $2.4 \times 10^{14} \text{ molecule cm}^{-3}$, was added to the majority of the experiments to minimize the concentrations of NO_3 radicals formed from the thermal decomposition of N_2O_5 and to scavenge any radical species formed in these reactions.

5. Investigation of Products of OH Radical Reactions with Organics

The reaction products and mechanisms of OH radical-initiated reactions with organics were studied in the 5800-liter evacuable chamber. In order to enhance the reactivity of the systems being studied, OH radical concentrations of $\geq 10^7 \text{ cm}^{-3}$ were generated by the photolysis at $\geq 290 \text{ nm}$ of part-per-million concentrations of CH_3ONO (see above). For the studies involving the chlorine-containing compounds, ethane was generally added to the reactant mixtures to scavenge any Cl atoms formed from the OH radical reactions. Additional relevant details of these experiments are given in the sections dealing with the individual compounds studied.

IV. EXPERIMENTAL RESULTS AND DISCUSSION

The experimental studies carried out and the data obtained are detailed below for the individual compounds investigated. The chemical compounds studied are dealt with either individually or grouped into series with analogous chemical structures.

A. Ethylene Oxide $\left(\begin{array}{c} \text{CH}_2 - \text{CH}_2 \\ \diagdown \quad \diagup \\ \quad \text{O} \end{array} \right)$

The available literature data show that the dominant chemical removal pathway for ethylene oxide from the troposphere is by reaction with the OH radical (Atkinson 1986). However, this atmospheric loss process is slow, with a calculated tropospheric lifetime due to OH radical reaction of approximately one year or longer, and hence wet and/or dry deposition could be important atmospheric removal routes.

At the request of the ARB staff, a series of experiments were carried out in the 5800-liter evacuable, Teflon-coated chamber to determine the loss rates of ethylene oxide as a function of the water vapor concentration. As noted in Section III, this chamber is equipped with an in situ White-type multiple reflection optical system interfaced to an FT-IR absorption spectrometer. Ethylene oxide and water concentrations were monitored during these experiments by FT-IR absorption spectroscopy, using a pathlength of 62.9 m and a resolution of 1 cm^{-1} . The water vapor concentrations were determined using calibration curves generated by vaporizing known amounts of liquid water into the evacuable chamber (Atkinson et al. 1986a). The initial ethylene oxide concentrations were approximately $1.4 \times 10^{14} \text{ molecule cm}^{-3}$ (6 ppm). All experiments were carried out in the dark at room temperature ($298 \pm 2 \text{ K}$).

The experimental conditions and observed loss rates of ethylene oxide are given in Table IV-1. Since the driest experiment exhibited the largest loss rate, the data presented in Table IV-1 indicated that there was no observable hydrolysis of ethylene oxide under our experimental conditions (the small losses of ethylene oxide observed are attributed to removal at the chamber walls).

Table IV-1. Experimental Conditions and Results for the Behavior of Ethylene Oxide in the Presence of Water Vapor

EC Run #	Diluent Gas	Relative Humidity (%)	Observed Ethylene Oxide Loss	Loss Rate (min^{-1})
1192	N ₂	<1	1.5% over 4 hrs	$\leq 7 \times 10^{-5}$
1193	N ₂	49	<0.5% over 2 hrs	$< 4 \times 10^{-5}$
1194	Air	49	4% over 29 hrs	$\leq 3 \times 10^{-5}$

These data yield an upper limit loss rate for ethylene oxide at ~50% relative humidity and room temperature of $\leq 3 \times 10^{-5} \text{ min}^{-1}$. Use of this upper limit yields a minimum atmospheric lifetime of ethylene oxide due to hydrolysis of 23 days, with the likelihood of a much longer lifetime due to this removal process.

These data concerning gas-phase hydrolysis and/or deposition of ethylene oxide at the chamber walls are consistent with the washout ratios measured by Terry Dana et al. (1985), which range from 4 at 278 K to 11 at 303 K. Thus, the wet removal of gaseous chemicals arises from equilibrium partitioning between rain and the gas phase, with the washout ratio W

$$W = C_{\text{rain}}/C_{\text{air}} = RT/H$$

defining the scavenging efficiency of gas-phase species, where C_{rain} and C_{air} are the concentrations in rain and air, respectively, R is the gas constant, T is temperature (K) and H is the Henry's law constant at that temperature. Since the washout ratios, W, for highly soluble, and hence readily wet deposited, species such as the phenols and particles are $\sim 10^4$ - 10^6 , it is clear that ethylene oxide is not a species which is readily wet deposited.

B. Vinyl Chloride, 1,1-Dichloroethene, cis- and trans-1,2-Dichloroethene, Trichloroethene and Tetrachloroethene

The chloroethenes are widely used toxic organic chemicals. Vinyl chloride and 1,1-dichloroethene are used as intermediates in the manufacture of polymers, while the other chloroethenes are used as commercial

solvents. Because of their high volatilities these compounds are also emitted in large quantities from waste chemical dumps and landfills. For example, the amounts of tri- and tetrachloroethene released into the atmosphere from all sources in the U. S. are estimated to be $\sim 2.5 \times 10^5$ and 1×10^5 metric tons per year, respectively (Gilbert et al. 1980, Thomas et al. 1981). In the California South Coast Air Basin alone, emissions of vinyl chloride, trichloroethene and tetrachloroethene are reported to be 2, 800 and 1.4×10^4 tons per year, respectively (SCAQMD 1983).

The chloroethenes do not absorb radiation at wavelengths < 300 nm to any significant extent, and they react very slowly with O_3 in the gas phase (Atkinson and Carter 1984). Absolute rate constants have been determined for the reaction of OH radicals with vinyl chloride and tri- and tetrachloroethene (Atkinson 1986), and recently a room temperature rate constant has been measured for 1,1-dichloroethene using a relative rate technique (Edney et al. 1986a). However, this latter measurement may have been complicated by secondary reactions involving Cl atoms, and no data are presently available for cis- and trans-1,2-dichloroethene. Additionally, rate constants for the gas-phase reactions of the chloroethenes with the NO_3 radical have not been determined.

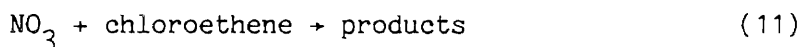
In the present investigation, kinetic data were obtained for the reactions of the OH radical with 1,1-dichloroethene and cis- and trans-1,2-dichloroethene and for the NO_3 radical with the entire series of chloroethenes. For the OH radical reactions, a relative rate technique was used under conditions where any Cl atoms generated in the OH radical reactions were scavenged. In addition, the products formed from the reactions of OH radicals with the entire series of chloroethenes were investigated by long pathlength FT-IR absorption spectroscopy.

1. Kinetics of NO_3 Radical Reactions

Experimental. The relative rate technique described in Section III above was used to determine NO_3 radical reaction rate constants. This technique involved monitoring the relative decay rates of the chloroethenes and ethene, the reference organic, in the presence of NO_3 radicals. Under these conditions,

$$\ln \left\{ \frac{[\text{chloroethene}]_{t_o}}{[\text{chloroethene}]_t} \right\} - D_t = \frac{k_{11}}{k_{12}} \left[\ln \left\{ \frac{[\text{ethene}]_{t_o}}{[\text{ethene}]_t} \right\} - D_t \right] \quad (\text{IX})$$

where $[\text{chloroethene}]_{t_0}$ and $[\text{ethene}]_{t_0}$ are the concentrations of the chloroethene and ethene, respectively, at time t_0 , $[\text{chloroethene}]_t$ and $[\text{ethene}]_t$ are the corresponding concentrations at time t , D_t is the dilution at time t caused by successive additions of N_2O_5 to the reactant mixture (0.0082 per N_2O_5 addition for the experiments carried out in the 2500-liter all-Teflon chamber), and k_{11} and k_{12} are the rate constants for reactions (11) and (12), respectively.



Hence plots of $\{\ln([\text{chloroethene}]_{t_0}/[\text{chloroethene}]_t) - D_t\}$ against $\{\ln([\text{ethene}]_{t_0}/[\text{ethene}]_t) - D_t\}$ should yield straight lines of slope k_{11}/k_{12} and zero intercept.

All rate constant determinations were carried out at 298 ± 2 K and atmospheric pressure (735-740 torr) in either a ~2500-liter all-Teflon chamber, with dry purified air as the diluent gas, or in the 5800-liter Teflon-coated evacuable chamber with synthetic air (80% N_2 + 20% O_2) as the diluent gas. In these experiments, the initial concentrations of the organic reactants and ethene were $(2-30) \times 10^{13}$ molecule cm^{-3} , and one or two injections of N_2O_5 [yielding initial concentrations in the chamber of $(2-4) \times 10^{14}$ molecule cm^{-3} per addition] were made to the chamber during an experiment. Ethane was also added, at concentrations of up to 1.2×10^{15} molecule cm^{-3} , to scavenge any Cl atoms produced from the reactions of the chloroethenes with NO_3 radicals.

Ethene and the chloroethenes were quantitatively monitored during these experiments by gas chromatography with flame ionization detection (GC-FID). Ethene was analyzed using a 5 ft. x 0.125 in. stainless steel (SS) column packed with Porapak N (80/100 mesh), operated at 333 K, while the chloroethenes were analyzed on a 10 ft. x 0.125 in. SS column of 10% Carbowax 600 on C-22 Firebrick, operated at 348 K. Known pressures of N_2O_5 (as measured by an MKS Baratron capacitance manometer) in Pyrex bulbs were flushed into the chambers for 2 min by a 9 liter min^{-1} flow of N_2 , with simultaneous rapid stirring by the chamber fans.

Results. The addition of ethane, in concentrations sufficient to intercept the majority of any Cl atoms produced from the reactions of NO₃ radicals with the chloroethenes, had no effect on the rate constant ratios obtained, within the experimental errors. Typical plots of equation (IX) are shown in Figures IV-1 and IV-2, and the rate constant ratios k_{11}/k_{12} determined from the slopes of such plots by least-squares analyses are given in Table IV-2.

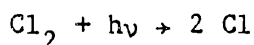
The data obtained are in good accord with equation (IX), although a significant amount of scatter was observed for the experiments involving 1,1-dichloroethene, probably due to the relatively large difference (a factor of ~6) in the amounts of 1,1-dichloroethene and ethene consumed during these experiments. The absence of any observable effects upon the addition of ethane to the reactant mixtures to scavenge any Cl atoms present in the experiments involving the chloroethenes suggests that Cl atoms are not formed in any significant yield from these NO₃ radical reactions since the Cl atom reactions with the chloroethenes and ethene have relative rate constants significantly different from the NO₃ radical reactions (see below).

The rate constant ratios k_{11}/k_{12} given in Table IV-2 can be placed on an absolute basis using a rate constant at 298 K of $k_{12}(\text{ethene}) = (2.3 \pm 0.4) \times 10^{-16} \text{ cm}^3 \text{ molecule}^{-1} \text{ s}^{-1}$, derived from the absolute rate constant for trans-2-butene (Ravishankara and Mauldin 1985) and our very recent relative rate data (Atkinson et al. 1987). The rate constants k_{11} so obtained are also given in Table IV-2.

2. Kinetics of Cl Atom Reactions

Experimental. The relative rate technique employed has been described previously (Atkinson and Aschmann 1985), and was based upon monitoring the relative disappearance rates of the chloroethenes and ethene, whose Cl atom reaction rate constant is reliably known.

Cl atoms were generated by the photolysis of Cl₂ in air at wavelengths $\geq 290 \text{ nm}$



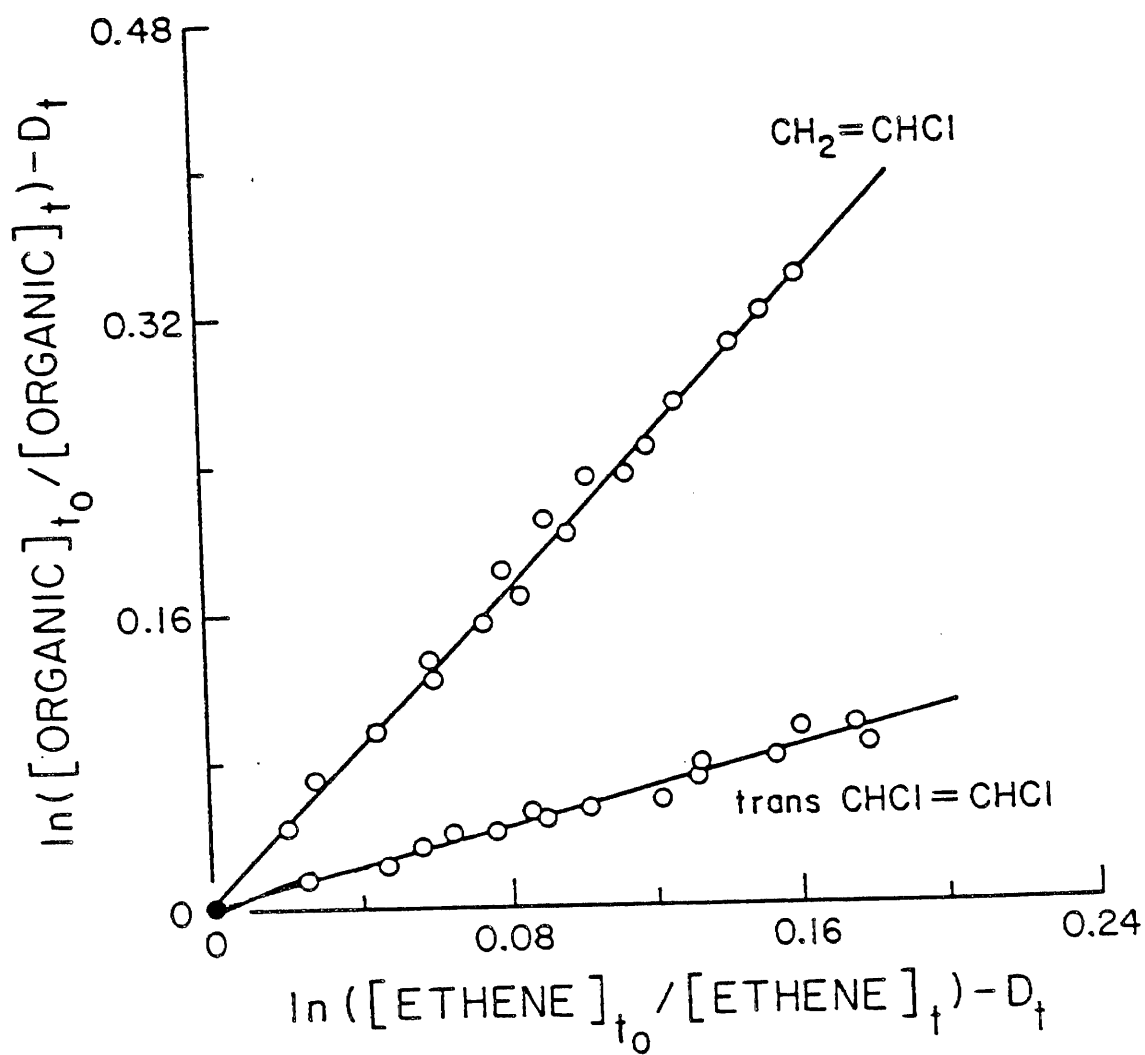


Figure IV-1. Plots of equation (IX) for the reaction of NO_3 radicals with vinyl chloride and trans-1,2-dichloroethene, with ethene as the reference organic.

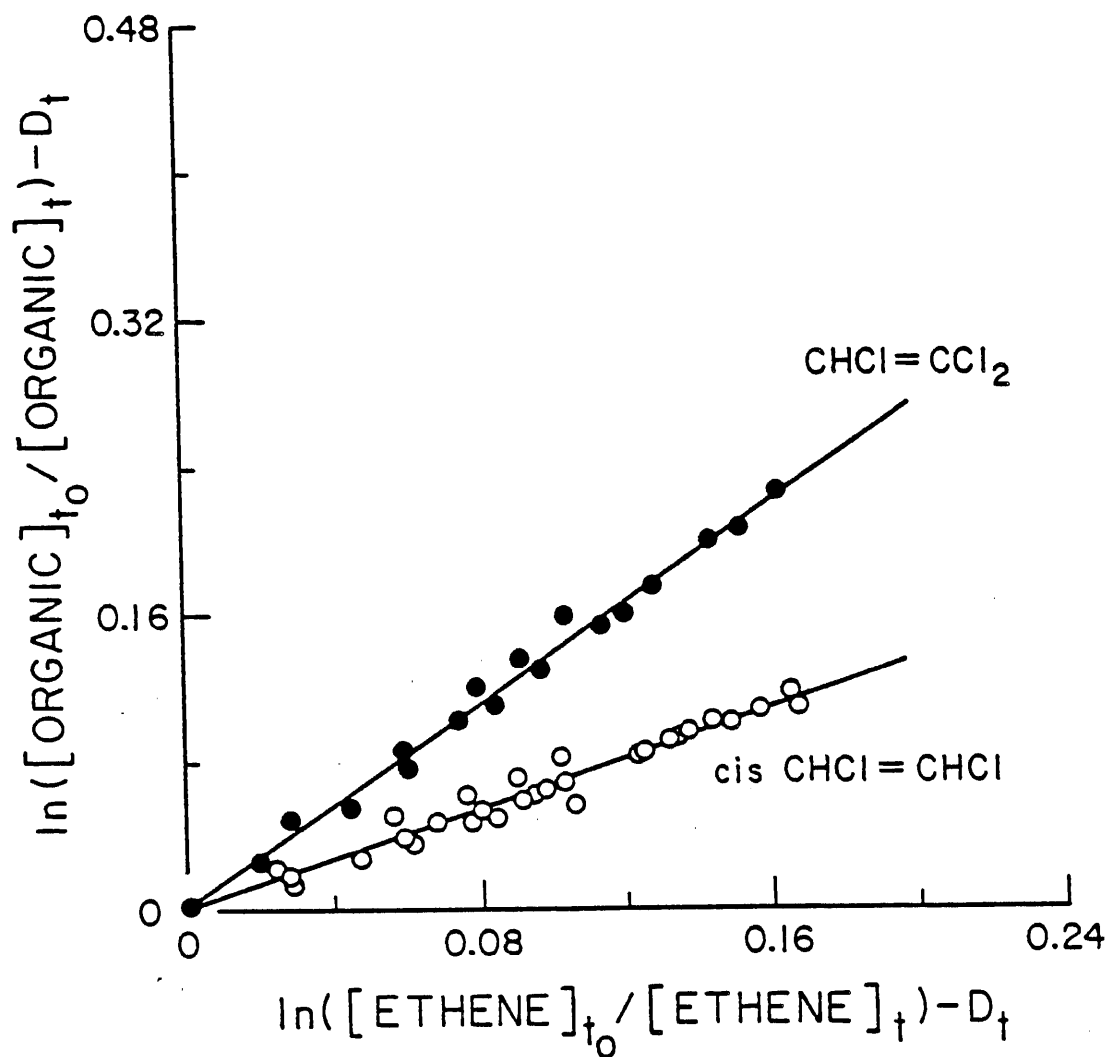


Figure IV-2. Plots of equation (IX) for reactions of NO_3 radicals with trichloroethene and cis-1,2-dichloroethene, with ethene as the reference organic.

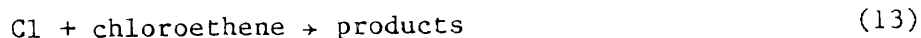
Table IV-2. Rate Constant Ratios k_{11}/k_{12} and Rate Constants k_{11} for the Gas-Phase Reactions of the NO_3 Radical with the Chloroethenes at 298 ± 2 K

Organic	k_{11}/k_{12}^a	$10^{16} \times k_{11}^{a,b}$ ($\text{cm}^3 \text{ molecule}^{-1} \text{ s}^{-1}$)
Vinyl Chloride	2.08 ± 0.09	4.8 ± 0.9
1,1-Dichloroethene	6.0 ± 0.7	14 ± 3
<u>cis</u> -1,2-Dichloroethene	0.68 ± 0.06	1.6 ± 0.4
<u>trans</u> -1,2-Dichloroethene	0.52 ± 0.05	1.2 ± 0.3
Trichloroethene	1.37 ± 0.08	3.2 ± 0.6
Tetrachloroethene	<0.25	<0.7

^aIndicated error limits are two least-squares standard deviations.

^bPlaced on an absolute basis by using a rate constant of $k_{12}(\text{ethene}) = (2.3 \pm 0.4) \times 10^{-16} \text{ cm}^3 \text{ molecule}^{-1} \text{ s}^{-1}$ (Ravishankara and Mauldin 1985, Atkinson et al. 1987).

and the reactions removing the organics were



Under the experimental conditions employed, then

$$\ln \left\{ \frac{[\text{chloroethene}]_{t_0}}{[\text{chloroethene}]_t} \right\} = \frac{k_{13}}{k_{14}} \ln \left\{ \frac{[\text{ethene}]_{t_0}}{[\text{ethene}]_t} \right\} \quad (\text{X})$$

where $[\text{chloroethene}]_{t_0}$ and $[\text{ethene}]_{t_0}$ are the concentrations of the chloroethene and ethene, respectively, at time t_0 , $[\text{chloroethene}]_t$ and $[\text{ethene}]_t$ are the corresponding concentrations at time t , and k_{13} and k_{14} are the rate constants for reactions (13) and (14), respectively. Hence plots of $\ln([\text{chloroethene}]_{t_0}/[\text{chloroethene}]_t)$ against $\ln([\text{ethene}]_{t_0}/[\text{ethene}]_t)$ should yield straight lines of slope k_{13}/k_{14} and zero intercept.

Irradiations were carried out in a ~60 liter cylindrical all-Teflon reaction bag surrounded by 24 GE F15T8-BL 15 watt blacklights. In this work eight of these blacklights were used, corresponding to a photolytic half-life of Cl_2 of ~20 mins. Prior to irradiation, the reaction bag/lamp assembly was kept in the dark to avoid any photolysis of the reactants. The approximate initial concentrations of the reactant mixtures were: Cl_2 , 7×10^{13} molecule cm^{-3} ; and the chloroethenes, ethane and ethene, 2.4×10^{13} molecule cm^{-3} each. Ultrazero air (Liquid Carbonic, <1 ppm hydrocarbons) was used as the diluent gas.

The organics were quantitatively analyzed during the experiments by gas chromatography with flame ionization detection. Ethane and ethene were analyzed using a 5 ft. x 0.125 in. stainless steel (SS) column with Porapak N (80/100 mesh), operated at 333 K; vinyl chloride using a 20 ft. x 0.125 in. SS column of 5% DC703/C20M on 100/120 mesh AW, DMCS Chromosorb G, operated at 333 K; and the di-, tri- and tetrachloroethenes using a 10 ft. x 0.125 in. SS column with 10% Carbowax C600 on C-22 Firebrick, operated at 348 K.

All rate constant determinations were carried out at 298 ± 2 K and atmospheric pressure (~735 torr).

Results. In order to avoid interferences in the gas chromatographic analyses, five sets of organics (ethene and tetrachloroethene; ethene, 1,1-dichloroethene and trichloroethene; ethene, ethane and vinyl chloride; ethene and cis-1,2-dichloroethene; and ethene and trans-1,2-dichloroethene) were employed. For each set of organics, two separate irradiations were carried out, with differing irradiation times (6-16 min) in order to vary the extent of reaction. The data obtained from these irradiations are plotted in accordance with equation (X) in Figures IV-3 and IV-4, and the rate constant ratios obtained from the slopes of these plots by least-squares analyses are given in Table IV-3. In all cases the least-squares intercepts of these plots were within two standard deviations of zero. The rate constant ratio of $k_{13}(\text{ethane})/k_{14} = 0.582 \pm 0.007$ determined in this study is in excellent agreement with that of 0.601 ± 0.022 derived from our previous measurements of the rate constant ratios $k(\text{ethane})/k(\text{n-butane})$ and $k(\text{ethene})/k(\text{n-butane})$ (Atkinson and Aschmann 1985).

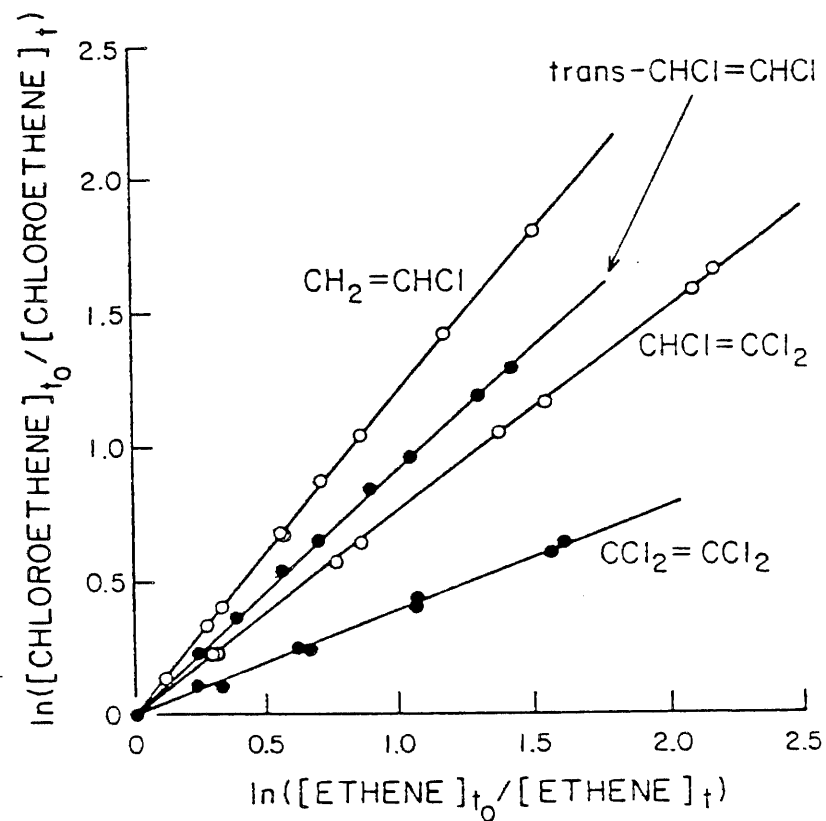


Figure IV-3. Plots of equation (X) for the reaction of Cl atoms with vinyl chloride, trans-1,2-dichloroethene, trichloroethene and tetrachloroethene, with ethene as the reference organic.

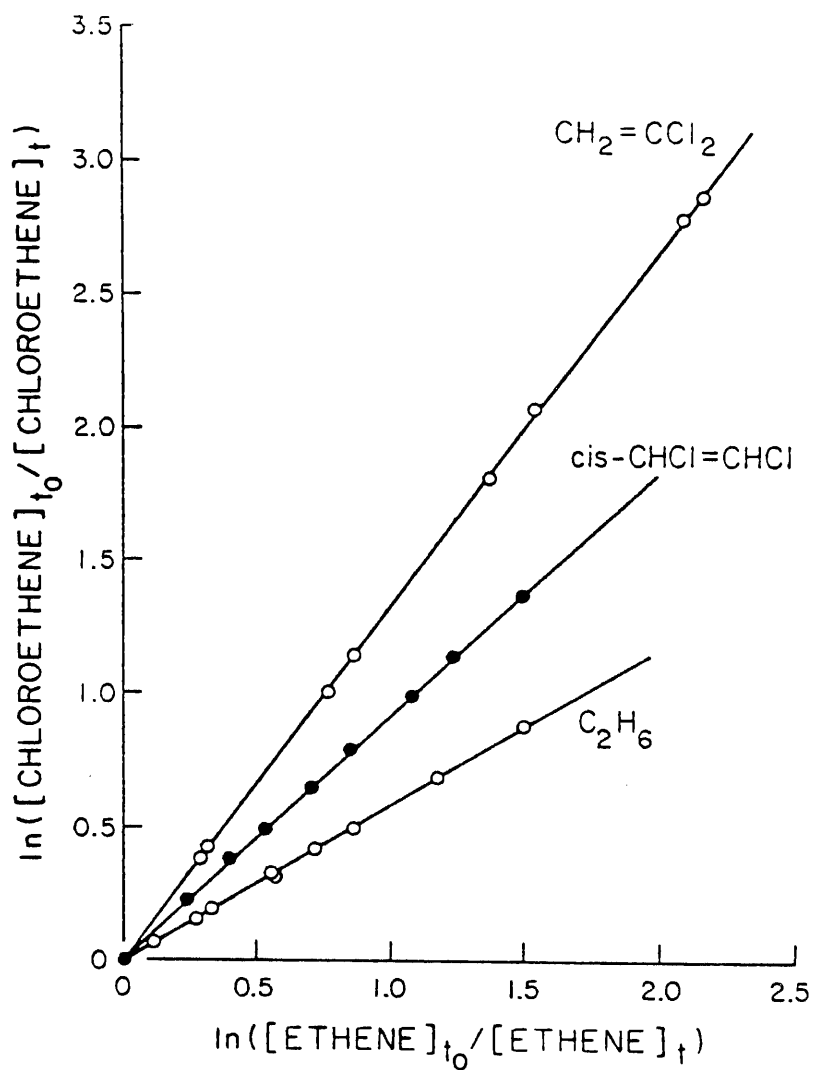


Figure IV-4. Plots of equation (X) for the reaction of Cl atoms with 1,1-dichloroethene, cis-1,2-dichloroethene and ethane, with ethene as the reference organic.

Table IV-3. Rate Constant Ratios k_{13}/k_{14} and Rate Constants k_{13} for the Gas-Phase Reactions of Cl Atoms with Ethane and the Chloroethenes at 298 ± 2 K and ~ 735 Torr Total Pressure of Air

Organic	k_{13}/k_{14}^a	$10^{11} \times k_{13}$ ($\text{cm}^3 \text{ molecule}^{-1} \text{ s}^{-1}$) ^{a,b}
$\text{CH}_2=\text{CHCl}$	1.20 ± 0.01	12.7 ± 0.2
$\text{CH}_2=\text{CCl}_2$	1.32 ± 0.01	14.0 ± 0.2
<u>cis</u> - $\text{CHCl}=\text{CHCl}$	0.910 ± 0.009	9.65 ± 0.10
<u>trans</u> - $\text{CHCl}=\text{CHCl}$	0.904 ± 0.016	9.58 ± 0.18
$\text{CHCl}=\text{CCl}_2$	0.762 ± 0.009	8.08 ± 0.10
$\text{CCl}_2=\text{CCl}_2$	0.390 ± 0.021	4.13 ± 0.23
C_2H_6	0.582 ± 0.007	6.17 ± 0.08

^aIndicated error limits are two least-squares standard deviations.

^bPlaced on an absolute basis by use of a rate constant for the reaction of Cl atoms with ethene of $k_{14} = (1.06 \pm 0.03) \times 10^{-10} \text{ cm}^3 \text{ molecule}^{-1} \text{ s}^{-1}$, at room temperature and atmospheric pressure (Atkinson and Aschmann 1985) which in turn is based on a room temperature rate constant for the reaction of Cl atoms with n-butane of $1.97 \times 10^{-10} \text{ cm}^3 \text{ molecule}^{-1} \text{ s}^{-1}$.

For the irradiations involving cis-1,2-dichloroethene, the formation of trans-1,2-dichloroethene was observed, and similarly cis-1,2-dichloroethene was formed from the Cl atom reaction with trans-1,2-dichloroethene. The formation yields of these geometric isomers during these reactions were determined using the kinetic data given in Table IV-3 to account for the reactions of these products with Cl atoms [as described previously (Atkinson et al. 1982c)]. Plots of the amounts of the geometric isomer formed, corrected for reaction with Cl atoms, against the amounts of cis- or trans-1,2-dichloroethene consumed during these Cl_2 -1,2-dichloroethene-air irradiations are shown in Figure IV-5. The geometric isomer product yields determined from least-squares analyses of these data were

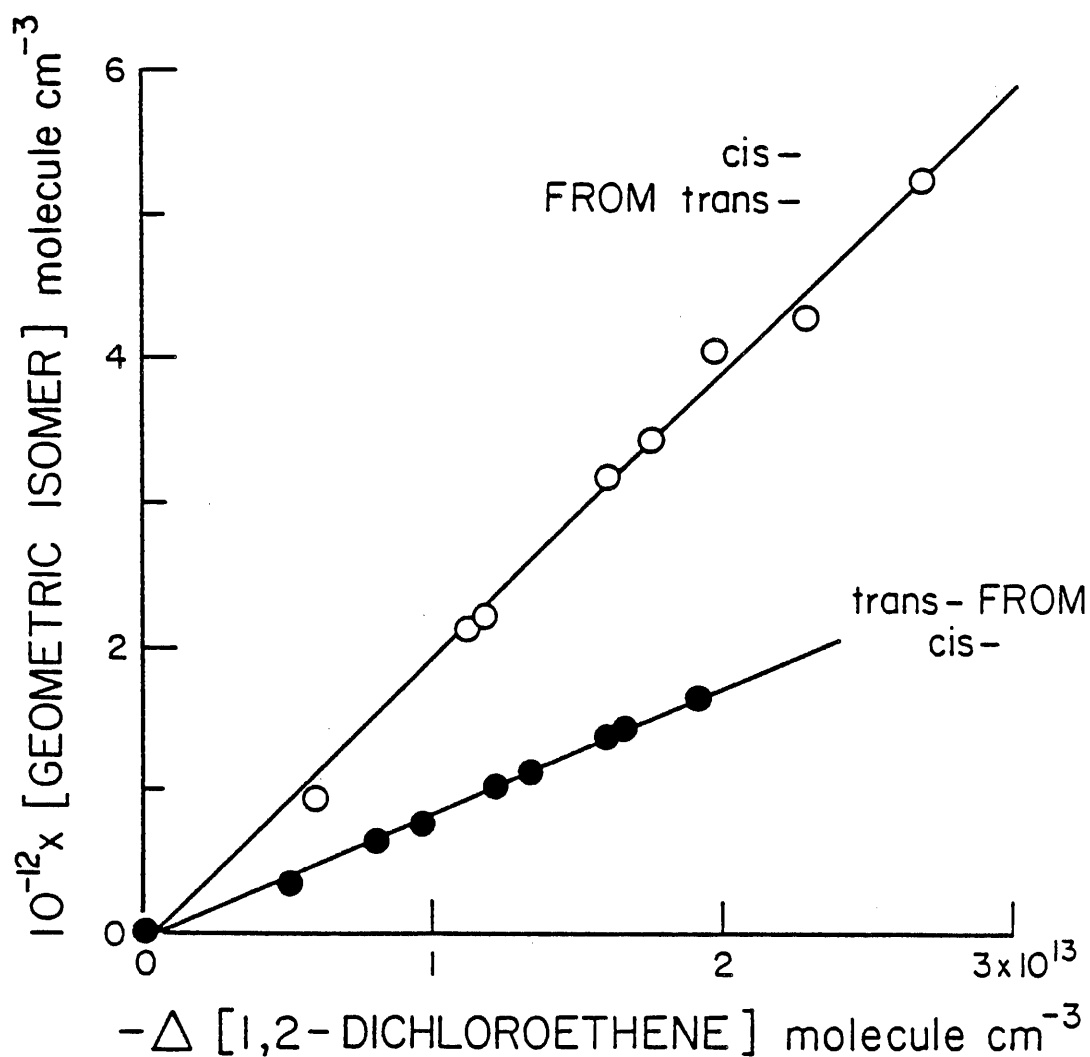


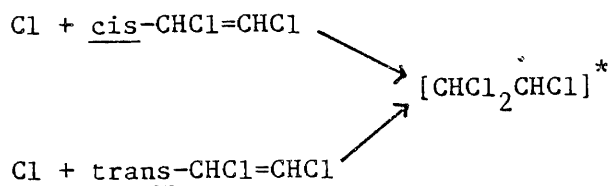
Figure IV-5. Plots of the amounts of cis- and trans-1,2-dichloroethene formed (corrected for secondary reactions with Cl atoms; see text) against the amounts of trans- or cis-1,2-dichloroethene, respectively, consumed in Cl_2 -1,2-dichloroethene-air irradiations.

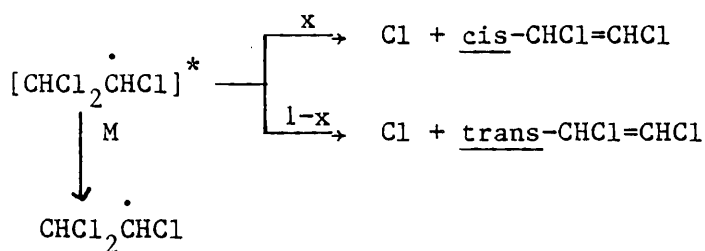
0.199 \pm 0.011 for formation of cis-1,2-dichloroethene from trans-1,2-dichloroethene, and 0.087 \pm 0.003 for formation of trans-1,2-dichloroethene from cis-1,2-dichloroethene, where the indicated error limits are the two least-squares standard deviations of the slopes of the plots shown in Figure IV-5.

The measured rate constant ratios k_{13}/k_{14} can be placed on an absolute basis using a rate constant for the reaction of Cl atoms with ethene at room temperature and ~735 torr total pressure of air of $k_{14} = (1.06 \pm 0.03) \times 10^{-10} \text{ cm}^3 \text{ molecule}^{-1} \text{ s}^{-1}$ (Atkinson and Aschmann 1985). This rate constant k_{14} was determined relative to that for the reaction of Cl atoms with n-butane of $1.97 \times 10^{-10} \text{ cm}^3 \text{ molecule}^{-1} \text{ s}^{-1}$, which was obtained from a least-squares fit of our relative rate data for ethane, propane, n-butane and 2-methylpropane (Atkinson and Aschmann 1985) to the literature room temperature absolute rate constants (Davis et al. 1970, Manning and Kurylo 1977, Ray et al. 1980, Lewis et al. 1980). The rate constants k_{13} so derived are also given in Table IV-3.

At room temperature and atmospheric pressure of air the Cl atom reactions with the chloroethenes are in the fall-off regime between second- and third-order kinetics. Thus, the rate constants k_{13} given in Table IV-3 for the chloroethenes are applicable only to the temperature and pressure (and third-body) conditions under which they were measured.

While the reactions of Cl atoms with the chloroethenes are fairly close to the limiting high pressure limits at 735 torr total pressure of air, the observed formation of cis-1,2-dichloroethene from trans-1,2-dichloroethene, and vice-versa for the cis-isomer, shows that for the 1,2-dichloroethenes the Cl atom reactions are not at the high-pressure limit at atmospheric pressure. Furthermore, the fraction, x, of cis-1,2-dichloroethene formed from the energy-rich $\text{CHCl}_2\dot{\text{CHCl}}$ radical



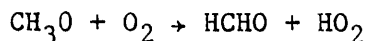
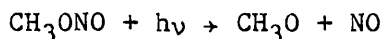


of 0.70 ± 0.05 [assuming, consistent with previous experimental data (Knox and Riddick 1966) that the $[\text{CHCl}_2\dot{\text{CHCl}}]$ radicals formed from cis and trans-1,2-dichloroethene decompose with virtually identical ratios of $x/(1-x)$] is in good agreement with the previous values of 0.78 (Knox and Riddick 1966) and ~ 0.60 -0.65 (Ayscough et al. 1966).

These kinetic data for the Cl atom reactions aid in the elucidation of the kinetics and products of the corresponding OH radical reactions.

3. Kinetics of the OH Radical Reactions with the Dichloroethenes

Experimental. The experimental techniques used were similar to those described in Section III above. Rate constants were determined using the relative rate technique in which the decay rates of the dichloroethenes were monitored relative to that of dimethyl ether, in the presence of OH radicals. Hydroxyl radicals were generated by the photolysis of methyl nitrite in air at wavelengths ≥ 300 nm.

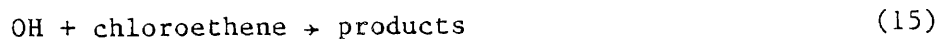


To minimize the formation of ozone during these irradiations, NO was also included in the reaction mixtures. In order to investigate the effect of Cl atoms which might have been produced during the reactions of the OH radical with the chloroethenes, separate irradiation experiments were conducted in which ethane was added to the reactant mixtures in concentrations sufficient to scavenge any Cl atoms generated. The initial reactant concentrations (in molecule cm^{-3} units) were: CH_3ONO , 2.4×10^{14} ; NO, $(1.2\text{-}2.4) \times 10^{14}$; the chloroethenes and CH_3OCH_3 , $(7\text{-}25) \times 10^{13}$ each; and ethane (when added), $(7\text{-}15) \times 10^{14}$.

Providing that reaction with the OH radical was the sole loss process for CH_3OCH_3 and the chloroethenes, then:

$$\ln \left\{ \frac{[\text{chloroethene}]_{t_0}}{[\text{chloroethene}]_t} \right\} = \frac{k_{15}}{k_{16}} \ln \left\{ \frac{[\text{CH}_3\text{OCH}_3]_{t_0}}{[\text{CH}_3\text{OCH}_3]_t} \right\} \quad (\text{XI})$$

where $[\text{chloroethene}]_{t_0}$ and $[\text{CH}_3\text{OCH}_3]_{t_0}$ are the concentrations of the chloroethene and CH_3OCH_3 , respectively, at time t_0 , $[\text{chloroethene}]_t$ and $[\text{CH}_3\text{OCH}_3]_t$ are the corresponding concentrations at time t , and k_{15} and k_{16} are the rate constants for reactions (15) and (16), respectively.



Hence, plots of $\ln([\text{chloroethene}]_{t_0}/[\text{chloroethene}]_t)$ against $\ln([\text{CH}_3\text{OCH}_3]_{t_0}/[\text{CH}_3\text{OCH}_3]_t)$ should yield straight lines with slopes of k_{15}/k_{16} and zero intercepts.

Results. The disappearance rates of CH_3OCH_3 , 1,1-dichloroethene, cis-1,2-dichloroethene, and trans-1,2-dichloroethene were monitored by FT-IR absorption spectroscopy during the irradiation of $\text{CH}_3\text{ONO-NO-chloroethene-CH}_3\text{OCH}_3$ -air and $\text{CH}_3\text{ONO-NO-chloroethene-CH}_3\text{OCH}_3$ -ethane-air mixtures, with reaction times of ~30-60 minutes. The data obtained are plotted in accordance with equation (XI) in Figures IV-6 through IV-8, and it can be seen from these figures that the experimental data obtained in both the presence and absence of ethane yielded good straight lines. The slopes of these plots determined by least-squares analyses of the data are given in Table IV-4.

Our kinetic data for the reactions of the Cl atom with the chloroethenes and ethane (see above), together with literature data for the rate constant of Cl atom reaction with CH_3OCH_3 (Michael et al. 1979), show that at room temperature and 740 torr total pressure of air the Cl atom reaction rate constants for the chloroethenes, ethane and dimethyl ether are all in the range $(4-18) \times 10^{-11} \text{ cm}^3 \text{ molecule}^{-1} \text{ s}^{-1}$. Consequently, both ethane and, especially, CH_3OCH_3 are good scavengers of Cl atoms in

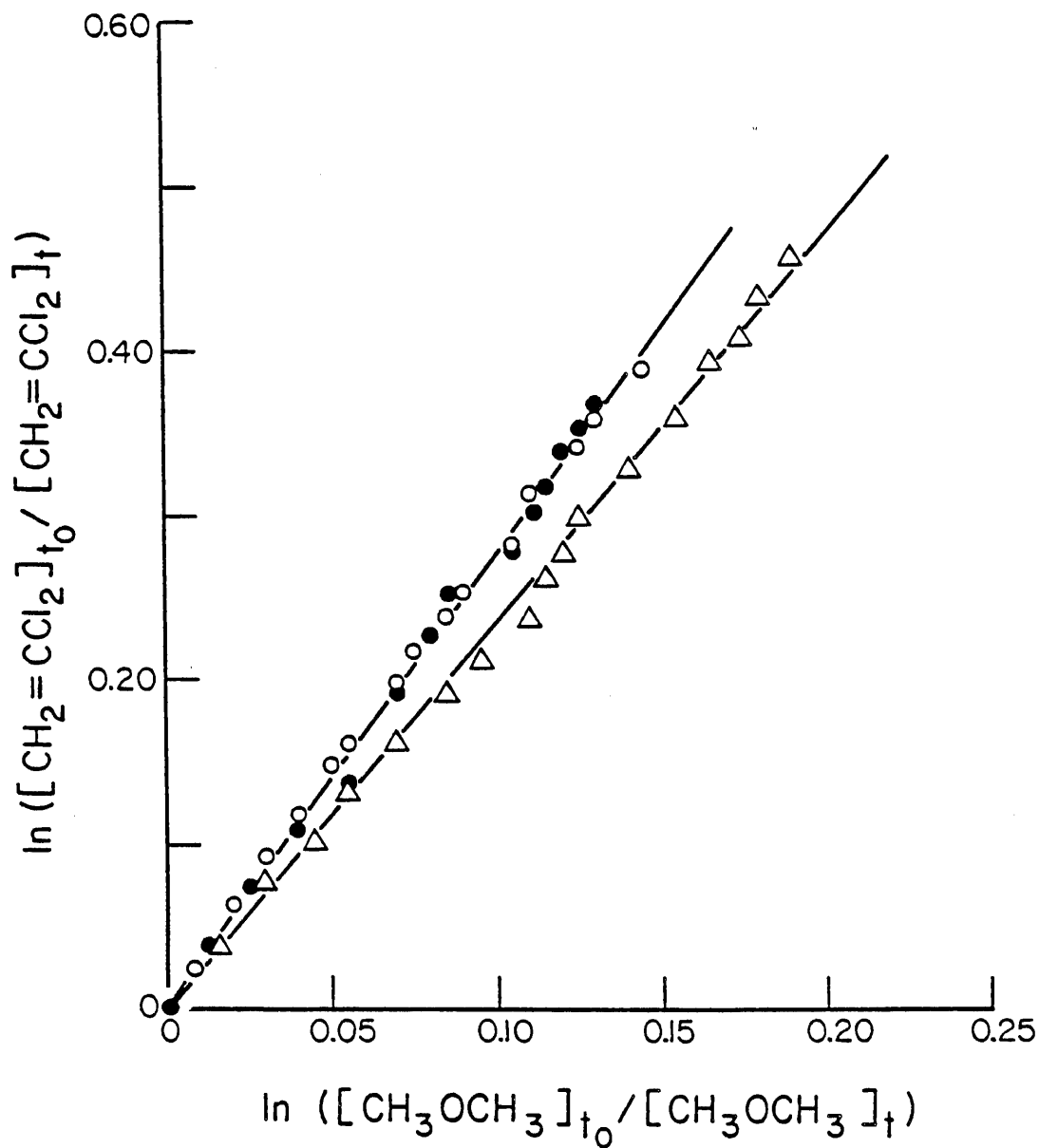


Figure IV-6. Plots of equation (XI) for 1,1-dichloroethene in the absence of ethane (Δ) and in the presence of 7×10^{14} molecule cm^{-3} (\circ) and 1.5×10^{15} molecule cm^{-3} (\bullet) of ethane.

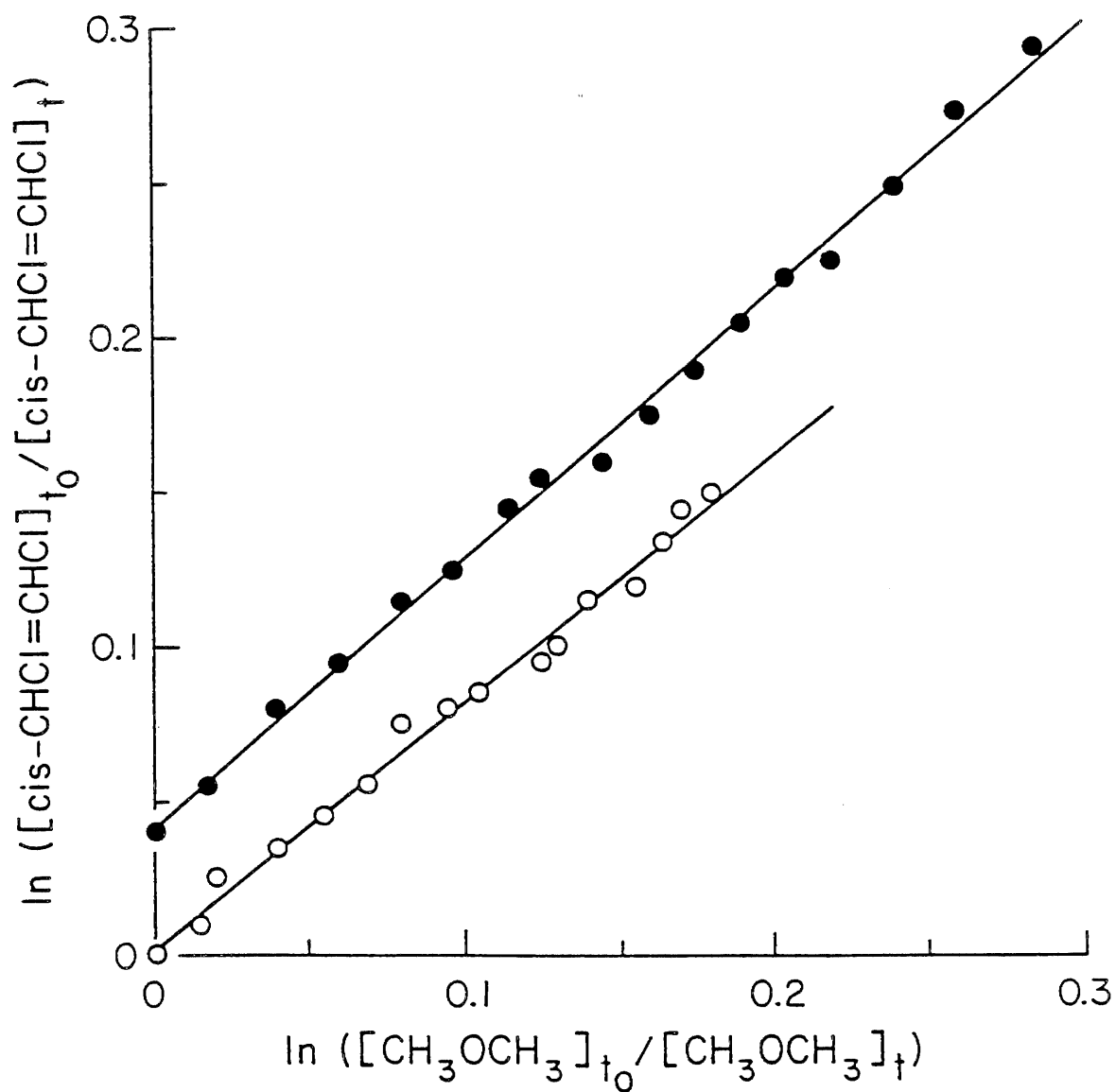


Figure IV-7. Plots of equation (XI) for cis-1,2-dichloroethene in the absence of ethane (●, displaced vertically by 0.04 units for clarity) and in the presence of 7×10^{14} molecule cm^{-3} of ethane (○).

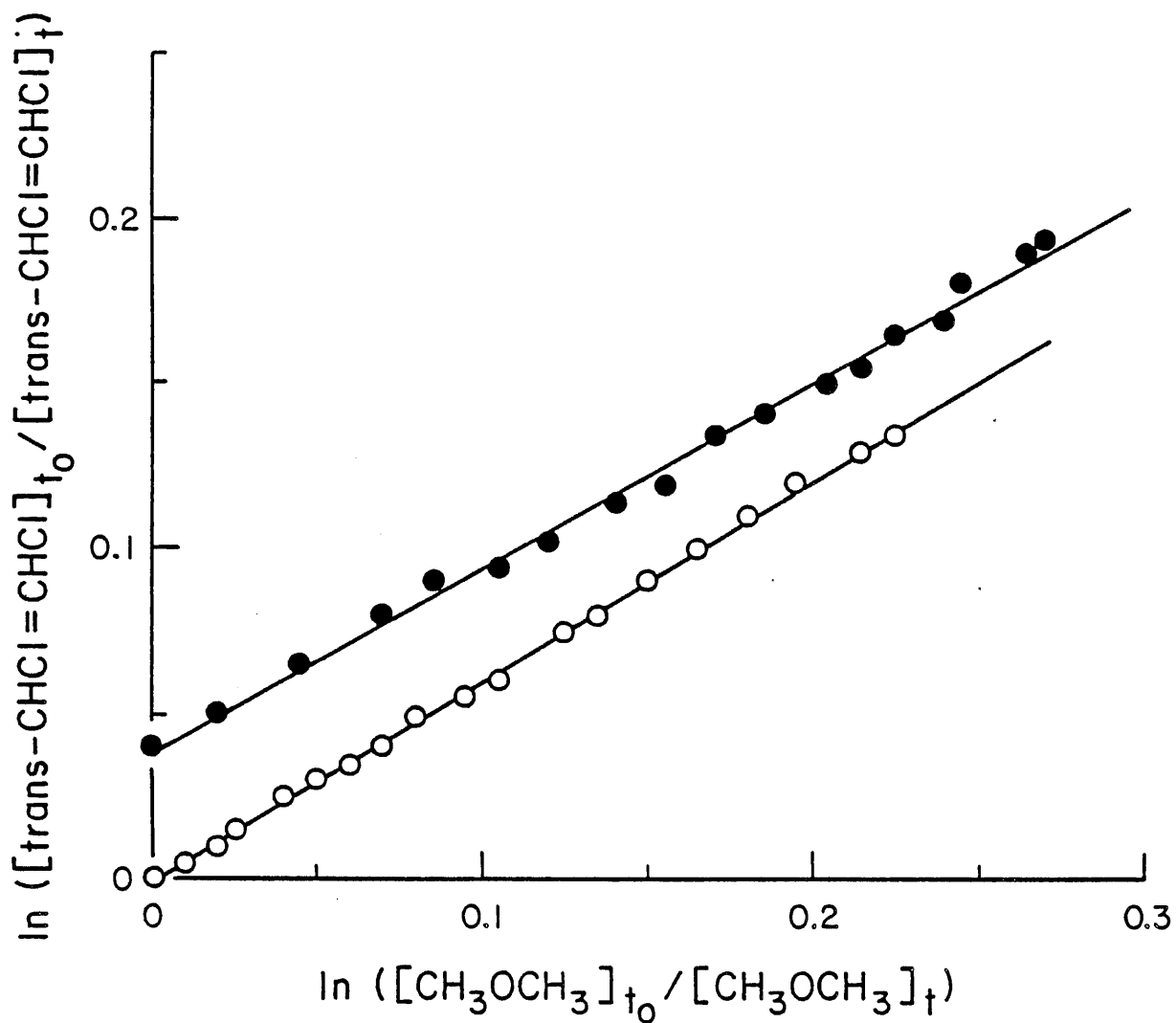


Figure IV-8. Plots of equation (XI) for trans-1,2-dichloroethene in the absence of ethane (●, displaced vertically by 0.04 units for clarity) and presence of 7×10^{14} molecule cm^{-3} of ethane (○).

Table IV-4. Slopes of the Plots of Equation (XI) Obtained at 298 ± 2 K and Atmospheric Pressure from Irradiated $\text{CH}_3\text{ONO-NO-Chloroethene-CH}_3\text{OCH}_3$ -Air Mixtures in the Absence and Presence of C_2H_6

Chloroethene	Slope ^a		$10^{12} \times k_{15}$ ($\text{cm}^3 \text{ molecule}^{-1} \text{ s}^{-1}$) ^{a,b}
	without C_2H_6	with C_2H_6 ($=k_{15}/k_{16}$)	
$\text{CH}_2=\text{CCl}_2$	2.37 ± 0.07	2.72 ± 0.08^c	8.11 ± 0.24
<u>cis</u> - $\text{CHCl}=\text{CHCl}$	0.872 ± 0.028	0.799 ± 0.045	2.38 ± 0.14
<u>trans</u> - $\text{CHCl}=\text{CHCl}$	0.559 ± 0.020	0.605 ± 0.010	1.80 ± 0.03

^aError limits are two least-squares standard deviations.

^bDerived from the rate constant ratios k_{15}/k_{16} obtained in the presence of $\geq 7 \times 10^{14} \text{ molecule cm}^{-3}$ of C_2H_6 by use of a rate constant for the reaction of OH radicals with CH_3OCH_3 of $k_{16} = 2.98 \times 10^{-12} \text{ cm}^3 \text{ molecule}^{-1} \text{ s}^{-1}$ (Atkinson 1986).

^cCombined value from irradiations with 7×10^{14} and $1.5 \times 10^{15} \text{ molecule cm}^{-3}$ of added C_2H_6 ; individual rate constant ratios of 2.69 ± 0.08 and 2.80 ± 0.12 , respectively, being determined.

these reaction mixtures. While, in absolute terms, the data presented in Table IV-4 show that the slopes of the plots of equation (XI) measured in the presence and absence of ethane are surprisingly similar (being within $\sim \pm 15\%$, with the largest effect being observed for 1,1-dichloroethene), the precision of the experimental data, and the product distributions obtained (see below), show unequivocally that in the absence of ethane other reaction processes occur, leading to secondary consumption of the chloroethenes and CH_3OCH_3 .

The slopes of the plots of equation (XI), obtained in the presence of sufficient ethane to suppress secondary reactions of Cl atoms, then allow the rate constant ratios k_{15}/k_{16} to be determined for the elementary reactions of the OH radical with the chloroethenes (Table IV-4). From these values of k_{15}/k_{16} , the rate constants k_{15} given in Table IV-4 were obtained using a rate constant for the reaction of the OH radical with CH_3OCH_3 of $k_{16} = 2.98 \times 10^{-12} \text{ cm}^3 \text{ molecule}^{-1} \text{ s}^{-1}$ at 298 K (Atkinson 1986).

Based upon the literature data for vinyl chloride, trichloroethene and tetrachloroethene (Atkinson 1986), the OH radical reactions with 1,1-dichloroethene and cis and trans-1,2-dichloroethene will be at the high pressure second-order limit at 740 torr total pressure of air. As noted above, there have been no previous reports of rate constants for the reactions of OH radicals with cis- and trans-1,2-dichloroethene. The present rate constant for the reaction of OH radicals with 1,1-dichloroethene of $(8.11 \pm 0.24) \times 10^{-12} \text{ cm}^3 \text{ molecule}^{-1} \text{ s}^{-1}$ at $298 \pm 2 \text{ K}$ is a factor of ~2 lower than that of $(1.49 \pm 0.21) \times 10^{-11} \text{ cm}^3 \text{ molecule}^{-1} \text{ s}^{-1}$ reported by Edney et al. (1986a). Edney et al. (1986a) attempted to circumvent problems associated with secondary reactions of the Cl atoms produced in the OH radical reactions of 1,1-dichloroethene and trichloroethene by working at sufficiently high reference organic/chloroethene concentration ratios that the Cl atoms were expected to react almost totally with the reference organic. However, it is possible that the method used by Edney et al. (1986a) did not allow complications from Cl atom reactions to be completely avoided and hence relative rate constants for the OH radical reactions to be correctly determined.

The kinetic data determined here for the reactions of the chloroethenes with NO_3 and OH radicals, together with the literature data for the O_3 reaction rate constants (Atkinson and Carter 1984), allow the atmospheric lifetimes and dominant atmospheric removal pathways to be assessed. Using ambient atmospheric concentrations appropriate to the cleaner, nonurban, areas of the troposphere of O_3 of $7 \times 10^{11} \text{ molecule cm}^{-3}$ (30 ppb) (Singh et al. 1978, Oltmanns 1981) throughout a 24-hr period, of OH radicals of $1 \times 10^6 \text{ molecule cm}^{-3}$ during a 12-hr daytime period (Crutzen 1982), and of NO_3 radicals of $2.4 \times 10^8 \text{ molecule cm}^{-3}$ (10 parts-per-trillion) during a 12-hr nighttime period (Platt et al. 1984, Atkinson et al. 1986b), the atmospheric lifetimes of the chloroethenes due to these three reaction routes can be calculated. Table IV-5 gives the room temperature rate constants for the NO_3 radical, OH radical and O_3 reactions, and the calculated atmospheric lifetimes due to each of these removal routes. This table shows that in the absence of high nighttime levels of NO_3 (i.e., NO_3 radical concentrations $\leq 10^9 \text{ molecule cm}^{-3}$), the dominant atmospheric removal process for all of the chloroethenes is by reaction with the OH radical. The calculated lifetimes range from

Table IV-5. Room Temperature Rate Constants for the Gas-Phase Reactions of NO₃ and OH Radicals and O₃ with the Chloroethenes, and the Calculated Atmospheric Lifetimes Due to These Reactions

Organic	Rate Constant (cm ³ molecule ⁻¹ s ⁻¹)			Atmospheric Lifetime Due to Reaction with ^a		
	NO ₃	OH	O ₃ ^b	NO ₃	OH	O ₃
Vinyl Chloride	4.8 x 10 ⁻¹⁶	6.6 x 10 ^{-12^c}	2.5 x 10 ⁻¹⁹	200 day	3.5 day	66 day
1,1-Dichloroethene	1.4 x 10 ⁻¹⁵	8.1 x 10 ⁻¹²	3.7 x 10 ⁻²¹	69 day	2.9 day	12 yr
<u>cis</u> -1,2-Dichloroethene	1.6 x 10 ⁻¹⁶	2.4 x 10 ⁻¹²	<5 x 10 ⁻²¹	1.7 yr	9.6 day	>9 yr
<u>trans</u> -1,2-Dichloroethene	1.2 x 10 ⁻¹⁶	1.8 x 10 ⁻¹²	1.5 x 10 ⁻¹⁹	2.2 yr	13 day	110 day
Trichloroethene	3.2 x 10 ⁻¹⁶	2.4 x 10 ^{-12^c}	<3 x 10 ⁻²⁰	300 day	9.6 day	>1.5 yr
Tetrachloroethene	<7 x 10 ⁻¹⁷	1.7 x 10 ^{-13^c}	<2 x 10 ⁻²³	3.8 yr	140 day	>2 x 10 ³ yr

^aFor concentrations of: O₃, 24-hr average of 7 x 10¹¹ molecule gm⁻³; OH, 12-hr daytime average of 1 x 10⁶ molecule cm⁻³; NO₃, 12-hr nighttime average of 2.4 x 10⁶ molecule cm⁻³.

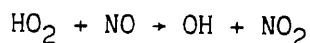
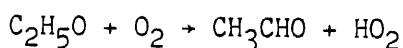
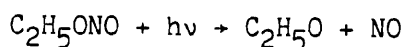
^bFrom Atkinson and Carter (1984).

^cFrom Atkinson (1986).

~3 days for vinyl chloride and 1,1-dichloroethene to ~6 months for tetrachloroethene.

4. Product Studies of the OH Radical Reactions

Experimental. For all of the chloroethenes, i.e., vinyl chloride, 1,1-dichloroethene, cis- and trans-1,2-dichloroethene, trichloroethene and tetrachloroethene, irradiations of CH₃ONO-NO-chloroethene-air mixtures, with and without ethane as an added Cl atom scavenger, were carried out for product analyses. In the case of cis- and trans-1,2-dichloroethene and 1,1-dichloroethene, product data were also obtained from the CH₃ONO-NO-dichloroethene-CH₃OCH₃-air and CH₃ONO-NO-dichloroethene-CH₃OCH₃-ethane-air irradiations which were used to obtain kinetic data. Since HCHO was an expected product from the OH radical reactions with vinyl chloride and 1,1-dichloroethene, and is formed from the photooxidation of CH₃ONO, ethyl nitrite was used as a source of OH radicals for the reactions with these two chloroethenes:



The kinetic and product studies were conducted in the 5800-liter evacuable Teflon-coated environmental chamber, using FT-IR absorption spectroscopy to monitor the reactants and products.

Results. The major products identified were formaldehyde (HCHO) and formyl chloride (HC(O)Cl) from vinyl chloride; HC(O)Cl from cis- and trans-1,2-dichloroethene; HCHO, phosgene (COCl₂) and chloroacetyl chloride (CH₂ClC(O)Cl) from 1,1-dichloroethene; HC(O)Cl, COCl₂ and dichloroacetyl chloride (CHCl₂C(O)Cl) from trichloroethene; and COCl₂ and trichloroacetyl chloride (CCl₃C(O)Cl) from tetrachloroethene. The calibrations for COCl₂ and the chloroacetyl chlorides were made by recording spectra of authentic samples. Reference calibration spectra of HC(O)Cl were obtained from the reaction of O₃ with excess trans-1,2-dichloroethene, based on a 1:1 stoichiometric yield of HC(O)Cl during the early stages of the reaction (Tuazon et al. 1984).

Infrared spectra of the products formed in the reaction mixtures with no added Cl atom scavengers are shown in Figures IV-9, IV-10 and IV-11 for 1,1-dichloroethene, trichloroethene and tetrachloroethene, respectively. In the case of 1,1-dichloroethene, absorption bands at $\sim 965\text{ cm}^{-1}$ and $\sim 1802\text{ cm}^{-1}$ (the latter not shown in Figure IV-9) were observed, distinct from the absorptions of chloroacetyl chloride but clearly associated with the -C(=O)Cl moiety (Pouchert 1975). The observed linear increase in the intensity of these bands with the amount of 1,1-dichloroethene consumed suggests that this product, which increased in yield by $\sim 50\%$ in the presence of ethane and ethane plus CH_3OCH_3 , has a rate constant of $\lesssim 1 \times 10^{-11}\text{ cm}^3\text{ molecule}^{-1}\text{ s}^{-1}$ for reaction with the OH radical. The increase in yield in the presence of a Cl atom scavenger shows that this product is formed from the OH radical reaction with 1,1-dichloroethene. Similarly, a product absorption band at 1139 cm^{-1} was observed in the irradiations involving trichloroethene (Figure IV-10). In this case, the relative product yield decreased with the extent of reaction, and increased markedly, by a factor of ~ 5 , in the presence of ethane. Again, this unidentified product must be formed from the OH radical reaction.

Since the products formed in these irradiations could react with OH radicals, it was necessary to take this loss process into account in order to determine the product yields, as we have described in detail previously (Atkinson et al. 1982c). While the OH radical reaction rate constant for HCHO is reliably known (Atkinson 1986), experimental data for the other products are lacking. Hence, the rate constants for the reactions of the OH radical with these other products were estimated using the method of Atkinson (1986, 1987). The rate constants used were (in units of $10^{-12}\text{ cm}^3\text{ molecule}^{-1}\text{ s}^{-1}$): HCHO, 9.0; HC(=O)Cl , 6.1; $\text{CH}_2\text{ClC(=O)Cl}$, 0.16; $\text{CHCl}_2\text{C(=O)Cl}$, 0.13; with COCl_2 and $\text{CCl}_3\text{C(=O)Cl}$ being unreactive towards the OH radical. The correction factors to take into account the secondary reactions of the products with the OH radical were always < 2.4 , and were generally $\lesssim 1.5$.

Typical plots of the product yields determined from RONO-NO-chloroethene-air irradiations in the presence of Cl atom scavengers, corrected for losses via reaction with the OH radical, are presented in Figure IV-12 for vinyl chloride and Figure IV-13 for 1,1-dichloroethene. Good straight line plots are observed, confirming that the corrections for secondary

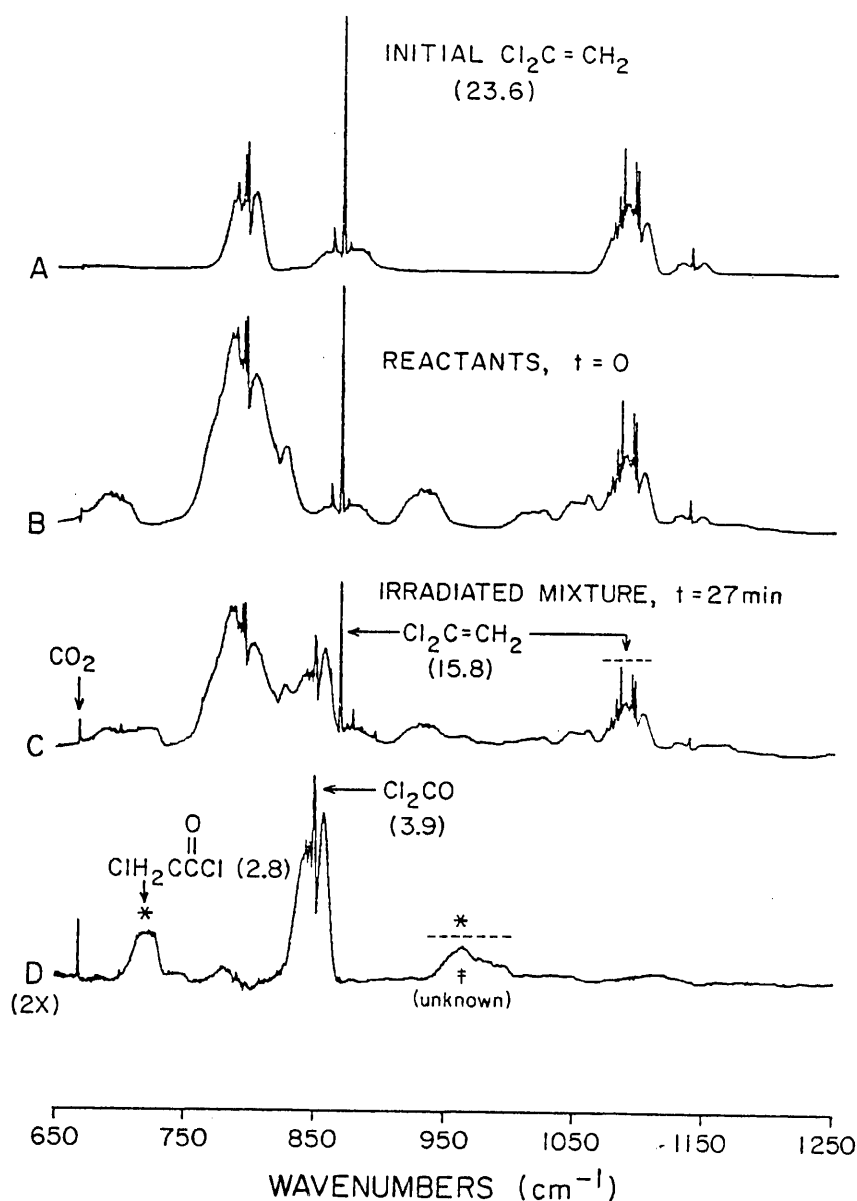


Figure IV-9. FT-IR absorption spectra obtained from a $\text{C}_2\text{H}_5\text{ONO-NO-1,1-dichloroethene-air}$ irradiation; concentrations in parentheses are in units of $10^{13} \text{ molecule cm}^{-3}$. (A) 1,1-dichloroethene; (B) initial mixture of 1,1-dichloroethene (23.6), ethyl nitrite (24.0) and nitric oxide (24.0); (C) mixture of products and reactants after 27 min of irradiation; (D) derived from (C) to show only the products arising from the reaction of 1,1-dichloroethene with the OH radical (see text for a discussion of the overlapped unknown band at $\sim 965 \text{ cm}^{-1}$).

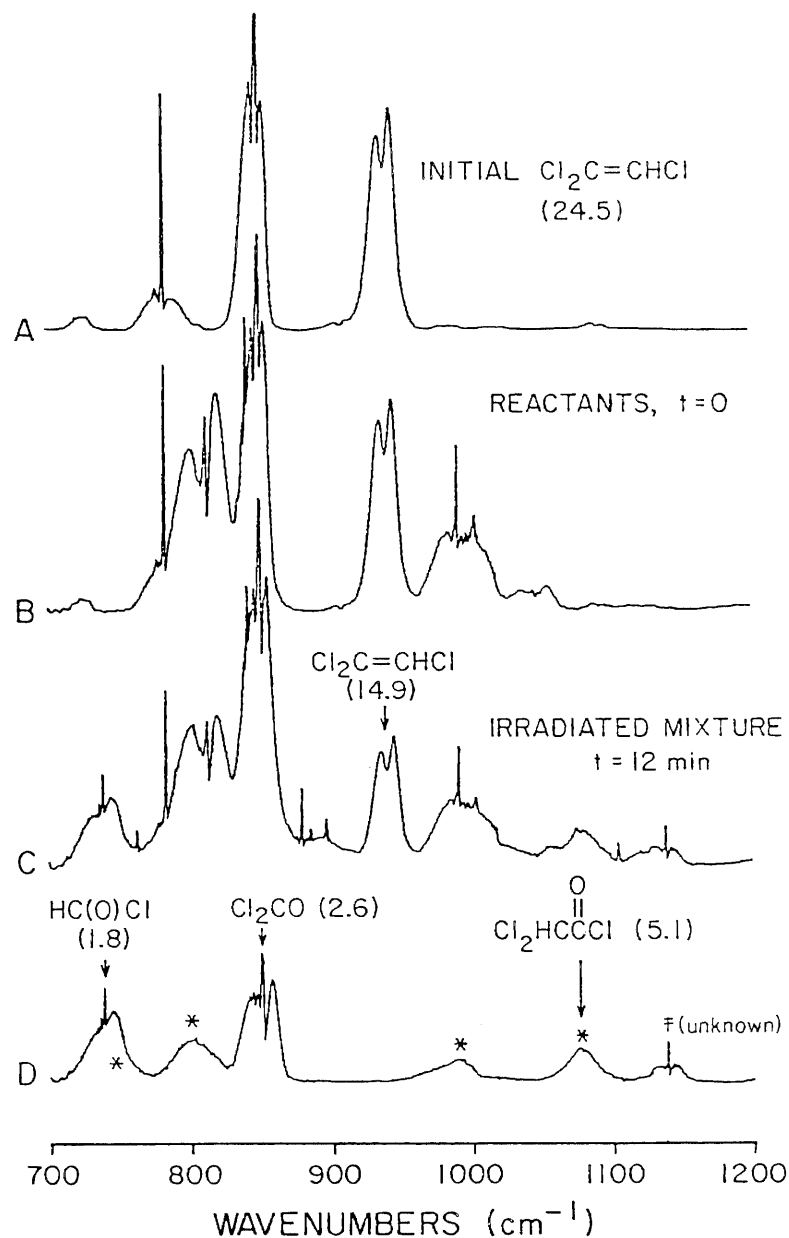


Figure IV-10. FT-IR absorption spectra obtained from a $\text{CH}_3\text{ONO-NO}$ -trichloroethene-air irradiation; concentrations in parentheses are in units of $10^{13} \text{ molecule cm}^{-3}$. (A) trichloroethene; (B) initial mixture of trichloroethene (24.5), methyl nitrite (24.0) and nitric oxide (12.0); (C) mixture of products and reactants after 12 min of irradiation; (D) derived from (C) to show only the products arising from the reaction of trichloroethene with the OH radical (the absorption at 1139 cm^{-1} is due to an unknown product).

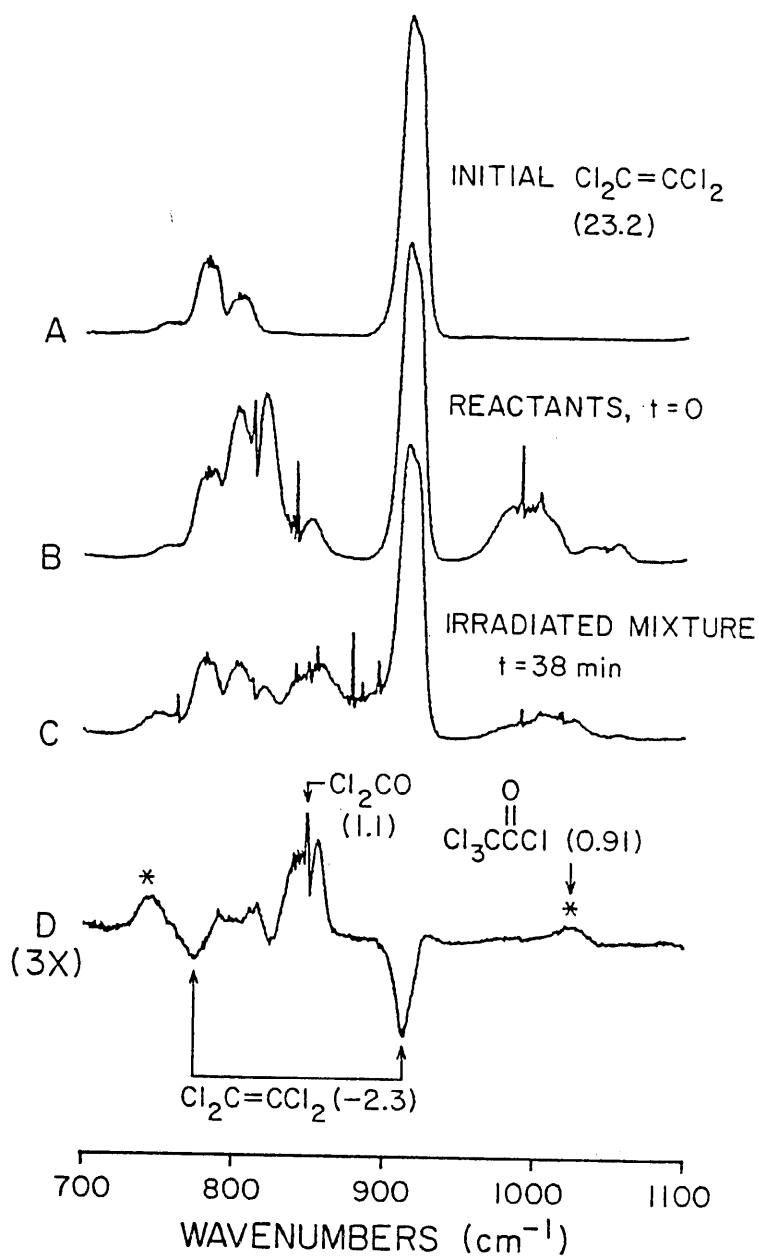


Figure IV-11. FT-IR absorption spectra obtained from a $\text{CH}_3\text{ONO}-\text{NO}$ -tetrachloroethene-air irradiation; concentrations in parentheses are in units of 10^{13} molecule cm^{-3} . (A) tetrachloroethene; (B) initial mixture of tetrachloroethene (23.2), methyl nitrite (24.0) and nitric oxide (12.0); (C) mixture of products and reactants after 38 min of irradiation; (D) derived from (C-B) to show only the consumption of tetrachloroethene and the formation of products from its OH radical reaction.

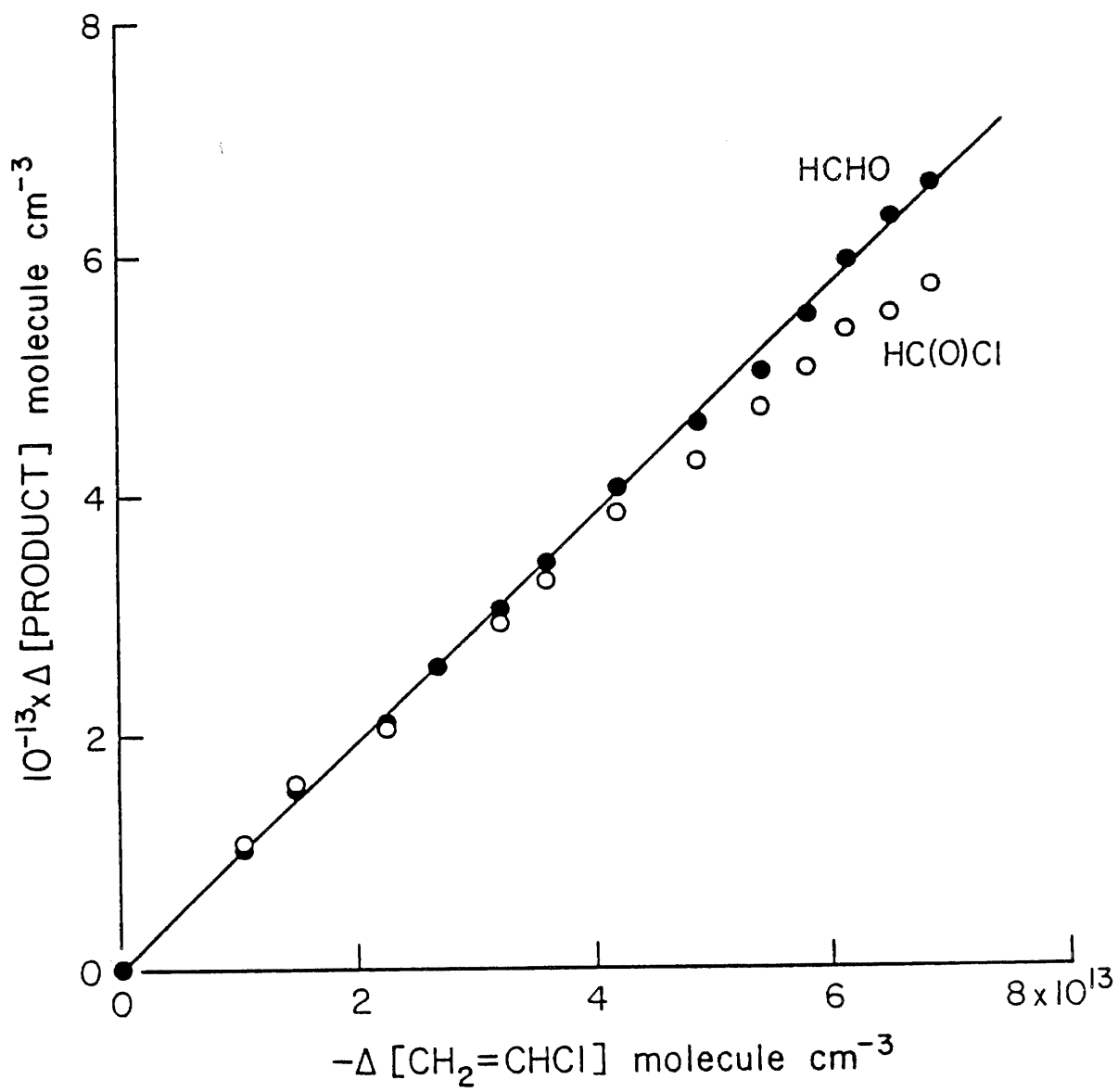


Figure IV-12. Plots of the amounts of HCHO (●) and HC(O)Cl (○) formed (corrected for loss by reaction with the OH radical, see text) against the amount of vinyl chloride consumed in a $\text{C}_2\text{H}_5\text{ONO-NO}$ -vinyl chloride-air irradiation in the presence of $7 \times 10^{14} \text{ molecule cm}^{-3}$ of ethane.

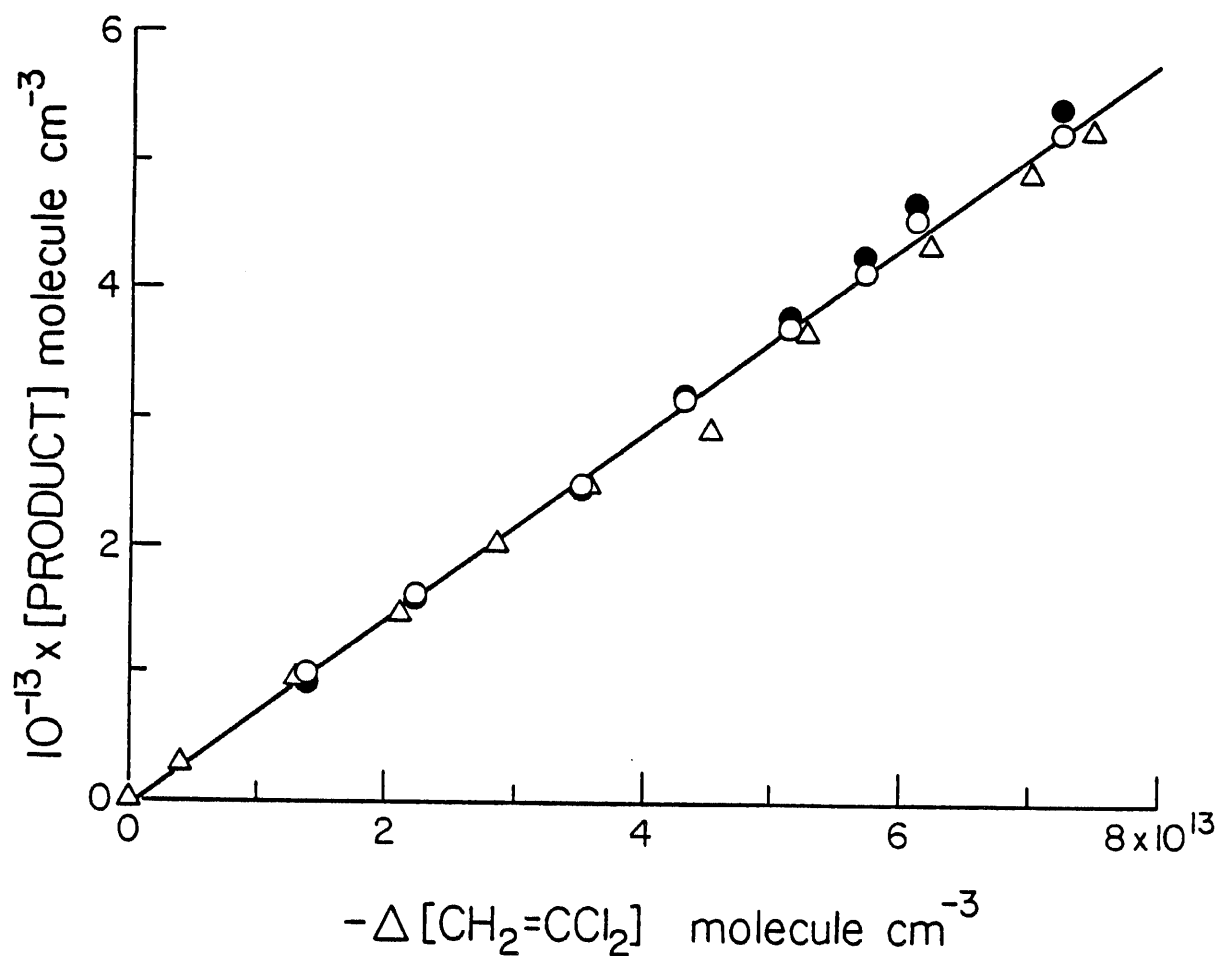


Figure IV-13. Plot of the amounts of HCHO (●) and COCl_2 (○, Δ) formed (those for HCHO corrected for loss by reaction with the OH radical, see text) against the amount of 1,1-dichloroethene consumed in $\text{C}_2\text{H}_5\text{ONO-NO-1,1-dichloroethene-air}$ (●, ○) and $\text{CH}_3\text{ONO-NO-1,1-dichloroethene-CH}_3\text{OCH}_3\text{-air}$ (Δ) irradiations in the presence of $7 \times 10^{14} \text{ molecule cm}^{-3}$ of ethane. The solid line is derived from a least-squares analysis of all of the data shown.

reactions of the products were adequate. It can be seen that for both of these chloroethenes the pair of products observed (HCHO and HC(O)Cl from vinyl chloride and HCHO and COCl_2 from 1,1-dichloroethene) were formed in essentially equal yields.

The yields of the products formed in the $\text{RONO-NO-chloroethene-air}$ irradiations in the absence and presence of ethane and/or CH_3OCH_3 are given in Table IV-6. The product yields in those irradiations in which Cl atoms were not completely scavenged would not be expected to be constant during the entire irradiation periods, and corrections to the product data which assumed that OH radical reactions were the only loss process for the products were probably incorrect. Nonlinear plots of the amount of product formed against the amount of chloroethene consumed were observed for certain irradiations (Table IV-6), but for the majority of the experiments good straight line plots of the corrected product yields against the amount of chloroethene consumed were obtained. While plots of the $\text{CCl}_3\text{C(O)Cl}$ concentrations against the amounts of tetrachloroethene consumed were curved, with the observed $\text{CCl}_3\text{C(O)Cl}$ formation yield appearing to decrease with reaction time, this effect could in part be due to wall loss or photolysis of $\text{CCl}_3\text{C(O)Cl}$, since $\text{CCl}_3\text{C(O)Cl}$ is not expected to react with OH radicals (or Cl atoms). These particular irradiations were also characterized by low conversions (~2-10%) of tetrachloroethene.

The data given in Table IV-6 show that the product yields depend on the presence or absence of the Cl atom scavengers ethane and/or CH_3OCH_3 , although the effect, if any, is very small for vinyl chloride. Furthermore, the observation of chloroacetyl chlorides, $\text{CH}_x\text{Cl}_{3-x}\text{C(O)Cl}$, from the reactions involving 1,1-dichloroethene, trichloroethene and tetrachloroethene in the absence of Cl atom scavengers, and the decrease in the yields of these chloroacetyl chlorides upon addition of ethane and/or CH_3OCH_3 shows that these compounds are products of the Cl atom reactions with the chloroethenes. Hence, as expected from the kinetic studies, the product data obtained from the irradiations with added ethane and CH_3OCH_3 correspond most closely to the OH radical reaction data.

Based upon our present knowledge of the gas-phase reactions of OH radicals with alkenes and haloalkenes (Atkinson 1986), these OH radical reactions proceed via initial OH radical addition to the carbon-carbon double bond, as shown in the following scheme for trichloroethene.

Table IV-6. Product Yields, Corrected for Reaction with the OH Radical, Determined from RONO-NO-Chloroethene-Air Irradiations in the Presence and Absence of Cl Atom Scavengers

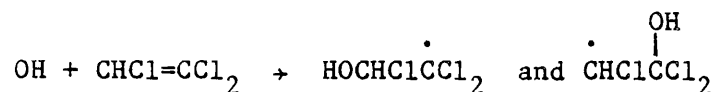
	Presence of		Yields (Corr)				
	C ₂ H ₆	CH ₃ OCH ₃	HCHO	HC(O)Cl	COCl ₂	CH ₂ ClC(O)Cl	CHCl ₂ C(O)Cl
CH ₂ =CHCl	x		0.96 ± 0.03	0.83 ± 0.03			CCl ₃ C(O)Cl
CH ₂ =CHCl			0.89 ± 0.02	0.80 ± 0.03			
<u>cis</u> -CHCl=CHCl	x	x		0.59 ± 0.04			
<u>cis</u> -CHCl=CHCl		x		0.67 ± 0.03			
<u>cis</u> -CHCl=CHCl				1.68 ± 0.12 ^a			
<u>trans</u> -CHCl=CHCl	x	x		0.72 ± 0.03			
<u>trans</u> -CHCl=CHCl		x		0.88 ± 0.03			
<u>trans</u> -CHCl=CHCl				1.85 ± 0.12 ^a			
CH ₂ =CCl ₂	x	x	b		0.69 ± 0.03	c	
CH ₂ =CCl ₂	x		0.76 ± 0.03		0.73 ± 0.02	0.090 ± 0.017	
CH ₂ =CCl ₂			0.57 ± 0.05		0.52 ± 0.03	0.32 ± 0.03	

(continued)

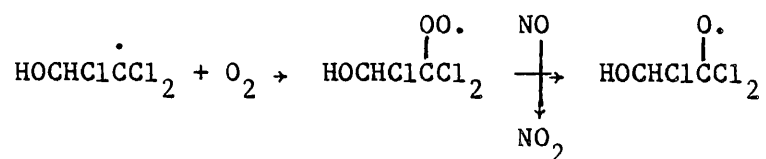
Table IV-6 (continued) - 2

	Presence of		Yields (Corr)				
	C ₂ H ₆	CH ₃ OCH ₃	HCHO	HC(O)Cl	COCl ₂	CH ₂ ClC(O)Cl	CHCl ₂ C(O)Cl
CHCl=CCl ₂				0.40 ± 0.05 ^a	0.29 ± 0.03		0.50 ± 0.05
CHCl=CCl ₂	x			0.067 ± 0.010	0.40 ± 0.06		0.19 ± 0.03
CHCl=CCl ₂				0.27 ± 0.01	0.27 ± 0.01		0.51 ± 0.02
CCl ₂ =CCl ₂					0.47 ± 0.02		0.39 ± 0.04 (~0.45) ^d
CCl ₂ =CCl ₂					0.52 ± 0.03		0.41 ± 0.05 (~0.50) ^d
CCl ₂ =CCl ₂					0.49 ± 0.05		
CCl ₂ =CCl ₂	x				0.47 ± 0.14		≤0.15

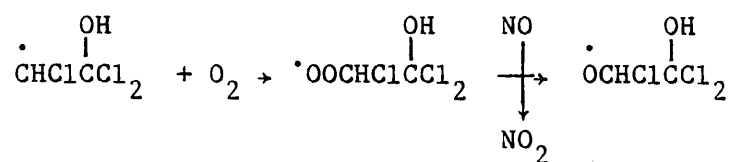
^aNon-linear plots of product formed (corrected for losses via OH radical reaction) against chloroethene consumed.^bNot measured; HCHO was also a product of CH₃ONO used as OH radical source in this experiment.^cNot detected.^dInitial value.



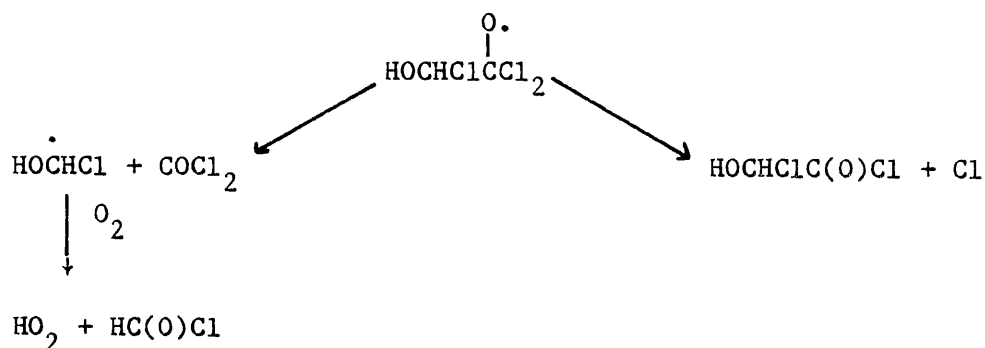
Under the experimental conditions employed in this study, the radicals formed in the initial reaction step are expected to rapidly add O_2 and then react with NO :



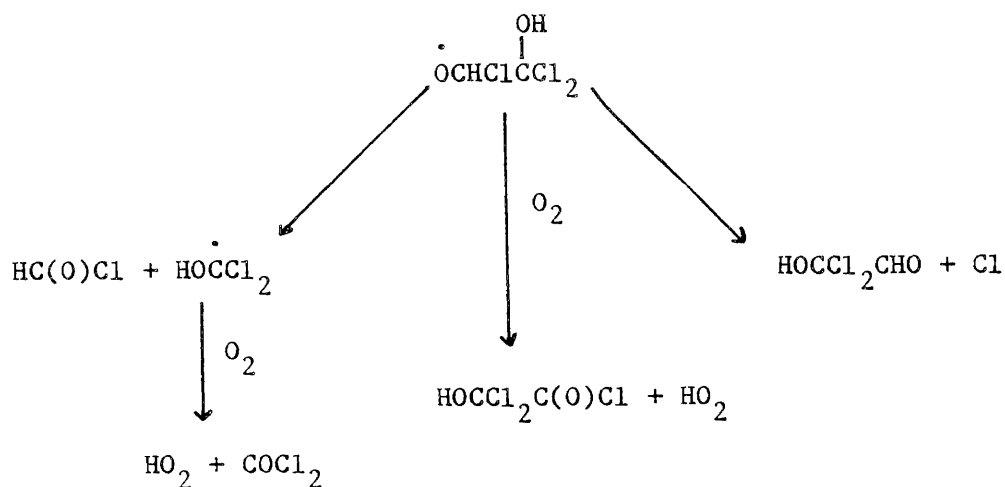
and



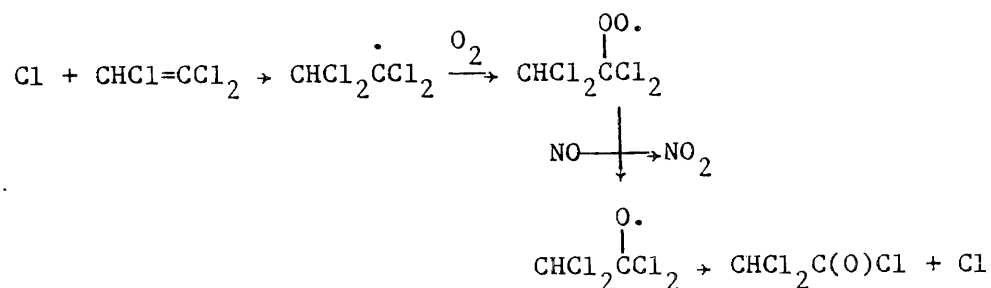
The subsequent reactions of these hydroxyethoxy radicals have not been elucidated at the present time, but the possible pathways involve cleavage at the carbon-carbon bond, Cl atom elimination and, probably less importantly, reaction with O_2 :



and



The subsequent reactions of the Cl atoms formed from the reaction of OH with the chloroethenes are expected to yield chloroacetyl chlorides, for example



Indeed, in the cases where chloroacetyl chlorides were observed as products, their yields (Table IV-6) were markedly decreased in the presence of ethane and/or dimethyl ether, which acted as Cl atom scavengers.

As seen from Table IV-6, not all of the products predicted above for trichloroethene, nor all of those predicted for the other chloroethenes following the same general reaction scheme, were observed. The simpler product distributions observed are indicative of the preferential decomposition pathways of the chloroethoxy radicals formed subsequent to OH radical and Cl atom additions. These chloroethoxy radicals are summarized for each chloroethene in Table IV-7 together with the predicted mode of decomposition for each radical. [Since the least chlorinated carbon is the most favored (by at least a factor of 10) site for Cl atom addition to the unsymmetrical chloroethenes (Sanhueza et al. 1976), only

Table IV-7. Ethoxy Radical Intermediates Formed from the Chloroethenes and their Predicted Modes of Reaction

Compound	Reaction with OH		Reaction with Cl ^a	
CH ₂ =CHCl	$\begin{array}{c} \text{O} \cdot \\ \\ \text{HOCH}_2\text{CHCl} \end{array}$	C-C cleavage	$\begin{array}{c} \text{O} \cdot \\ \\ \text{CH}_2\text{ClCHCl} \end{array} (+4)$	C-C cleavage
	$\begin{array}{c} \text{OH} \\ \\ \cdot\text{OCH}_2\text{CHCl} \end{array}$	C-C cleavage		
CHCl=CHCl (<u>cis</u> or <u>trans</u>)	$\begin{array}{c} \text{O} \cdot \\ \\ \text{HOCHClCHCl} \end{array}$	C-C cleavage	$\begin{array}{c} \text{O} \cdot \\ \\ \text{CHCl}_2\text{CHCl} \end{array} (+6)$	C-C cleavage
CH ₂ =CCl ₂	$\begin{array}{c} \text{O} \cdot \\ \\ \text{HOCH}_2\text{CCl}_2 \end{array}$	Cl elimination	$\begin{array}{c} \text{O} \cdot \\ \\ \text{CH}_2\text{ClCCl}_2 \end{array} (-9.2)$	Cl elimination
	$\begin{array}{c} \text{OH} \\ \\ \cdot\text{OCH}_2\text{CCl}_2 \end{array}$	C-C cleavage		
CHCl=CCl ₂	$\begin{array}{c} \text{O} \cdot \\ \\ \text{HOCHClCCl}_2 \end{array}$	Cl elimination	$\begin{array}{c} \text{O} \cdot \\ \\ \text{CHCl}_2\text{CCl}_2 \end{array} (-3)$	Cl elimination
	$\begin{array}{c} \text{OH} \\ \\ \cdot\text{OCHClCCl}_2 \end{array}$	C-C cleavage		
CCl ₂ =CCl ₂	$\begin{array}{c} \text{O} \cdot \\ \\ \text{HOCCl}_2\text{CCl}_2 \end{array}$	C-C cleavage and Cl elimination	$\begin{array}{c} \text{O} \cdot \\ \\ \text{CCl}_3\text{CCl}_2 \end{array} (+3)$	C-C cleavage and Cl elimination

^aValues in parentheses are the bond energy differences [D(C-Cl)-D(C-C)], in kcal mol⁻¹, from Sanhueza et al. (1976).

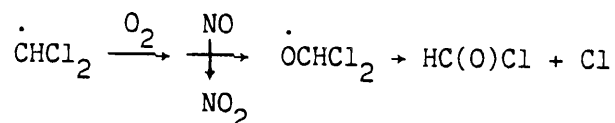
the chloroethoxy radicals which result from this preferential Cl atom addition are given in Table IV-7.]

In a review of the Cl-atom initiated oxidation of haloethenes, Sanhueza et al. (1976) correlated the preferred decomposition modes of the chloroethoxy radicals with the difference in the bond energies between the C-Cl bond of the oxygen-bearing carbon atom and the C-C bond. It was concluded that when the bond energy difference $[D(C-Cl)-D(C-C)]$ is ≥ 6 kcal mol⁻¹, the chloroethoxy radical reacts through C-C bond scission; when $[D(C-Cl)-D(C-C)]$ is < -3 kcal mol⁻¹, almost all of the decomposition proceeds through Cl atom elimination (Sanhueza et al. 1976). The bond energy differences calculated by Sanhueza et al. (1976) are included in Table IV-7 for the respective chloroethoxy radicals.

It is expected that the values of $[D(C-Cl)-D(C-C)]$ for the hydroxyethoxy radicals formed subsequent to the OH reactions will be similar to those in which a Cl atom instead of a hydroxyl group is attached to the β -carbon, since mesomeric effects are not operative and the inductive effects of a Cl atom and the hydroxyl oxygen atom are quite similar. Thus, the mode of decomposition, either C-C cleavage or Cl elimination, is expected to be similar for corresponding ethoxy radicals such as $HOCH_2C(O^\bullet)CCl_2$ and $CH_2ClC(O^\bullet)CCl_2$.

Many of the qualitative aspects of the product yields summarized in Table IV-6 can be explained in terms of the predicted modes of chloroethoxy radical decomposition given in Table IV-7. Thus, the high yields (approaching 100%) of HCHO and HC(O)Cl from vinyl chloride are consistent with the $HOCH_2CH(\dot{O})Cl$ and $\dot{O}CH_2CH(OH)Cl$ radicals decomposing mainly via C-C bond cleavage.

For cis- and trans-1,2-dichloroethene, C-C cleavage of the corresponding hydroxydichloroethoxy radical produces HC(O)Cl as well as HOCHCl. Formation of Cl from the oxidation of HOCHCl and subsequent Cl reaction with the 1,2-dichloroethene could explain, in part, the higher HC(O)Cl yields observed in the absence of Cl atom scavengers. This arises because the cleavage of the C-C bond of the $CHCl_2CH(\dot{O})Cl$ radical formed in the Cl atom reaction generates directly one HC(O)Cl plus another from the subsequent oxidation of the $\dot{C}HCl_2$ fragment, which generates a Cl atom to maintain the chain reaction.



Since COCl_2 was not observed as a product from the cis- and trans- 1,2-dichloroethenes in the absence of ethane and CH_3OCH_3 , this confirms that the $\dot{\text{OCHCl}}_2$ radicals do not react with O_2 to yield COCl_2 and an HO_2 radical (Niki et al. 1980). However, an explanation for the low absolute yields of HC(O)Cl of 0.6-0.9 (instead of the expected 1-2 in the presence of Cl atom scavengers) is not immediately obvious.

Cl atom elimination is predicted to be an important mode of decomposition for the ethoxy radicals formed in the OH and Cl reactions with 1,1-dichloroethene, trichloroethene and tetrachloroethene. As seen from Figures IV-9 through IV-11, chloroacetyl chlorides are obvious products of the reaction of Cl with these chloroethenes, and indeed their yields are markedly reduced in the presence of Cl atom scavengers.

As noted above, for 1,1-dichloroethene infrared absorption bands associated with an acid chloride, but distinct from those of $\text{CH}_2\text{ClC(O)Cl}$, were observed. These bands are most likely due to $\text{HOCH}_2\text{C(O)Cl}$, which is formed by Cl elimination from the $\text{HOCH}_2\dot{\text{CCl}}_2$ radical, and which presumably accounts for the balance of the products in Table IV-6. The observed increase in the relative yield of this compound, as well as those of HCHO and COCl_2 , in the presence of added ethane is due to the suppression of the subsequent reactions of Cl atoms leading to $\text{CH}_2\text{ClC(O)Cl}$ formation.

The formation of HOCHClC(O)Cl by Cl atom elimination from $\text{HOCHCl}\dot{\text{CCl}}_2$ is predicted for trichloroethene. However, the only residual infrared band observed which was distinct from those of the products HC(O)Cl , COCl_2 and $\text{CHCl}_2\text{C(O)Cl}$ was definitely not due to an acid chloride. Furthermore, the results of the trichloroethene irradiations (Table IV-6) were unusual with respect to the high variability of the HC(O)Cl yield, particularly in the experiment with added ethane, where the extent of Cl atom reactions was still significant as evidenced by the yield of $\text{CHCl}_2\text{C(O)Cl}$. The cause for the very low observed yield of HC(O)Cl in the presence of added ethane is not known. It is interesting to note, however, that Sanhueza et al. (1976) invoked reaction channels leading to an energetic HC(O)Cl molecule, which always decomposes to CO and HCl, in explaining the results of the

Cl-atom sensitized oxidation of the chloroethenes. [The generally low yields of HC(O)Cl from cis- and trans-1,2-dichloroethene may also be related to this cause].

The observed yields of COCl_2 and $\text{CCl}_3\text{C(O)Cl}$ from tetrachloroethene can be accounted for by the decomposition of the alkoxy radicals (Table IV-7) via both C-Cl cleavage and Cl elimination. The reaction of tetrachloroethene with the Cl atom in the chain process which forms $\text{CCl}_3\text{C(O)Cl}$ is presumably initiated by Cl atom elimination from the $\text{HOCCl}_2\text{CCl}_2$ radical, a step which would also form $\text{HOCCl}_2\text{C(O)Cl}$. The formation of this latter compound could not be ascertained due to the low conversion of tetrachloroethene during the irradiation experiments (~8-10% and ~2%, respectively, in the absence and presence of ethane for irradiations lasting ~2 hr).

It is clear from the above discussion that the involvement of Cl atoms in these reactions greatly complicates the reaction pathways subsequent to the initial OH radical attack on the chloroethenes. Although the routes leading to the major products are reasonably well accepted reactions, the general scheme still requires the identification of hydroxy-acetyl chlorides from trichloroethene and tetrachloroethene.

The kinetic data obtained in this and previous studies demonstrate that the chloroethenes will be relatively long-lived in the troposphere with respect to chemical removal processes. These compounds will therefore be dispersed over substantial distances from their emission sources. The present product studies indicate that in addition to concerns over the toxicity of the chlorinated alkenes themselves, the possible health impacts of their atmospheric reaction products must also be taken into account.

C. Allyl Chloride ($\text{CH}_2=\text{CHCH}_2\text{Cl}$)

At the time our program commenced, no data were available concerning the atmospheric lifetimes and fates of allyl chloride. Accordingly, we studied the kinetics of the gas-phase reactions of allyl chloride with OH and NO_3 radicals and with O_3 , and studied the products of the OH radical reaction, the dominant removal pathway. These studies are described below.

1. Kinetics of the Ozone Reaction

The rate constant for the reaction of O_3 with allyl chloride was determined as described in Section III above. Allyl chloride was monitored in the reaction bag, after mixing of the O_3 and allyl chloride reactants, by GC-FID, using a 10 ft. x 0.125 in. stainless steel column of 10% Carbowax 600 on C-22 Firebrick, operated at 348 K. The O_3 decays were always exponential, and the O_3 decay rates at the allyl chloride concentrations studied are given in Table IV-8. A plot of the O_3 decay rate against the allyl chloride concentration is shown in Figure IV-14. A good straight line relationship is observed, and a least-squares analysis of the data yields the rate constant

$$k(O_3 + \text{allyl chloride}) = (1.60 \pm 0.18) \times 10^{-18} \text{ cm}^3 \text{ molecule}^{-1} \text{ s}^{-1}$$

at 296 ± 2 K, where the indicated error limit is two least-squares standard deviations combined with a 10% uncertainty in the GC-FID calibration of allyl chloride.

This rate constant is in excellent agreement with that of $(1.5 \pm 0.2) \times 10^{-18} \text{ cm}^3 \text{ molecule}^{-1} \text{ s}^{-1}$ recently reported by Edney et al. (1986b).

Table IV-8. Experimental Data for the Gas-Phase Reaction of O_3 with Allyl Chloride at 296 ± 2 K^a

$10^{-14} \times [\text{Allyl Chloride}]$ (molecule cm^{-3})	$10^3 \times O_3$ Decay Rate (s^{-1})
-	0.0033
4.78	0.832
7.24	1.18
9.73	1.58
2.13	0.402

^aExperiments are given in the order carried out.

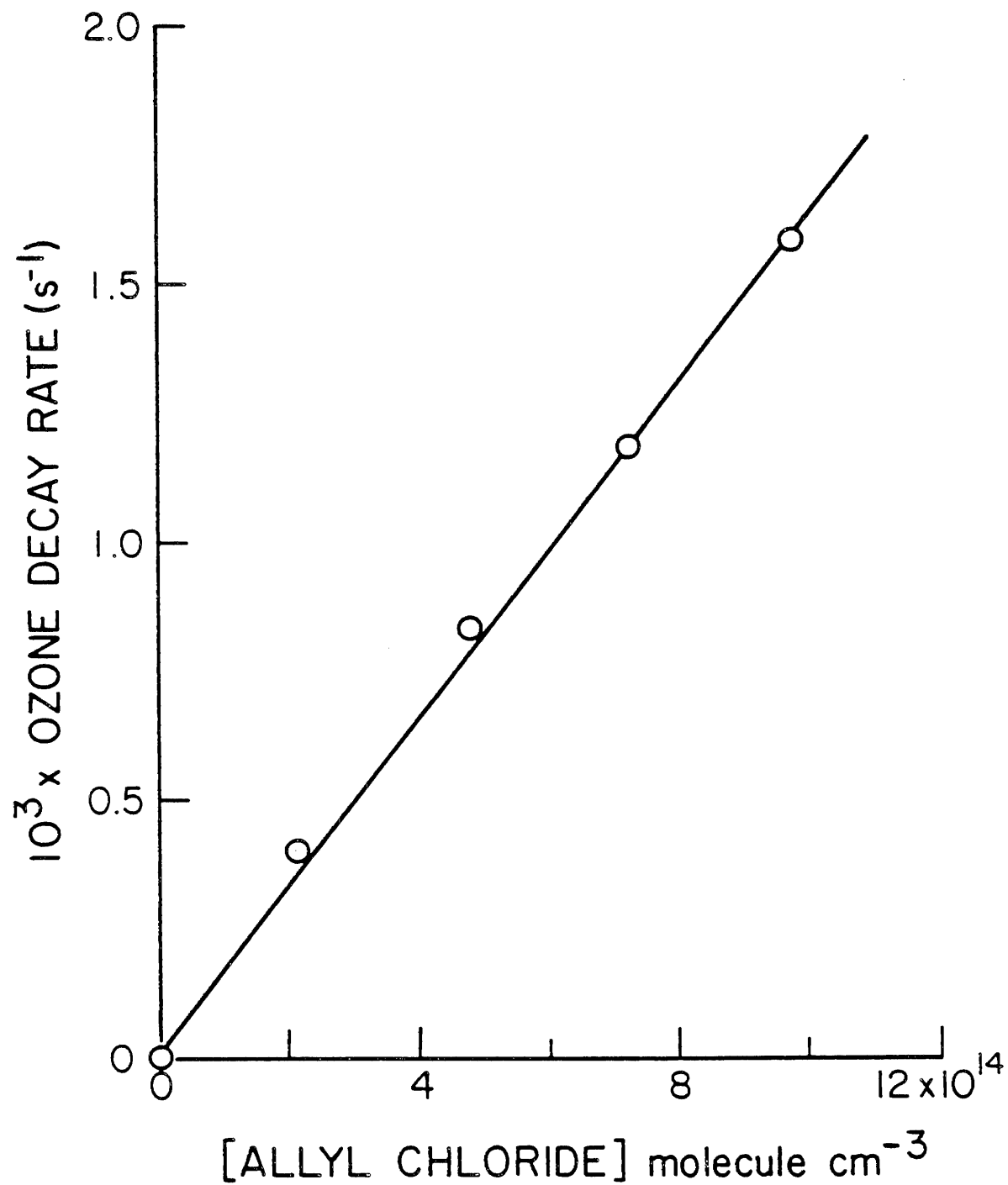


Figure IV-14. Plot of the O_3 decay rate against the allyl chloride concentration at $296 \pm 2 \text{ K}$.

2. Kinetics of the NO₃ Radical Reaction

The rate constant for the reaction of NO₃ with allyl chloride was determined using the relative rate technique described in Section III above. Experiments were carried out in a 2500-liter all-Teflon chamber, with ethene as the reference organic. Allyl chloride and ethene were monitored by GC-FID. The data obtained are plotted in accordance with equation (VII) in Figure IV-15, and a least-squares analysis yields the rate constant ratio

$$k(\text{allyl chloride})/k(\text{ethene}) = 2.61 \pm 0.10$$

where the error limit is two least-squares standard deviations. Use of a rate constant for the reaction of NO₃ radicals with ethene of $(2.3 \pm 0.4) \times 10^{-16} \text{ cm}^3 \text{ molecule}^{-1} \text{ s}^{-1}$ (Ravishankara and Mauldin 1985, Atkinson et al. 1987) allows this rate constant ratio to be placed on an absolute basis, yielding

$$k(\text{NO}_3 + \text{allyl chloride}) = (6.0 \pm 1.1) \times 10^{-16} \text{ cm}^3 \text{ molecule}^{-1} \text{ s}^{-1}$$

at $298 \pm 2 \text{ K}$.

3. Determination of the Rate Constant for OH Radical Reaction

Experimental. The kinetics of the reaction of allyl chloride with the OH radical were studied using the relative rate method described in Section III above. Propene was used as the reference organic and both propene and allyl chloride were monitored by long pathlength FT-IR spectroscopy. The initial concentrations of the reactants were CH₃ONO, $2.4 \times 10^{14} \text{ molecule cm}^{-3}$; NO, $(1.2\text{--}2.4) \times 10^{14} \text{ molecule cm}^{-3}$; allyl chloride, $(3.8\text{--}4.8) \times 10^{14} \text{ molecule cm}^{-3}$; and propene $(3.6\text{--}4.8) \times 10^{14} \text{ molecule cm}^{-3}$. Since, as discussed above for the chloroethenes, Cl atoms may be generated from the reaction of OH radicals with allyl chloride, an irradiation was also carried out with $1.9 \times 10^{15} \text{ molecule cm}^{-3}$ of ethane added to the reactant mixture to scavenge any Cl atoms formed.

Results. The data obtained are plotted in accordance with equation (III) in Figure IV-16, and it can be seen that all of the data, including those with added ethane, fit a good straight line. This shows that either Cl atoms are not produced from the reaction of OH radicals with allyl

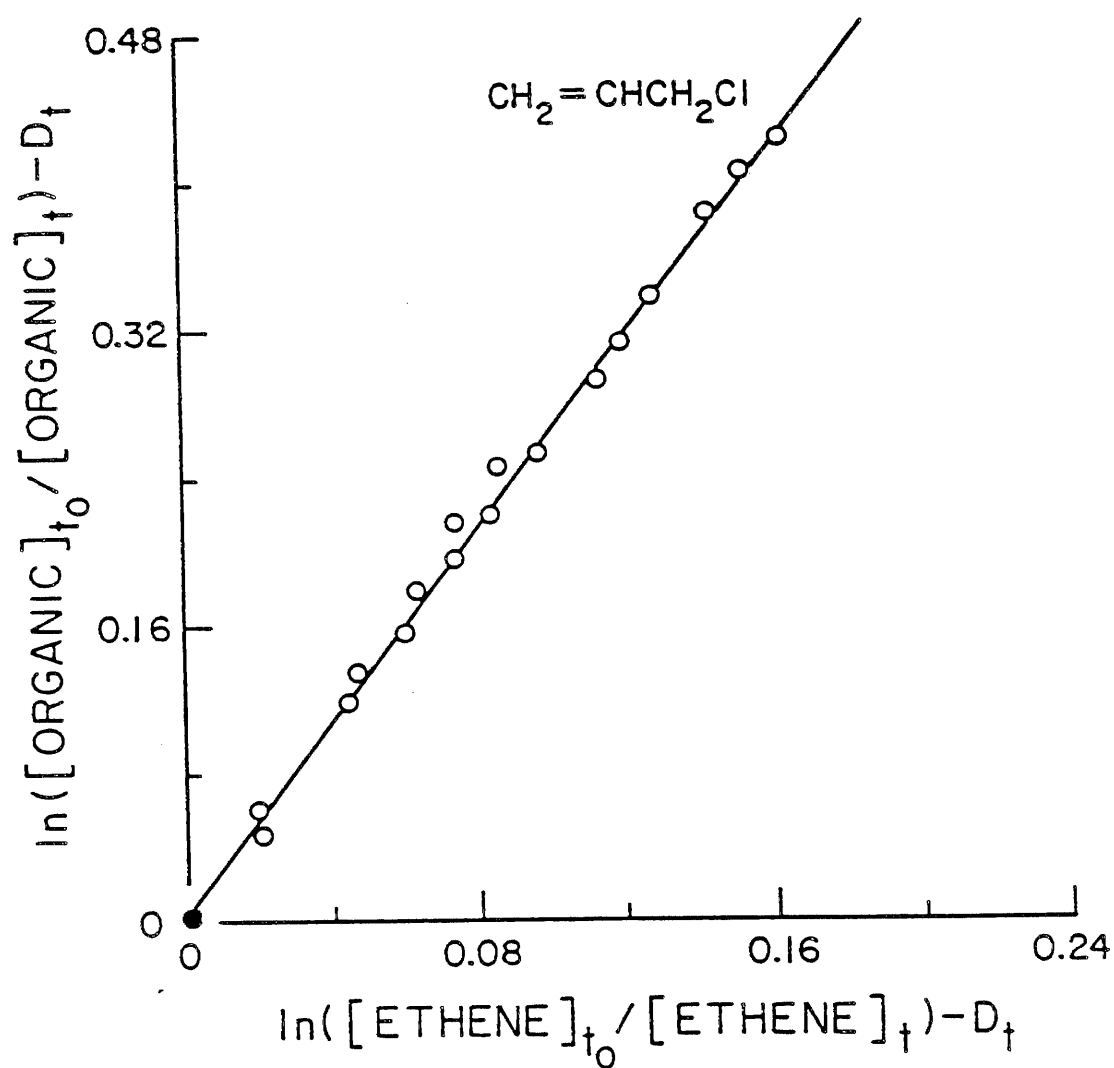


Figure IV-15. Plot of equation (VII) for the reaction of NO_3 radicals with allyl chloride, with ethene as the reference organic.

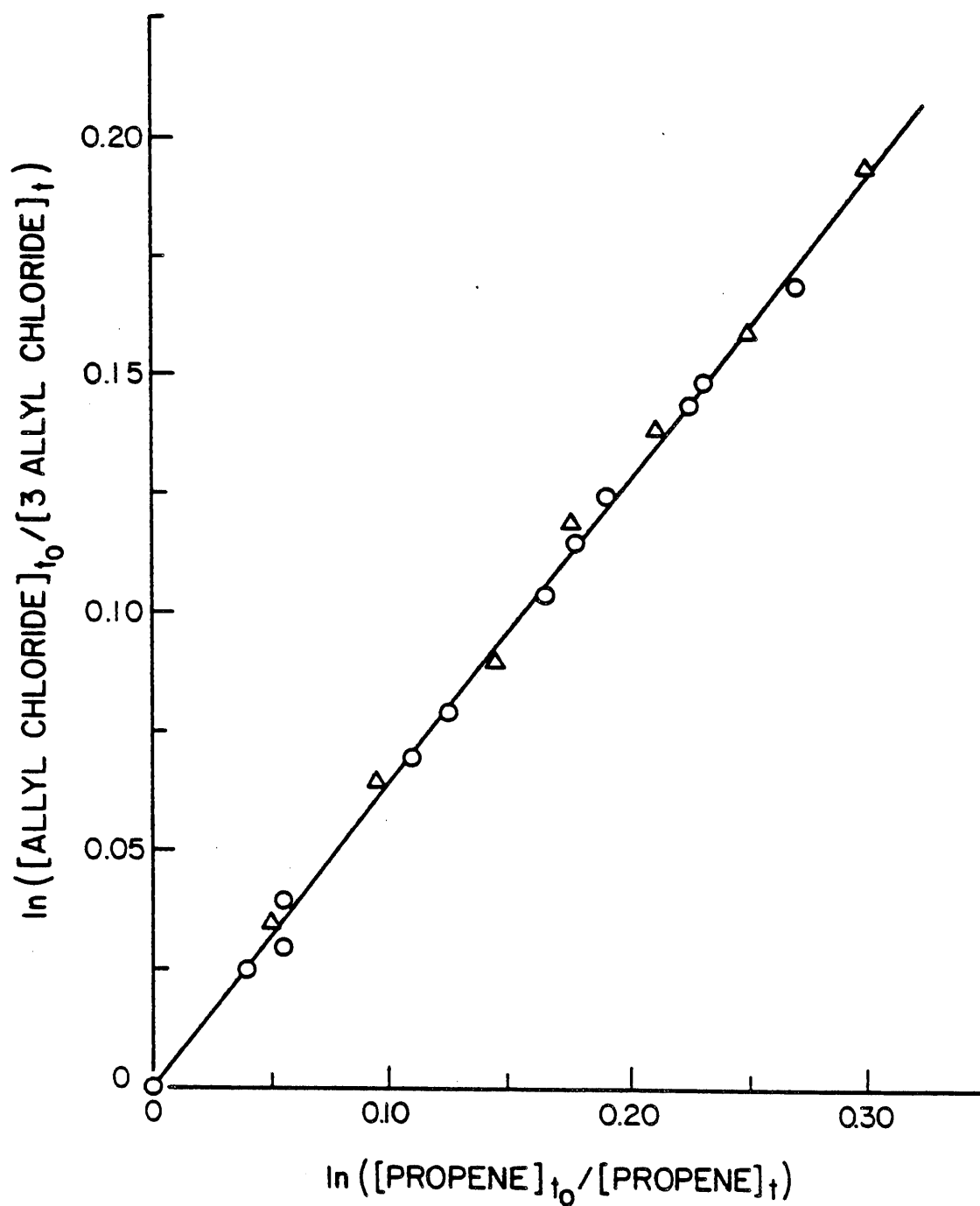


Figure IV-16. Plot of the equation (III) for the reaction of OH radicals with allyl chloride, with propene as the reference organic (O - data obtained in the absence of added ethane, Δ - data obtained in the presence of 1.9×10^{15} molecule cm^{-3} of added ethane).

chloride, or that the rate constant ratios for the reactions of OH radicals and Cl atoms with allyl chloride and propene are essentially identical. Since the recent study of Edney et al. (1986b) shows that Cl atoms are produced from this OH radical reaction, the rate constant ratios for Cl atoms and OH radicals must be very similar.

Least squares analysis of the data obtained in the presence of ethane (sufficient to scavenge ~50% of the Cl atoms produced) gave a slope of the plot of equation (III) identical (to within <1%) to that obtained from least-squares analysis of the total data set. The rate constant ratio obtained was

$$k(\text{allyl chloride})/k(\text{propene}) = 0.643 \pm 0.026$$

where the error limit is two least squares standard deviations of the data obtained in the presence of ethane. Using a rate constant for the reaction of OH radicals with propene of $2.63 \times 10^{-11} \text{ cm}^3 \text{ molecule}^{-1} \text{ s}^{-1}$ (Atkinson 1986) leads to

$$k(\text{OH} + \text{allyl chloride}) = (1.69 \pm 0.07) \times 10^{-11} \text{ cm}^3 \text{ molecule}^{-1} \text{ s}^{-1}$$

at $298 \pm 2 \text{ K}$, where the error limits are two least squares standard deviations. This value is in excellent agreement with that of $(1.7 \pm 0.7) \times 10^{-11} \text{ cm}^3 \text{ molecule}^{-1} \text{ s}^{-1}$ reported by Edney et al. (1986b).

These rate constants for the reactions of allyl chloride with OH and NO_3 radicals and O_3 allow the atmospheric lifetimes of allyl chloride to be calculated for each of these potential removal pathways, as given in Table IV-9. The dominant atmospheric loss process is clearly by reaction with the OH radical. Hence we studied the products of the OH radical reaction, as discussed below.

4. Product Study of the OH Radical Reaction

Reactions were carried out in the 5800-liter evacuable chamber, as described in Section III above. Due to the expected formation of HCHO from allyl chloride, OH radicals were generated from the photolysis of $\text{C}_2\text{H}_5\text{ONO}$ in air. The reactants and products were monitored by long pathlength FT-IR absorption spectroscopy.

Table IV-9. Calculated Atmospheric Lifetimes of Allyl Chloride Due to Reaction with NO_3 and OH Radicals and O_3

Reactive Species	Concentration (molecule cm^{-3})	Lifetime of Allyl Chloride
OH	1×10^6 (12-hr daytime)	1.4 days
NO_3	2.4×10^8 (12-hr nighttime)	160 days
O_3	7×10^{11} (24-hr period)	10 days

A reference spectrum of allyl chloride is shown in Figure IV-17A, while that of an initial mixture of 4.9×10^{14} molecule cm^{-3} of $\text{CH}_2=\text{CHCH}_2\text{Cl}$, 2.4×10^{14} molecule cm^{-3} of $\text{C}_2\text{H}_5\text{ONO}$ and 1.9×10^{14} molecule cm^{-3} of NO is given in Figure IV-17B. The spectrum of all products and reactants after 9 min of irradiation, when ~25% of allyl chloride has been consumed, is depicted in Figure IV-17C. Figure IV-18A shows the resulting spectrum after subtracting the absorptions due to the reactants, the product species HNO_3 and HONO , and the photooxidation products of $\text{C}_2\text{H}_5\text{ONO}$ (i.e., CH_3CHO and PAN) from Figure IV-17C. The products which are attributed to reaction of allyl chloride are HCHO , HOCH_2CHO (very weak absorption bands), HC(O)Cl (labeled in Figure IV-18A), CH_2ClCHO (labeled in Figure IV-18B), and as yet unidentified species (residual spectrum of Figure IV-18C).

The time-concentration data obtained for this $\text{C}_2\text{H}_5\text{ONO}$ - NO -allyl chloride-air irradiation are given in Table IV-10. The errors accompanying the analyses for glycolaldehyde (HOCH_2CHO) and chloroacetaldehyde (CH_2ClCHO) are ~25%, compared to <10% for HCHO and HC(O)Cl , due to the inherently weak bands of glycolaldehyde and the overlapped bands of chloroacetaldehyde.

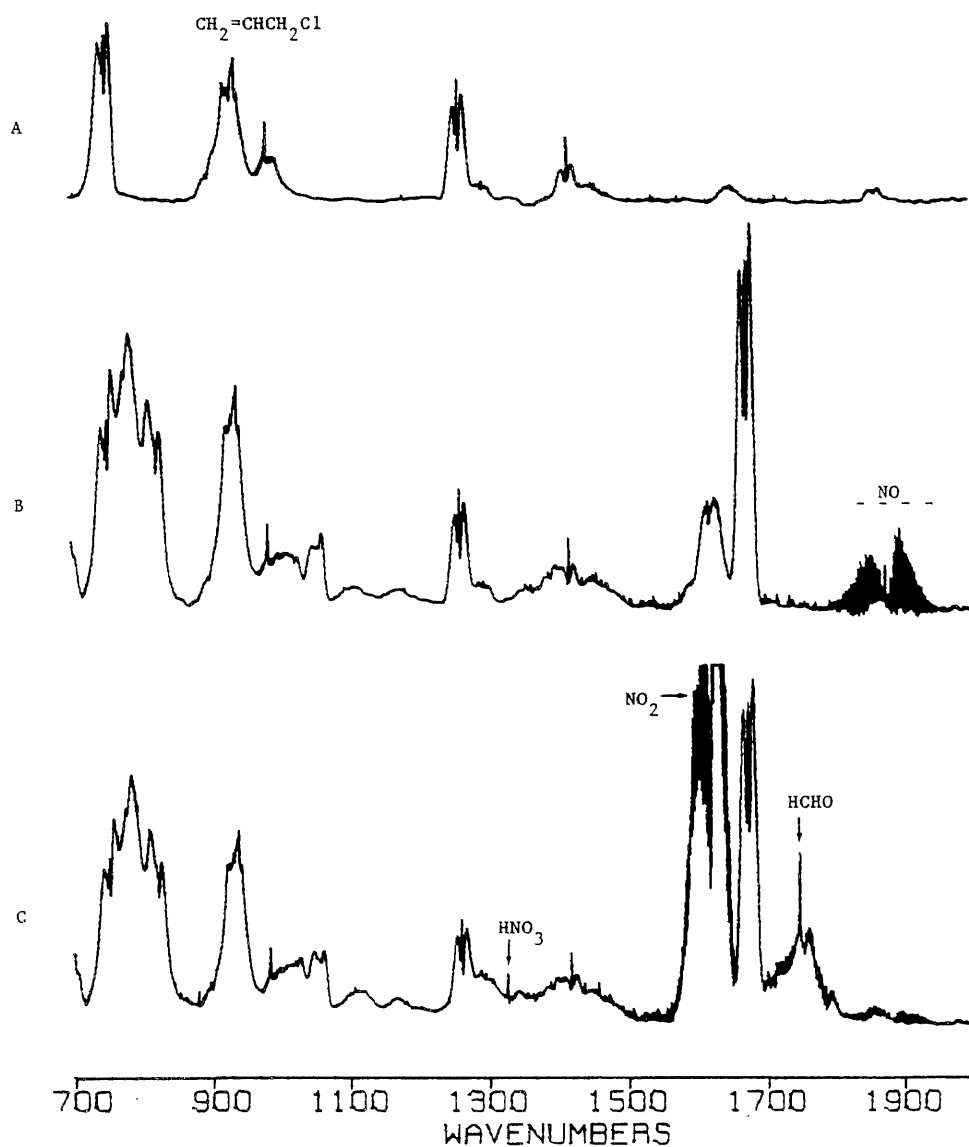


Figure IV-17. FT-IR spectra from the allyl chloride + OH reaction. (A) $\text{CH}_2=\text{CHCH}_2\text{Cl}$; (B) initial mixture of $\text{CH}_2=\text{CHCH}_2\text{Cl}$ (4.9×10^{14}), $\text{C}_2\text{H}_5\text{ONO}$ (2.4×10^{14}) and NO (1.9×10^{14}) [concentrations in units of molecule cm^{-3}]; (C) product spectrum after 9 min of irradiation.

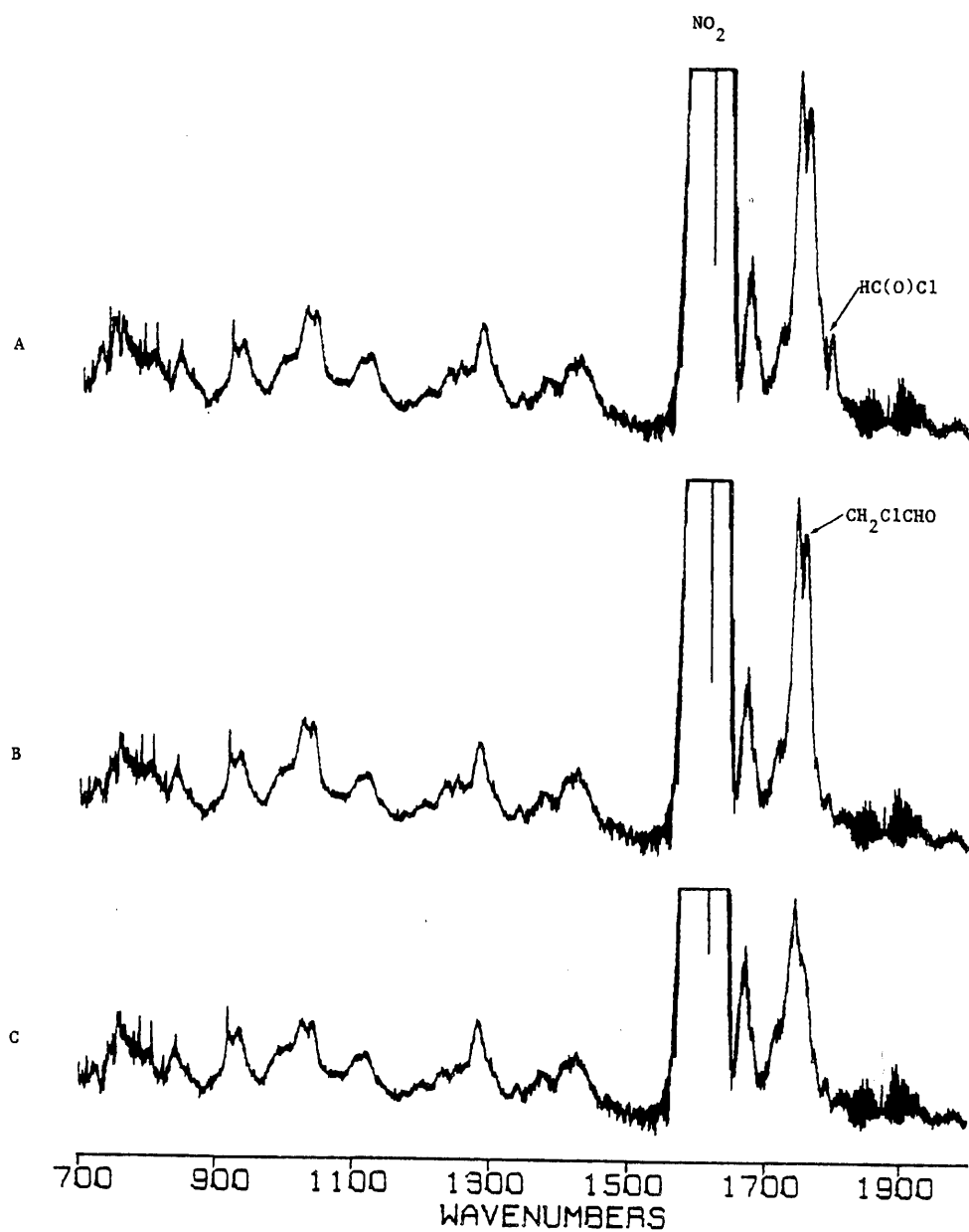
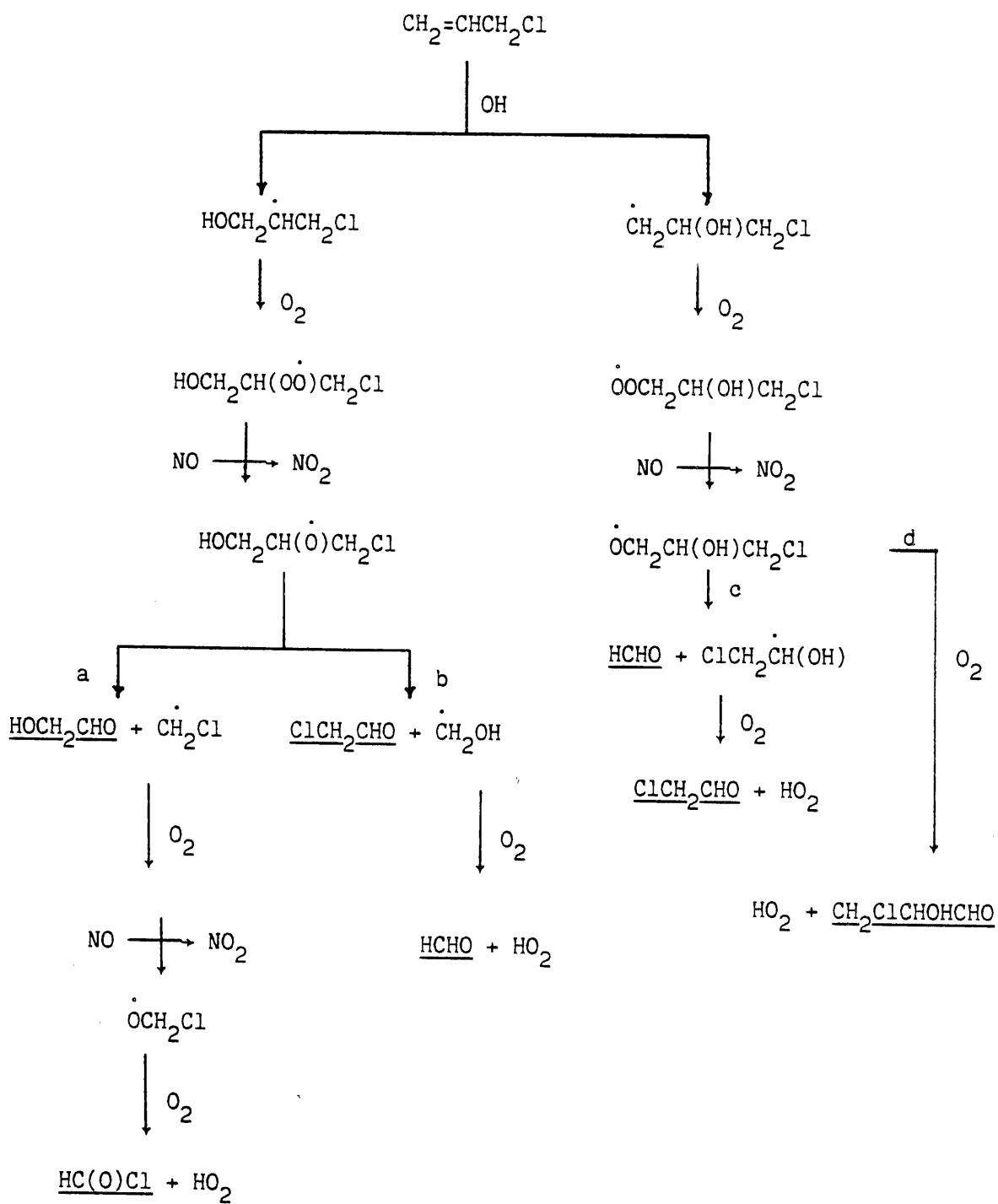


Figure IV-18. FT-IR spectra of products from allyl chloride. (A) Derived from Figure IV-17C by subtraction of absorptions by the reactants, HNO_3 , HONO , CH_3CHO , PAN, and HCHO ; (B) spectrum A minus HC(O)Cl absorptions; (C) residual spectrum of the unknown product(s) (after subtraction of CH_2ClCHO absorptions from spectrum B).

Table IV-10. Time-Concentration Data for an Irradiated $C_2H_5ONO-NO$ -Allyl Chloride-Air Mixture

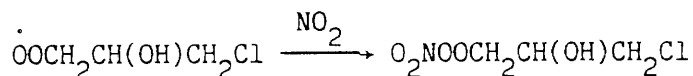
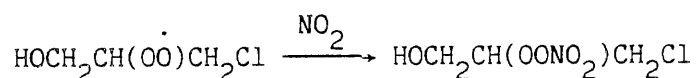
Irradiation Time (min)	10^{-13} x Concentration (molecule cm^{-3})				
	$CH_2=CHCH_2Cl$	HCHO	$HC(O)Cl$	$HOCH_2CHO$	$ClCH_2CHO$
-5	48.7				
1	44.9	0.70	-	-	1.1
5	40.3	2.09	0.26	0.2	2.4
9	36.7	3.00	0.36	0.5	3.1
13	35.0	3.62	0.46	0.7	3.6
17	33.8	3.91	0.48	0.7	4.1

Addition to the carbon-carbon double bond is calculated to be the favored mode of OH attack on allyl chloride (Atkinson 1986, 1987), with H-atom abstraction from the $-CH_2Cl$ group accounting for ~2% of the overall reaction.

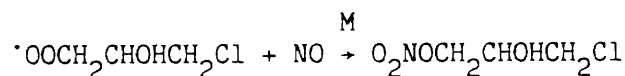
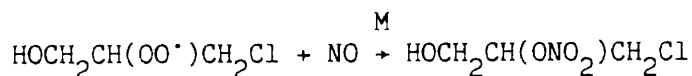


The above reaction scheme, where the "stable" products are underlined, is consistent with the product data summarized in Table IV-10. Thus, the yield of HCHO is equal to that of ClCH₂CHO, as are those of HC(O)Cl and HOCH₂CHO, within the error limits.

However, the above four products observed account only for 30-35% of the amount of allyl chloride reacting. Hence, the more likely explanations to account for the carbon balance, as well as interpret some features in the residual spectrum of Figure IV-18C involve alternative routes of reactions of the peroxy and/or alkoxy radicals which are formed following the initial OH attack on the double bond. Thus, the peroxy radical intermediates may react with NO₂ to yield peroxy nitrates

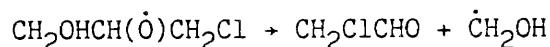


and with NO to yield, part of the time, nitrates



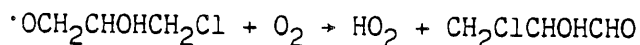
The infrared absorption bands characteristic of the alkyl peroxy nitrates (ROONO₂) are found at ~790, ~1300 and ~1730 cm⁻¹ (Niki et al. 1978). There are bands in Figure IV-18C at the approximate positions and the correct relative intensities which suggest the possible presence of the above organic peroxy nitrates. However, mere coincidences cannot be discounted since these bands may be overlapped by absorptions of other compounds. The distinct absorption bands at ~1670, ~1280 and ~850 cm⁻¹ strongly support the presence of an organic -ONO₂ group.

It is expected that the alkoxy radical CH₂OHCH(O·)CH₂Cl will decompose rather than react with O₂, with the major decomposition route being route (b) above.



The low yields of the identified products may also mean that for the ·OCH₂CHOHCH₂Cl radical, decomposition is not important, but that reaction

with O₂



predominates [route (d) above].

The overlap of C=O stretches with nearby peroxyxynitrate absorptions may indeed be the reason for the broad envelope of the total band at ~1750 cm⁻¹. Thus, the spectral evidence supports to a certain extent the speculation that the alkoxy radical intermediates from allyl chloride are sufficiently stable to undergo further reactions with O₂ to form products in addition to those which arise from their fragmentation.

D. Acrolein (CH₂=CHCHO)

The kinetics of the O₃ and OH radical reactions have been determined previously (Atkinson and Carter 1984, Atkinson 1984). Of these two reactions, that with OH radicals is calculated to dominate as an atmospheric loss process for acrolein (~1 day for the OH radical reaction versus ~60 days for the O₃ reaction). Therefore, we determined the rate constant at room temperature for the NO₃ radical reaction and, since this reaction was also calculated to be of minor importance as an atmospheric loss process compared to the OH radical reaction, carried out a product study of the OH radical reaction. These investigations are described below.

1. Kinetics of the NO₃ Radical Reaction

The experimental technique was that described in Section III. Experiments were carried out in the 5800-liter evacuable chamber, and acrolein and the reference organic (ethene) were monitored by long path-length FT-IR absorption spectroscopy. Acrolein was observed to react significantly faster than did ethene, and because of this disparity in the relative rate constants, the data exhibited an appreciable amount of scatter. Least-squares analysis of the experimental data obtained yield a rate constant ratio of

$$k(\text{acrolein})/k(\text{ethene}) = 5.4 \pm 0.8$$

where the error limit is two least-squares standard deviations. Use of a rate constant for the reaction of NO₃ radicals with ethene of $(2.3 \pm 0.4) \times 10^{-16} \text{ cm}^3 \text{ molecule}^{-1} \text{ s}^{-1}$ (Ravishankara and Mauldin 1984, Atkinson et al.

1987) allows this rate constant ratio to be placed on an absolute basis, yielding

$$k(\text{NO}_3 + \text{acrolein}) = (1.2 \pm 0.3) \times 10^{-15} \text{ cm}^3 \text{ molecule}^{-1} \text{ s}^{-1}$$

Use of this rate constant, together with those for the OH radical and O_3 reactions [$2.0 \times 10^{-11} \text{ cm}^3 \text{ molecule}^{-1} \text{ s}^{-1}$ and $2.8 \times 10^{-19} \text{ cm}^3 \text{ molecule}^{-1} \text{ s}^{-1}$, respectively (Atkinson and Carter 1984, Atkinson 1986)] allows the atmospheric lifetimes of acrolein due to these removal pathways to be calculated. As shown in Table IV-11, the OH radical reaction is clearly the dominant chemical tropospheric removal process for acrolein. Accordingly, we then studied the products of the OH radical reaction, as described below.

Table IV-11. Calculated Atmospheric Lifetimes of Acrolein Due to Reaction with OH and NO_3 Reactions and O_3

Reactive Species	Concentration (molecule cm^{-3})	Lifetime of Acrolein
OH	1×10^6 (12-hr daytime)	1.2 days
NO_3	2.4×10^8 (12-hr nighttime)	80 days
O_3	7×10^{11} (24-hr period)	60 days

2. Products of the OH Radical Reaction

Experiments were carried out in the 5800-liter evacuable chamber, as described in Section III above. Because of the expected formation of HCHO from acrolein, OH radicals were generated by photolysis of $\text{C}_2\text{H}_5\text{ONO}$ in air. The products of an irradiated mixture of acrolein ($3.8 \times 10^{14} \text{ molecule cm}^{-3}$), ethyl nitrite ($2.4 \times 10^{14} \text{ molecule cm}^{-3}$) and nitric oxide ($1.9 \times 10^{14} \text{ molecule cm}^{-3}$) were analyzed by FT-IR spectroscopy. The spectra of acrolein and the initial mixture of reactants are shown in Figure IV-19. Figure IV-20 is the spectrum after 18 min of irradiation

minus that prior to irradiation (Figure IV-19B), thus depicting the consumption of reactants and the formation of the various products. The products which are attributed to acrolein are CO, CO₂, HCHO, glycolaldehyde (HOCH₂CHO), ketene (H₂C=C=O), and a PAN-type compound which is being identified here as acryloyl peroxyxynitrate [CH₂=CHC(O)OONO₂]. The infrared spectral signatures of the latter three products are more clearly seen in the residual spectrum presented in Figure IV-20B, where the absorptions due to HCHO and CO have also been subtracted.

The absorption bands marked with asterisks in Figure IV-20B strongly support the identification of acryloyl peroxyxynitrate, since they are comprised of those characteristic of the PAN-compounds (~795, 1075, 1300, 1745 and 1820 cm⁻¹) [Stephens 1969] and those which indicate the presence of a vinyl group (~935 and 990 cm⁻¹). Furthermore, it was observed that the decomposition of this product in the dark was significantly enhanced (~60% loss in 50 min at room temperature) by addition of excess NO, a reaction which has been observed for other organic peroxyxynitrates (Niki et al. 1985).

The calibration for all reactants and relevant products were made with authentic samples, except for ketene and the peroxyxynitrate compound. For ketene an absorptivity value (base 10) of 16.0 cm⁻¹ atm⁻¹ for the R-branch at 2164 cm⁻¹ has been adopted from the literature (Hatakeyama et al. 1985). Acryloyl peroxyxynitrate was generated by irradiation of a mixture of acrolein (2.4 x 10¹⁴ molecule cm⁻³), Cl₂ (1.0 x 10¹⁴ molecule cm⁻³) and NO₂ (1.9 x 10¹⁴ molecule cm⁻³), from which a nitrogen balance yielded an absorptivity (base 10) of 6.6 cm⁻¹ atm⁻¹ for the 1075 cm⁻¹ band.

The time-concentration data for the above C₂H₅ONO-NO-acrolein-air irradiation are summarized in Table IV-12. The formation of most of the products are seen to be generally linear with respect to the amounts of acrolein reacting, with approximate yields of: CO, 62%; HCHO, 35%; H₂C=C=O, initially ~15%, decreasing during the irradiation; and HOCH₂CHO, 14%. However, the yield of acryloyl peroxyxynitrate rose from ~16% after 1 min to ~53% after 18 min of irradiation, suggesting that the delayed but rapid rise in concentration was dependent on the build-up of sufficient concentrations of NO₂.

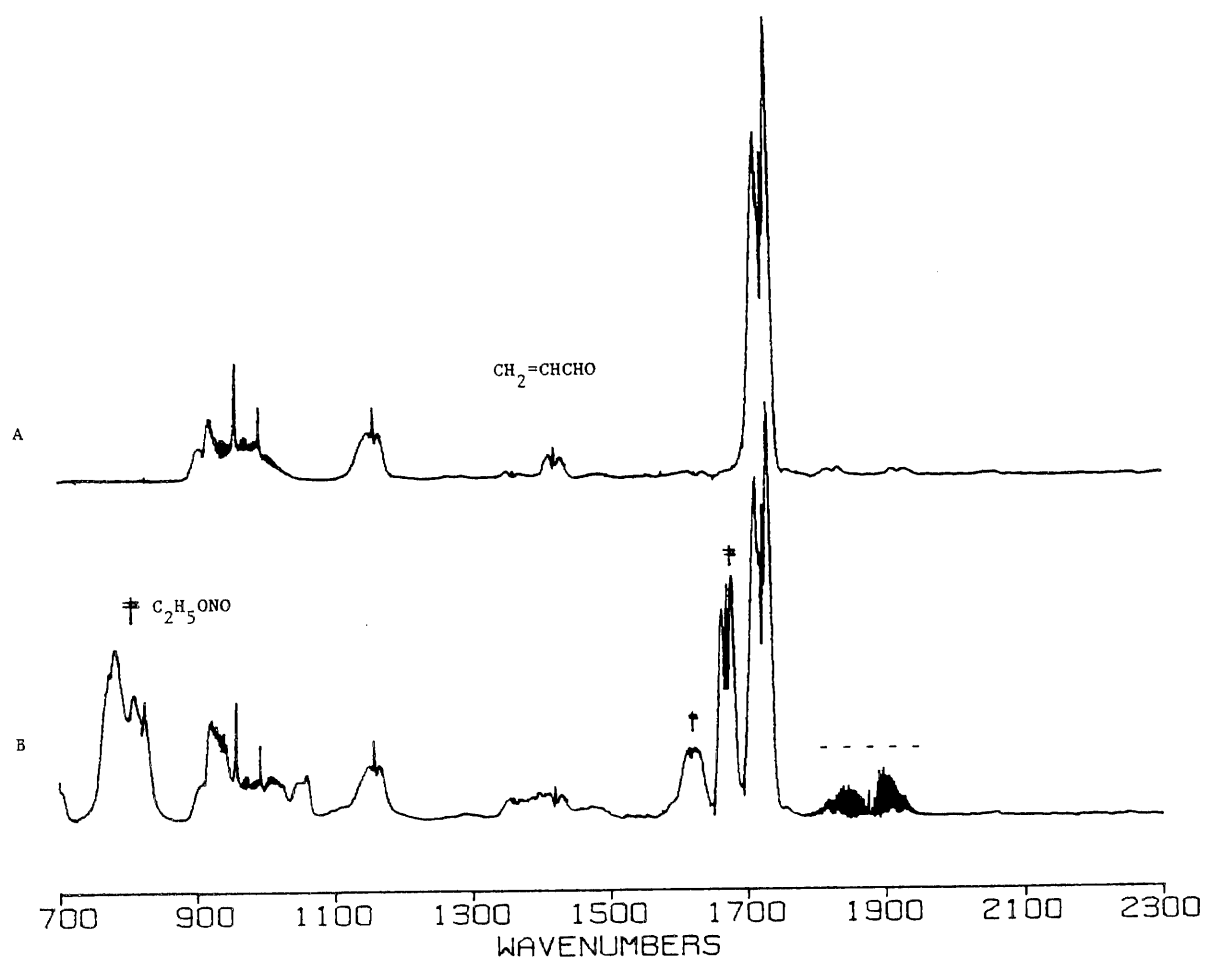


Figure IV-19. FT-IR absorption spectra of (A) acrolein and (B) the $\text{C}_2\text{H}_5\text{ONO}$ -NO-acrolein-air reactant mixture.

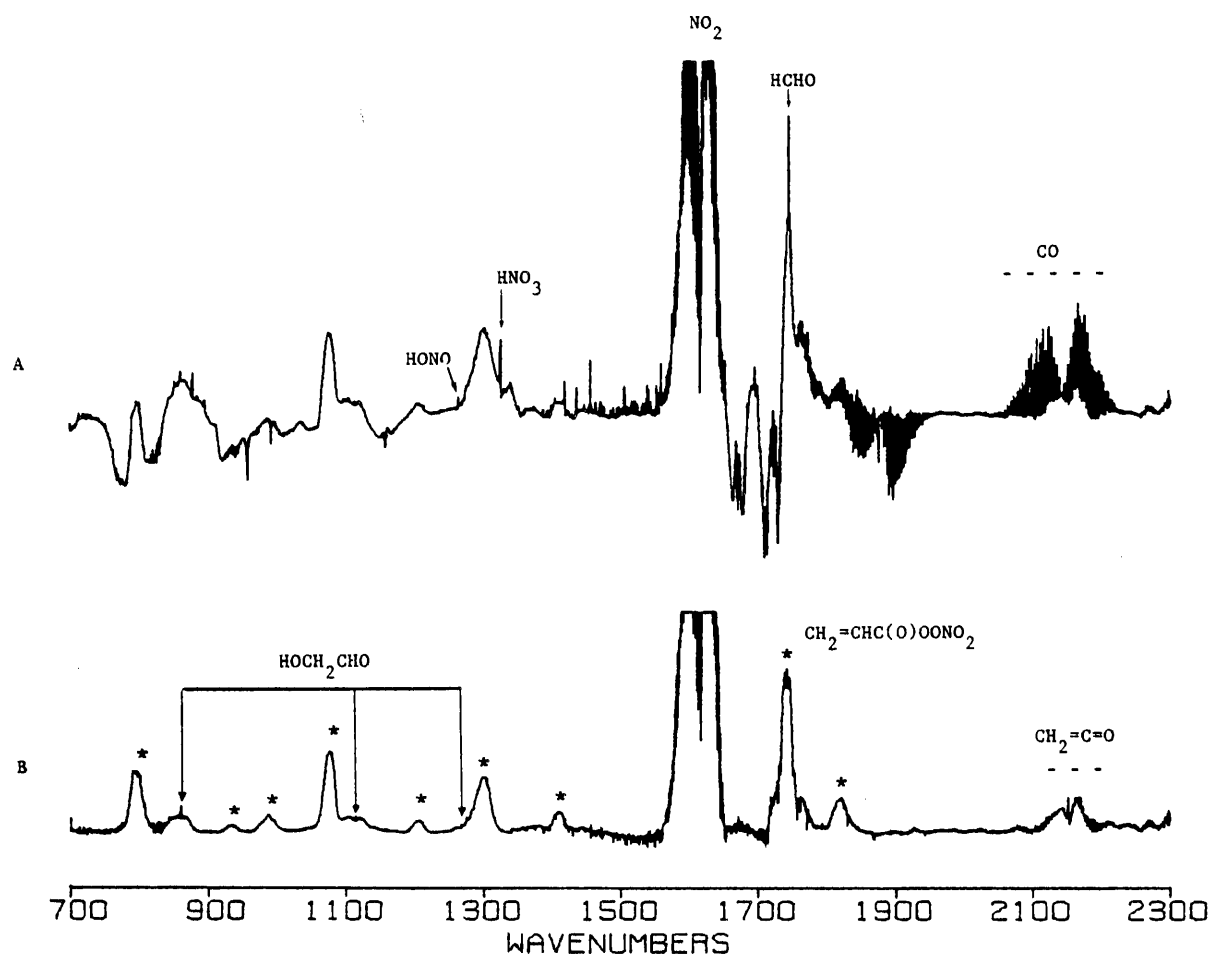


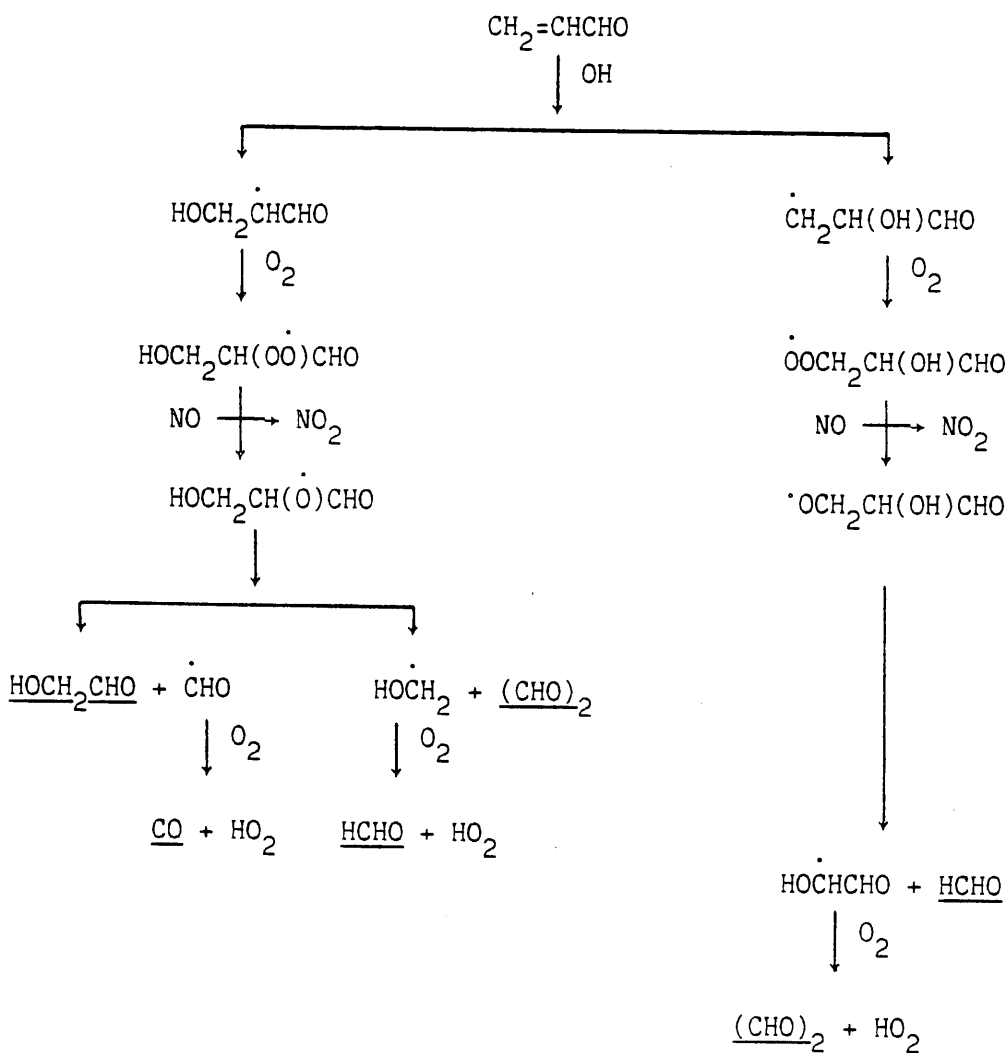
Figure IV-20. FT-IR absorption spectra of (A) the reactant mixture after 18 min irradiation, with the initial reactant spectrum (Figure IV-19B) subtracted and (B) after subtraction of absorptions due to CO and HCHO.

Table IV-12. Time-Concentration Data for an Irradiated $\text{CH}_2=\text{CHCHO}/\text{C}_2\text{H}_5\text{ONO}/\text{NO}$ -Air Mixture^{a,b}

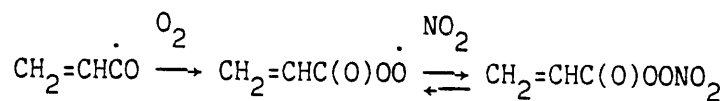
Elapsed Time (min)	$10^{-13} \times \text{Concentration (molecule cm}^{-3}\text{)}$					
	$\text{CH}_2=\text{CHCHO}$	CO	HCHO	HOCH_2CHO	$\text{CH}_2=\text{CHC(O)OONO}_2$	$\text{CH}_2=\text{C=O}$
-	38.6					
1	36.0	1.63	0.98	0.22	0.41	0.38
4	33.4	3.38	1.92	0.77	1.39	0.53
10	29.8	5.28	2.90	1.32	3.58	0.84
18	27.4	6.86	3.67	1.85	5.93	1.03

^aInitial concentration (molecule cm^{-3}): $\text{CH}_2=\text{CHCHO}$, 3.86×10^{14} ; $\text{C}_2\text{H}_5\text{ONO}$, 2.40×10^{14} ; NO, 1.92×10^{14} .

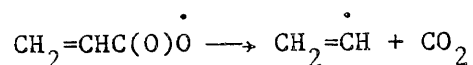
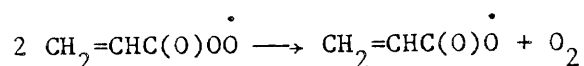
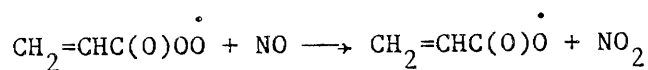
From a consideration of the observed products it appears that both addition and abstraction routes occur in the reaction of OH radicals with acrolein. This is consistent with inferences drawn from kinetic data, with Atkinson (1986) concluding that H-atom abstraction from the -CHO group is the dominant reaction pathway. The generally well-accepted scheme for OH radical addition to the carbon-carbon double bond is given below for acrolein, with the "stable" products being underlined. This is consistent with the observed formation of HOCH_2CHO , HCHO and CO. The scheme also predicts glyoxal $(\text{CHO})_2$ to be a major product of the OH radical addition route, with its yield being equal to that of the HCHO formed from the OH radical addition route. Due to the nature of interferences in the C=O stretch and C-H stretch regions of the infrared spectrum, and the inherently weak band intensities of glyoxal, its presence as a product could not be established at concentrations below an estimated detection limit of $\sim 3.6 \times 10^{13}$ molecule cm^{-3} .



The observed high yields of acryloyl peroxyxynitrate (Table IV-12) indicate that abstraction of the aldehydic hydrogen (Atkinson 1986) is the dominant initial mode of attack of the OH radical on acrolein:

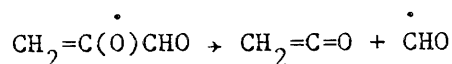
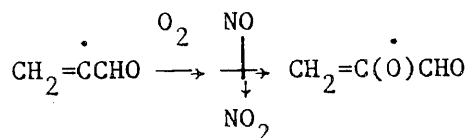


The organic peroxy radical can also undergo the following processes (Atkinson and Lloyd 1984):



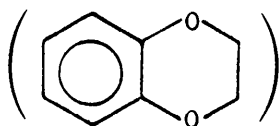
which explains the apparent lag in the formation of the peroxyacrylate during the early part of the irradiation when the NO/NO₂ concentration ratio was high. If vinyl (CH₂=CH[•]) radicals are indeed formed, they react with O₂ to yield HCHO and HCO (Slagle et al. 1984), and this may contribute to the observed yields of HCHO and CO.

The observed formation of ketene is difficult to rationalize, but appears consistent only with the (unlikely) occurrence of H-abstraction from the carbon atom adjacent to the carbonyl group:

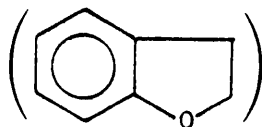


It was shown that the formation of ketene did not involve the peroxy radical CH₂CHC(O)OO[•], since the addition of excess NO to the reaction mixture resulted in the accelerated decomposition of acryloyl peroxyacrylate, to produce the peroxy radical, but was not accompanied by an increase in the concentration of ketene.

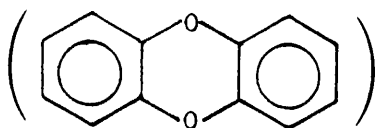
E. 1,4-Benzodioxan



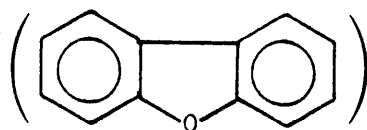
and 2,3-Dihydrobenzofuran



As discussed in Section II, these two compounds were chosen as volatile model compounds for the dibenzo-p-dioxans



and the dibenzofurans



As described below, we investigated the kinetics of the reactions of OH and NO₃ and O₃ with these compounds, and determined that the OH radical reactions were important loss processes for these two model compounds, and that the OH radical reaction will be the sole important chemical loss process for the dibenzo-p-dioxans and dibenzofurans and their chlorinated and brominated homologues. Accordingly, we studied the products of the OH radical reactions with 1,4-benzodioxan and 2,3-dihydrobenzofuran.

1. Kinetics of the Reactions with O₃

The rate constants for the reactions of O₃ with 1,4-benzodioxan and 2,3-dihydrobenzofuran were determined using the technique described in Section III above. The concentrations of the organic reactants were calculated from the amounts of compound introduced into the reaction chamber and the measured volume of the bag. The measured O₃ decay rates for these experiments are given in Table IV-13. The O₃ decay rates in the presence of 1,4-benzodioxan and 2,3-dihydrobenzofuran were indistinguishable from the background O₃ decay rates in the absence of added reactant,

Table IV-13. Experimental Data for the Reactions of O_3 with 1,4-Benzodioxan and 2,3-Dihydrobenzofuran at 297 ± 2 K

Compound	Concentration (molecule cm^{-3})	$10^5 \times O_3$ Decay Rate (s^{-1})
1,4-Benzodioxan	2.5×10^{14}	1.8
	1.25×10^{15}	1.5
	-	1.7
	-	2.8
2,3-Dihydrobenzofuran	2.8×10^{14}	2.8

within the experimental error limits. Thus, only upper limits to the rate constants could be obtained. Making the conservative assumption that all of the observed O_3 decay rates were due to reaction with 1,4-benzodioxan and 2,3-dihydrobenzofuran, the following upper limits to the O_3 reaction rate constants at 297 ± 2 K are obtained:

$$k(1,4\text{-benzodioxan}) < 1.2 \times 10^{-20} \text{ cm}^3 \text{ molecule}^{-1} \text{ s}^{-1}$$

$$k(2,3\text{-dihydrobenzofuran}) < 1.0 \times 10^{-19} \text{ cm}^3 \text{ molecule}^{-1} \text{ s}^{-1}$$

2. Kinetics of the Reactions with NO_3 Radicals

The rate constants for the gas-phase reactions of the NO_3 radical with 1,4-benzodioxan and 2,3-dihydrobenzofuran were determined using the experimental technique described in Section III above. Experiments were carried out in the 5800-liter evacuable chamber. 1,4-Benzodioxan was monitored by long pathlength FT-IR absorption spectroscopy, while 2,3-dihydrobenzofuran was analyzed by GC-FID, using a 6 ft. x 0.25 in. glass column packed with Super Pak 20M, temperature programmed from 328 to 373 K at 4 K min^{-1} . For these analyses, gas samples of 100 cm^3 volume were collected from the chamber onto Tenax GC solid adsorbent, and then thermally desorbed at $\sim 525 \text{ K}$ onto the head of the GC column which was at 328 K, followed by the temperature programming noted above. Propene and

trans-2-butene were used, respectively, as the reference compounds for the experiments involving 1,4-benzodioxan and 2,3-dihydrobenzofuran. These alkenes were monitored by GC-FID, using a 20 ft. x 0.125 in. stainless steel (SS) column with 5% DC703/C20M on 100/120 mesh AW, DMCS Chromosorb G, operated at 333 K for trans-2-butene and a 36 ft. x 0.125 in. SS column of 10% 2,4-dimethylsulfolane on C-22 firebrick (60/80 mesh), operated at 273 K for propene.

1,4-Benzodioxan was observed to decay in the chamber in the dark, presumably to the walls, with a decay rate of $\sim 6 \times 10^{-6} \text{ s}^{-1}$, and this dark decay rate was taken into account in the derivation of the rate constant ratio for this compound. However, because of the low amounts of 1,4-benzodioxan consumed in these experiments (6-8%), the corrections for the dark decays were a substantial fraction of the overall disappearance rate of 1,4-benzodioxan, leading to relatively large uncertainties in the rate constant ratio derived.

For 2,3-dihydrobenzofuran, experiments were carried out with the initial NO_2 concentrations being varied between 5×10^{13} and 2.4×10^{14} molecule cm^{-3} . The data obtained for 2,3-dihydrobenzofuran are plotted in Figure IV-21, and the rate constant ratio derived by least-squares analysis of these data is given in Table IV-14. Using rate constants for the reaction of NO_3 radicals with propene and trans-2-butene of $(9.2 \pm 1.1) \times 10^{-15} \text{ cm}^3 \text{ molecule}^{-1} \text{ s}^{-1}$ and $(3.8 \pm 0.4) \times 10^{-13} \text{ cm}^3 \text{ molecule}^{-1} \text{ s}^{-1}$, respectively (Ravishankara and Mauldin 1985, Atkinson et al. 1987), these lead to rate constants at $298 \pm 2 \text{ K}$ of

$$k(\text{NO}_3 + 1,4\text{-benzodioxan}) = (5.8 \pm 3.0) \times 10^{-16} \text{ cm}^3 \text{ molecule}^{-1} \text{ s}^{-1}$$

and

$$k(\text{NO}_3 + 2,3\text{-dihydrobenzofuran}) = (1.1 \pm 0.3) \times 10^{-13} \text{ cm}^3 \text{ molecule}^{-1} \text{ s}^{-1}$$

3. Kinetics of OH Radical Reactions with 1,4-Benzodioxan and 2,3-Dihydrobenzofuran

The rate constants for the reactions of OH radicals with 1,4-benzodioxan and 2,3-dihydrobenzofuran were determined using the relative rate technique described in Section III above. Experiments were carried out in the 5800-liter evacuable chamber with 1,4-benzodioxan and 2,3-

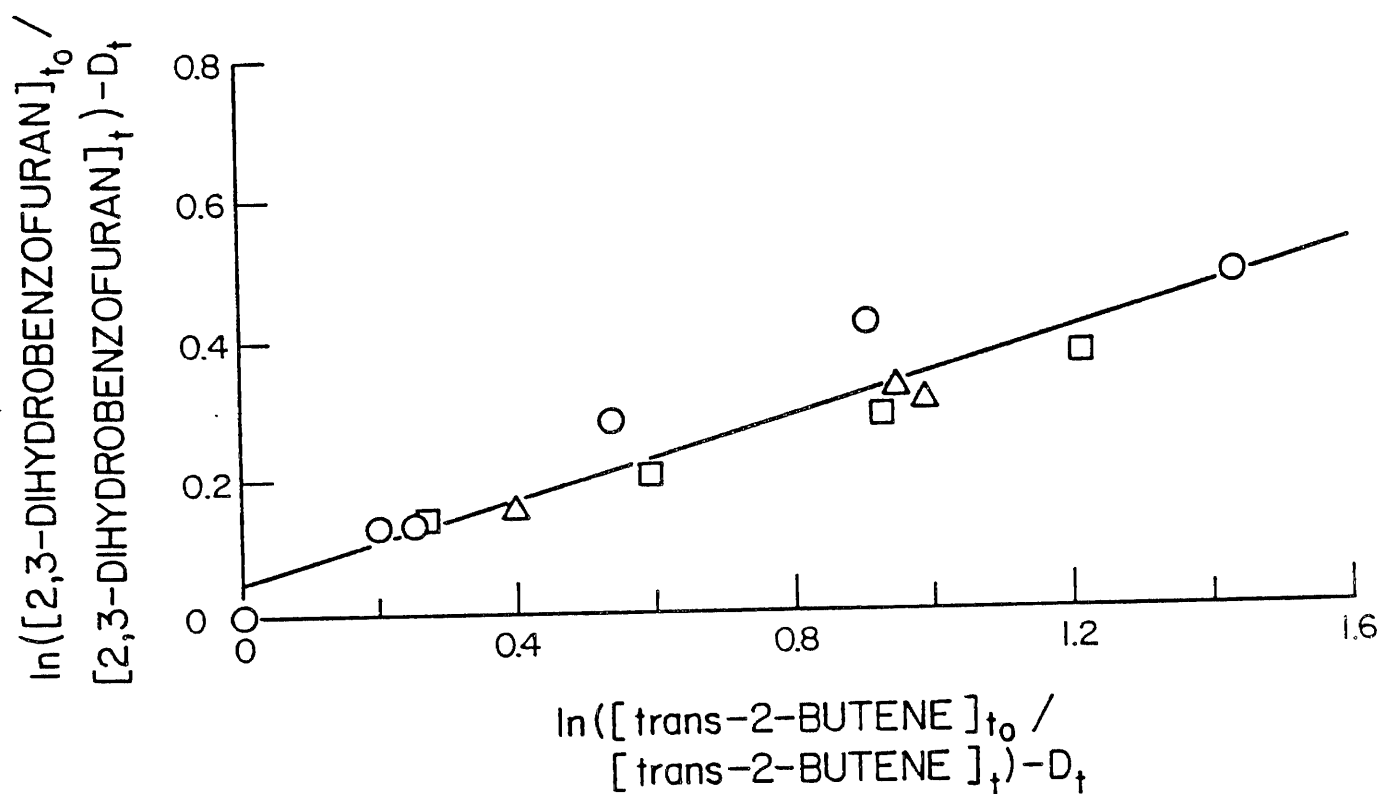


Figure IV-21. Plot of equation (VII) for the reaction of NO_3 radicals with 2,3-dihydrobenzofuran, with trans-2-butene as the reference alkene. The initial NO_2 concentrations were: Δ - 5×10^{13} molecule cm^{-3} , \square - 1.2×10^{14} molecule cm^{-3} , and \circ - 2.4×10^{14} molecule cm^{-3} .

Table IV-14. Rate Constant Ratios for the Gas-Phase Reactions of 1,4-Benzodioxan and 2,3-Dihydrobenzofuran with NO_3 Radicals at 298 ± 2 K

Aromatic	Rate Constant Ratio	
	Relative to $k(\text{propene}) = 1.00$	Relative to $k(\text{trans-2-butene}) = 1.00$
1,4-Benzodioxan	0.063 ± 0.031	
2,3-Dihydrobenzofuran		0.295 ± 0.063

^aIndicated error limits are two deviations least-squares standard deviations.

dihydrobenzofuran being monitored by long pathlength FT-IR absorption spectroscopy. Propene, which was used as the reference organic, was also monitored by long pathlength FT-IR absorption spectroscopy.

The experimental data obtained are plotted in accordance with equation (III) in Figure IV-22, and the rate constant ratios determined from the slopes of these plots by least-squares analyses are given in Table IV-15. These rate constant ratios can be placed on an absolute basis by using a rate constant for the reaction of OH radicals with propene of $2.63 \times 10^{-11} \text{ cm}^3 \text{ molecule}^{-1} \text{ s}^{-1}$ (Atkinson 1986), and these rate constants are also given in Table IV-15.

Based upon the rate constants for the reactions of 1,4-benzodioxan and 2,3-dihydrobenzofuran with OH and NO_3 radicals and the upper limits to the rate constants for the O_3 reactions, the atmospheric lifetimes due to those reaction processes can be calculated. These calculated atmospheric lifetimes, using ambient atmospheric concentrations of O_3 of $7 \times 10^{11} \text{ molecule cm}^{-3}$ (Singh et al. 1978, Oltmans 1981), of OH radicals of $1 \times 10^6 \text{ molecule cm}^{-3}$ during daytime hours (Crutzen 1982) and of NO_3 radicals of $2.4 \times 10^8 \text{ molecule cm}^{-3}$ during nighttime hours (Platt et al. 1984, Atkinson et al. 1986b), are given in Table IV-16.

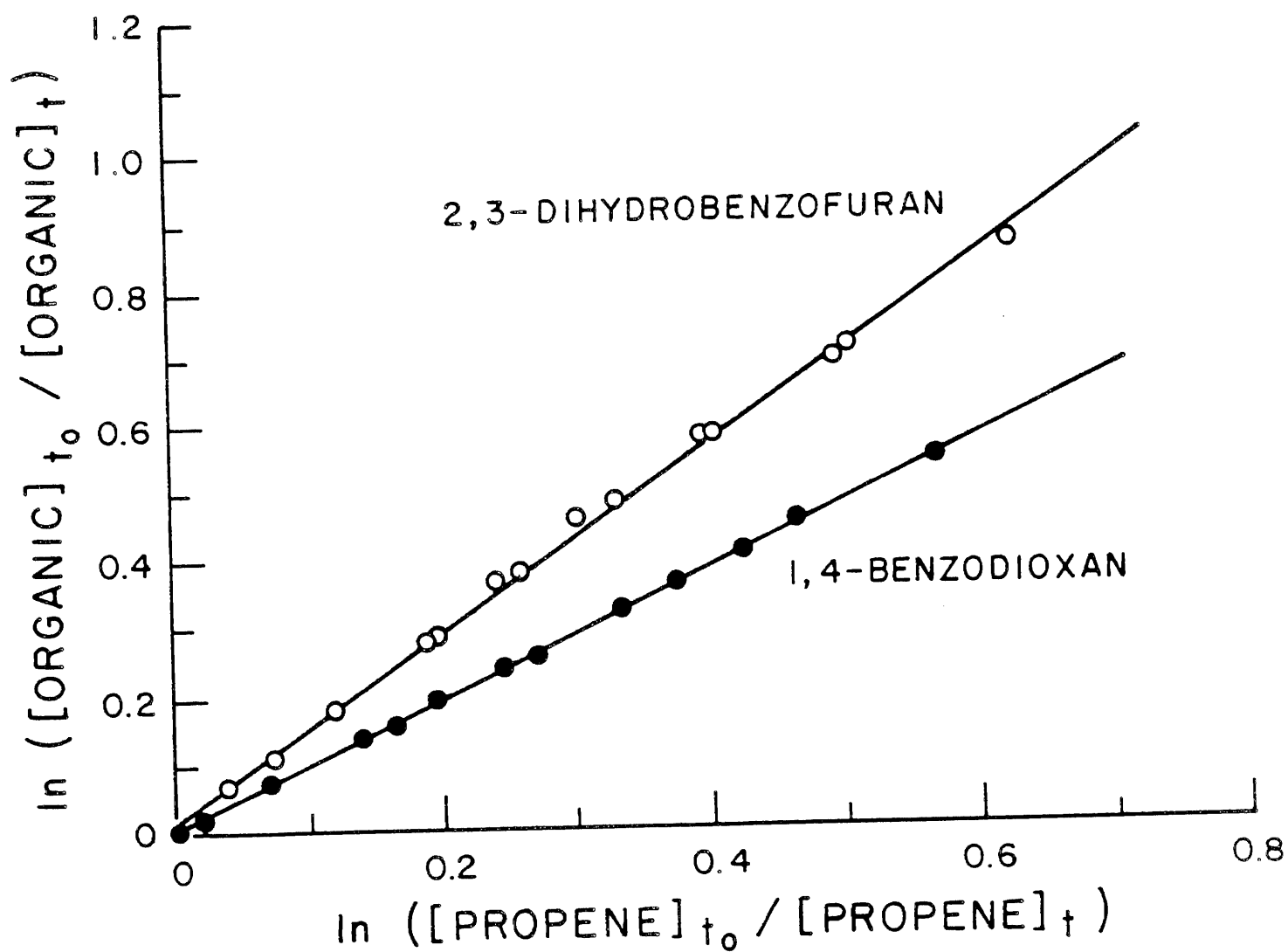


Figure IV-22. Plot of equation (III) for the gas-phase reaction of OH radicals with 1,4-benzodioxan and 2,3-dihydrobenzofuran, with propene as the reference organic.

Table IV-15. Rate Constant Ratios and Rate Constants for the Reactions of OH Radicals with 1,4-Benzodioxan and 2,3-Dihydrobenzofuran

Aromatic	Rate Constant	
	Ratio ^a	$10^{11} \times k^{\text{OH}}$ ($\text{cm}^3 \text{ molecule}^{-1} \text{ s}^{-1}$) ^{a,b}
1,4-Benzodioxan	0.959 ± 0.013	2.52 ± 0.04
2,3-Dihydrobenzofuran	1.39 ± 0.04	3.66 ± 0.11

^aIndicated errors are two least-squares standard deviations.

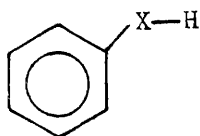
^bPlaced on an absolute basis by use of a rate constant for the reaction of OH radicals with propene of $2.63 \times 10^{-11} \text{ cm}^3 \text{ molecule}^{-1} \text{ s}^{-1}$ (Atkinson 1986).

Table IV-16. Calculated Atmospheric Lifetimes of 1,4-Benzodioxan and 2,3-Dihydrobenzofuran Due to Reaction with OH and NO₃ Radicals and O₃

Aromatic	Lifetime Due to Reaction with		
	OH	NO ₃	O ₃
1,4-Benzodioxan	11 hr	165 days	>3.8 yr
2,3-Dihydrobenzofuran	7.6 hr	11 hr	>165 days

The data in this table show that for 1,4-benzodioxan the dominant atmospheric chemical removal process is by OH radical reaction, while 2,3-dihydrobenzofuran is calculated to be removed from the atmosphere by reaction with both OH and NO₃ radicals. However, the kinetic data obtained to date for the reaction of NO₃ radicals with aromatic compounds indicate that the NO₃ radical reaction with 2,3-dihydrobenzofuran proceeds mainly via H-atom abstraction from the -CH₂- group attached to the aromatic ring.

Thus, the room temperature NO_3 radical rate constants for phenol and the cresols are a factor of $\sim 10^5$ higher than that for methoxybenzene, and that for 1,4-benzodioxan is lower by an order of magnitude than the NO_3 radical rate constant for tetralin (Table IV-17). This shows that NO_3 radical addition to the aromatic ring cannot be the important overall process. Indeed, these data indicate that the higher room temperature NO_3 radical reaction rate constants are associated with aromatic compounds having the general structure,



with $\text{X} = \text{C}$ or O . As suggested by Carter et al. (1981), this structural requirement allows the formation of a six-membered ring transition state after (reversible) addition of NO_3 radicals to the aromatic ring, which is expected to facilitate the overall H-atom abstraction process.

Since the rate constant for the reaction of NO_3 radicals with 2,3-dihydrobenzofuran is a factor of ~ 200 higher than that for 1,4-benzodioxan, the NO_3 radical reaction with 2,3-dihydrobenzofuran presumably proceeds via overall H-atom abstraction from the $-\text{CH}_2-$ group attached to the aromatic ring. It appears, however, that these NO_3 radical reaction rate constants are sensitive to the actual substituent groups and their configuration, since it would be expected that the room temperature rate constant for 2,3-dihydrobenzofuran would be approximately the same or lower than that for tetralin. However, the NO_3 radical rate constant for 2,3-dihydrobenzofuran is a factor of ~ 10 higher than that for tetralin.

These data indicate that NO_3 radical addition to aromatic ring systems to yield stable NO_3 -aromatic adducts is of negligible importance as an atmospheric loss process. Hence, it can be concluded that the gas-phase reactions of the NO_3 radical with dibenzo-p-dioxan and dibenzofuran, and with their chlorinated and brominated homologues, will be of negligible importance as atmospheric loss processes. For this reason, we investigated only the products of the OH radical reactions with 1,4-benzodioxan and 2,3-dihydrobenzofuran, as described below.

Table IV-17. Rate Constants k for the Gas-Phase Reaction of NO_3 Radicals with a Series of Aromatic Compounds at Room Temperature

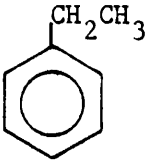
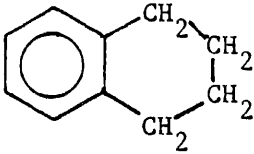
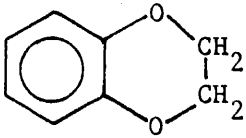
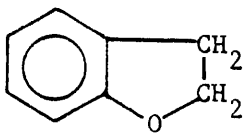
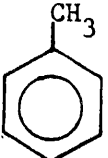
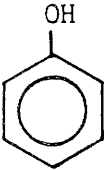
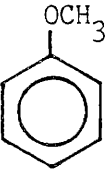
Aromatic Compound	Structure	k ($\text{cm}^3 \text{ molecule}^{-1} \text{ s}^{-1}$)
Ethylbenzene		$\leq 6 \times 10^{-16}^a$
Tetralin		$1.1 \times 10^{-14}^a$
1,4-Benzodioxan		$5.8 \times 10^{-16}^a$
2,3-Dihydrobenzofuran		$1.1 \times 10^{-13}^a$
Toluene		$7.1 \times 10^{-17}^b$

Table IV-17 (continued) - 2

Aromatic Compound	Structure	k (cm ³ molecule ⁻¹ s ⁻¹)
Phenol		3.8 x 10 ⁻¹² ^b
Methoxybenzene		~2 x 10 ⁻¹⁶ ^b

^aFrom this study.^bFrom Atkinson et al. (1984c), re-evaluated to be consistent with the rate constants for the reference compounds used in this work.

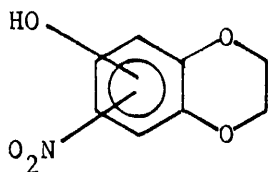
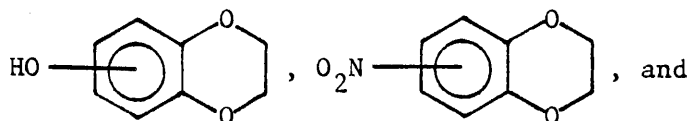
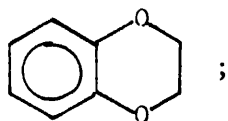
4. Products of the OH Radical Reactions with 1,4-Dibenzodioxan and 2,3-Dihydrobenzofuran

Experiments to investigate the products of the gas-phase reactions of the OH radical with these aromatic compounds were carried out, in the presence of NO_x, in both the 5800-liter evacuable and 6400-liter all-Teflon chambers. In both chambers, OH radicals were generated by the photolysis of CH₃ONO in air.

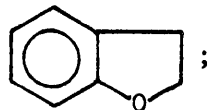
Initial reactions were carried out in the 6400-liter all-Teflon chamber, with the initial reactant concentrations being (in molecule cm⁻³ units): CH₃ONO, ~2.4 x 10¹⁴; NO, ~2.4 x 10¹⁴; 1,4-benzodioxan or 2,3-dihydrobenzofuran, 2.4 x 10¹³. These reactant mixtures were irradiated for either 1.0 min (2,3-dihydrobenzofuran) or 2.0 min (1,4-benzodioxan), and in both cases gas samples of ~3000-4000 liters were collected on

polyurethane foam (PUF) plugs. The 1,4-benzodioxan and 2,3-dihydrobenzofuran concentrations at the termination of the irradiations were measured by GC-FID, with no observable amount of 1,4-benzodioxan remaining after the 2.0-min irradiation period, and with 1.4×10^{13} molecule cm^{-3} (or ~60%) of the 2,3-dihydrobenzofuran remaining after the 1.0-min irradiation. After extraction with dichloromethane, the reactants and products were analyzed by combined gas chromatography-mass spectrometry (GC-MS) using a Finnigan 3200 GC-MS interfaced to a Technivent data system. The total ion chromatograms (TIC) obtained from these two experiments are shown in Figures IV-23 and IV-24, together with tentative identifications based on the masses of the ions observed. These data show that the following products were tentatively identified from the OH radical-initiated reactions:

From



From



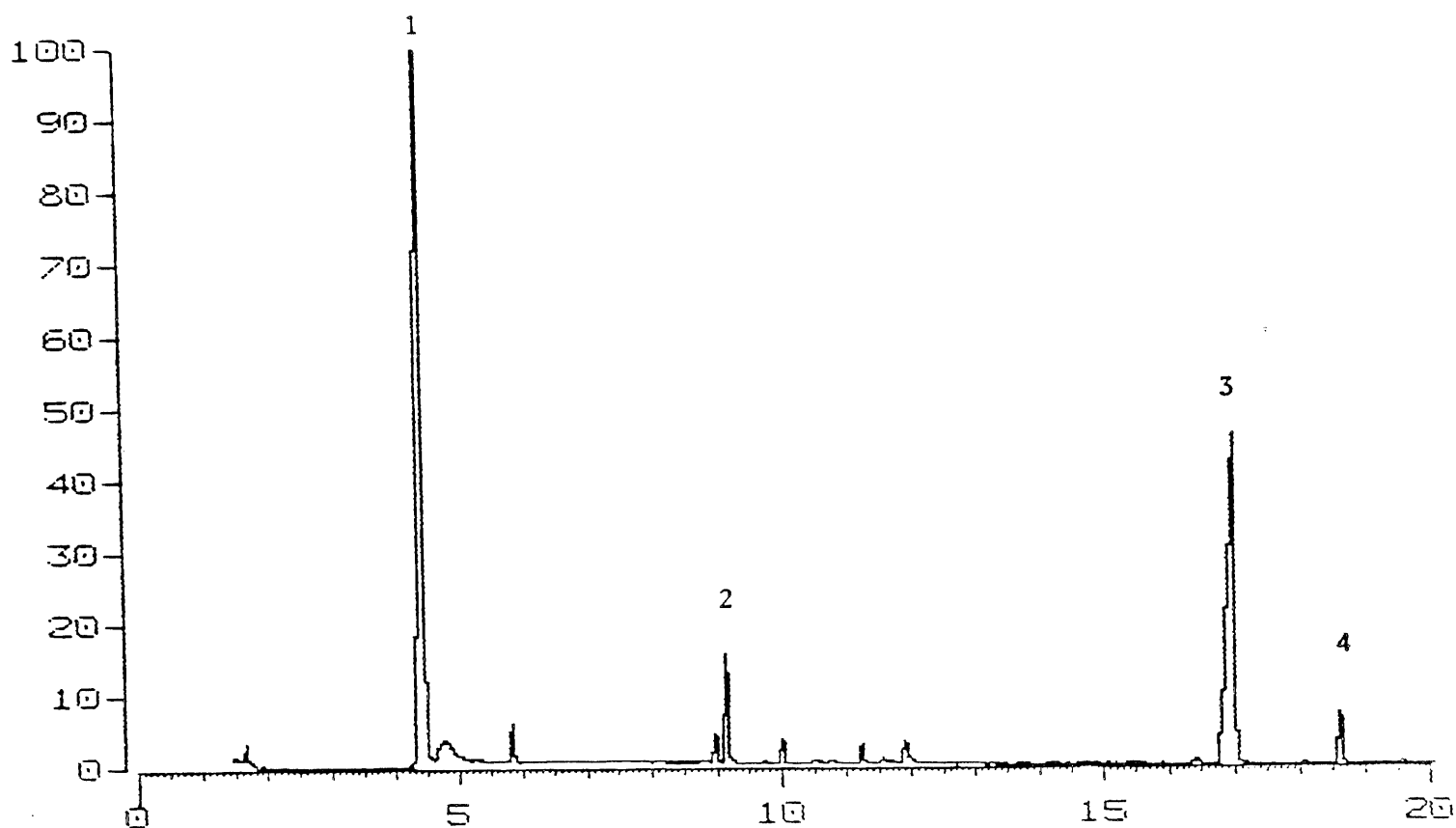


Figure IV-23. Total ion current (TIC) trace for the GC/MS analysis of the dichloromethane extract of a ~4000-liter PUF plug chamber sample from the OH radical reaction of 1,4-benzodioxan. Peak #1 is unreacted 1,4-benzodioxan. The product peaks are tentatively identified from their mass spectra as: peak #2, hydroxy-; peak #3, nitro-; and peak #4, hydroxynitro-derivatives of 2,4-benzodioxan.

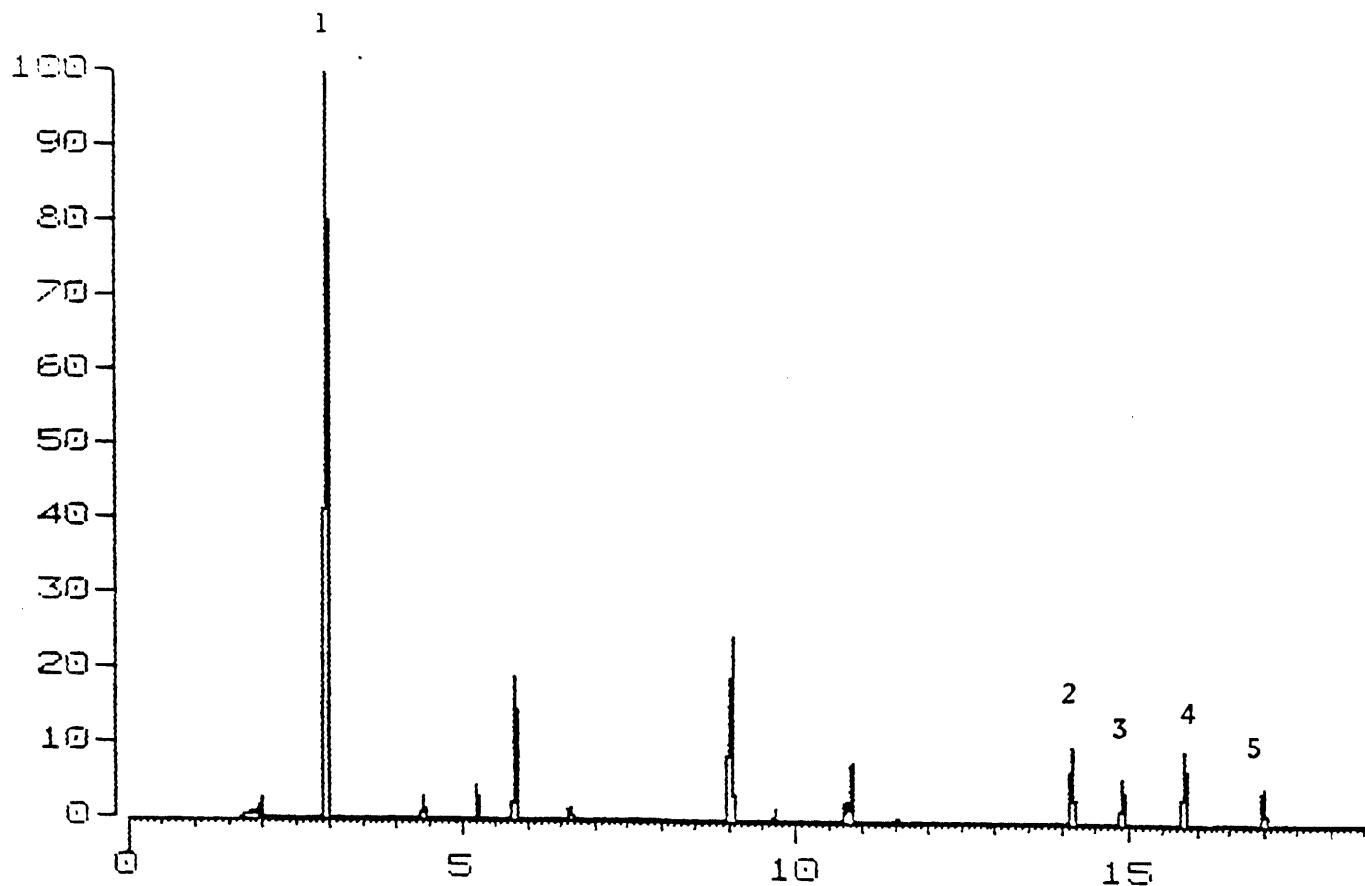
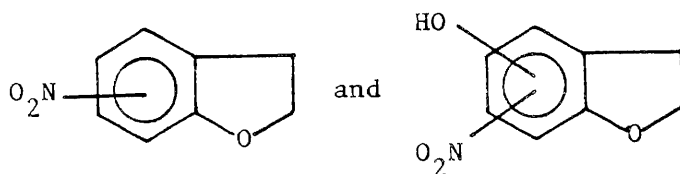


Figure IV-24. TIC trace for the GC/MS analysis of the dichloromethane extract of a ~4000-liter PUF plug chamber sample from the OH radical reaction of 2,3-dihydrobenzofuran. Peak #1 is unreacted 2,3-dihydrobenzofuran. The product peaks, numbers 2, 3, 4 and 5, have been tentatively identified from their mass spectra as: peaks 2 and 3, nitro-isomers of 2,3-dihydrobenzofuran; peaks 4 and 5, hydroxynitro-isomers of dihydrobenzofuran.



Due to lack of authentic samples of these compounds, isomer-specific identification of these products was not possible.

In an effort to further investigate the products of these reactions, corresponding irradiations were carried out in the 5800-liter evacuable chamber with long pathlength FT-IR analysis of products. The initial reactant concentrations for these irradiations were (in molecule cm^{-3}): 1,4-benzodioxan or 2,3-dihydrobenzofuran, 1.7×10^{14} ; CH_3ONO , 2.4×10^{14} ; and NO , 2.4×10^{14} . In addition, Cl atom sensitized oxidation of 1,4-benzodioxan and 2,3-dihydrobenzofuran were carried out by irradiations of similar concentrations of these two compounds with Cl_2 (1.8×10^{14}) and NO (9×10^{13}), with the objective of generating some products common with those of the OH radical reaction in a "spectroscopically simpler" system. Reference spectra of 1,4-benzodioxan and 2,3-dihydrobenzofuran are given in Figure IV-25 and residual spectra characterizing the products are presented in Figures IV-26 and IV-27.

Figure IV-26A is the spectrum of products from the 1,4-benzodioxan- CH_3ONO - NO -air irradiation after 10 mins irradiation when 1.0 ppm (2.4×10^{13} molecule cm^{-3}) of 1,4-benzodioxan has reacted, while Figure IV-26B is the spectrum after 43 min of irradiation, with a corresponding 3.3 ppm (7.9×10^{13} molecule cm^{-3}) loss of the reactant. There are at least two major groups of bands in the above residual spectra, with the pair at ~ 1520 and ~ 1345 cm^{-1} being the most conspicuous because of their accelerated growth during the course of the irradiation. The positions of these two bands are consistent with the presence of $-\text{NO}_2$ group substitution in the aromatic ring. The growth of a band in the $\text{C}=\text{O}$ stretch region indicates that products are being formed which most likely arise from the attack of the OH radical on the saturated ring.

Figure IV-26C is the residual spectrum from the 1,4-benzodioxan- Cl_2 - NO -air irradiation after 17 min of irradiation when 3 ppm (7.2×10^{13} molecule cm^{-3}) of the organic reactant has been consumed. There are clearly groups of absorption bands that are common to the spectra of the

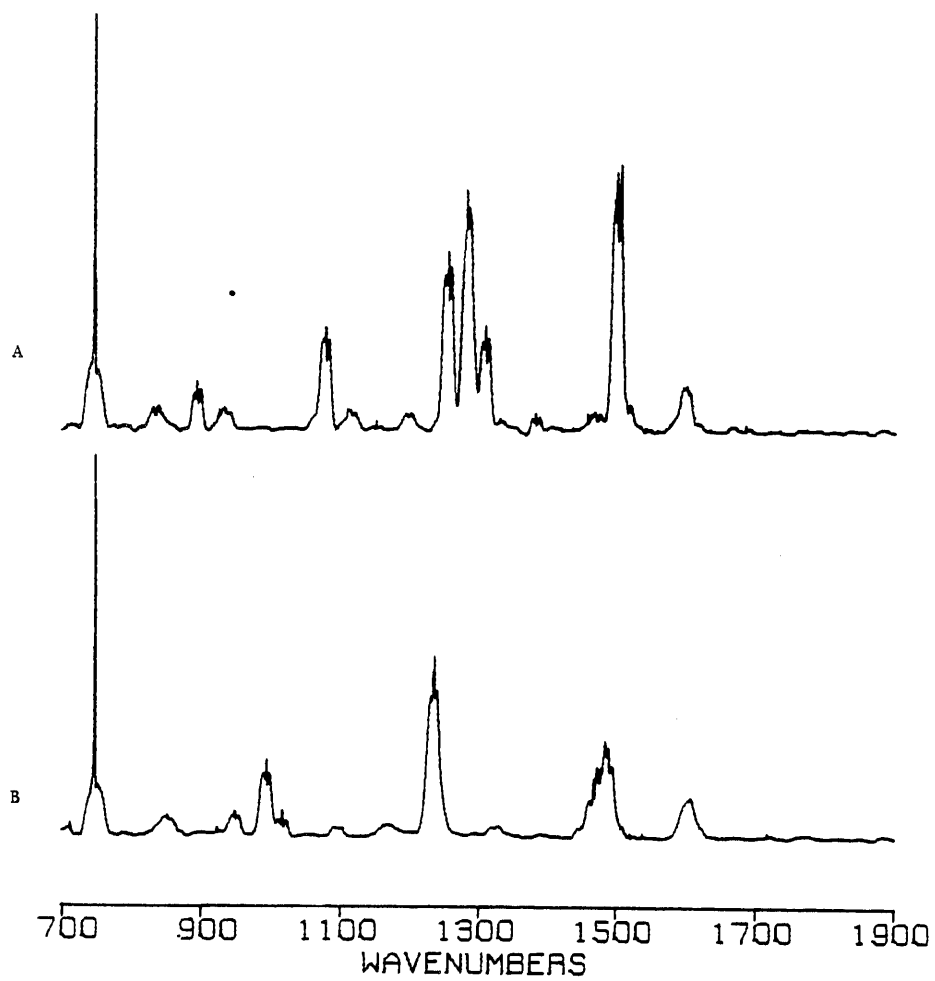


Figure IV-25. Infrared spectra of (A) 1,4-benzodioxan and (B) 2,3-dihydrobenzofuran.

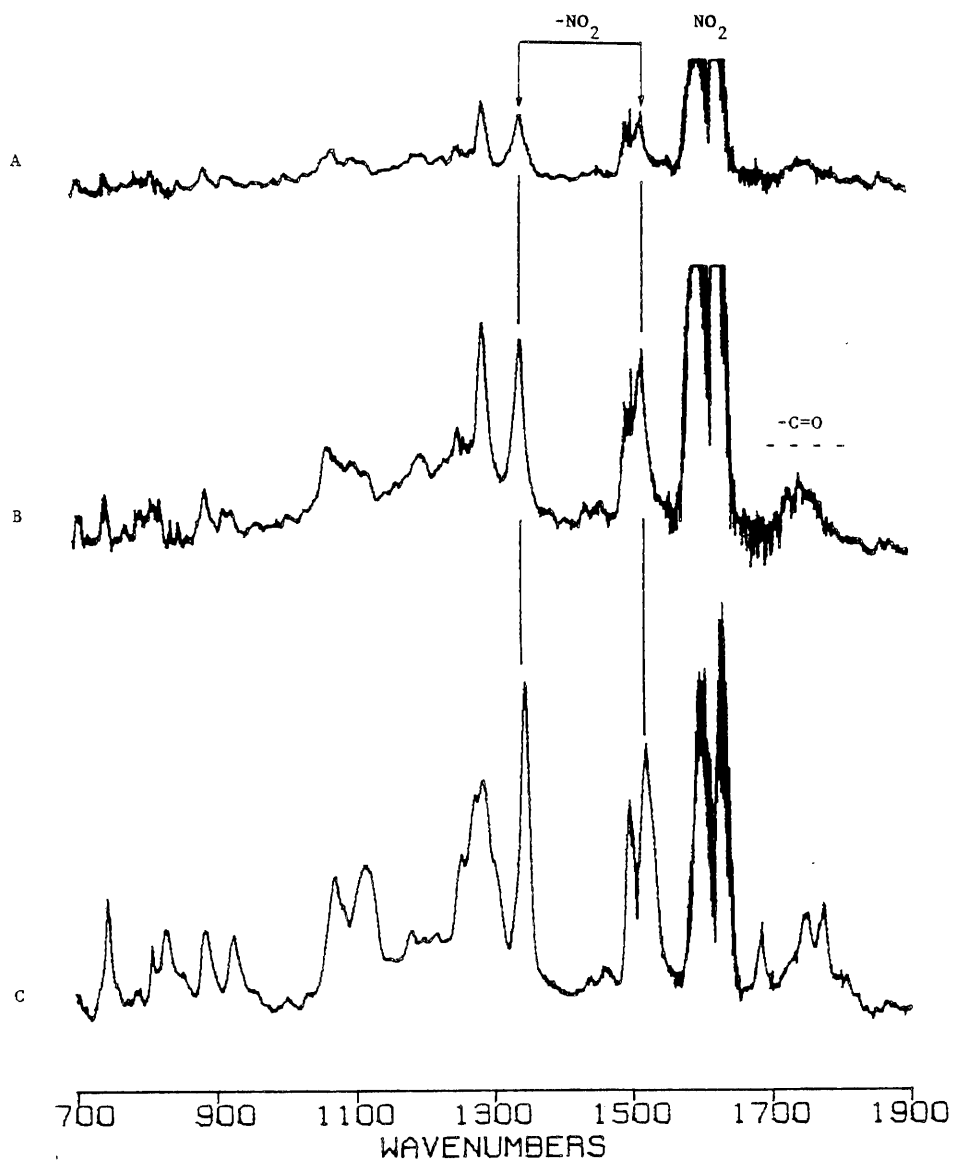


Figure IV-26. Product spectra from (A) 1,4-benzodioxan- CH_3ONO - NO -air mixture after 10 min of irradiation; (B) same mixture after 43 min of irradiation; (C) irradiated 1,4-benzodioxan- Cl_2 - NO -air mixture.

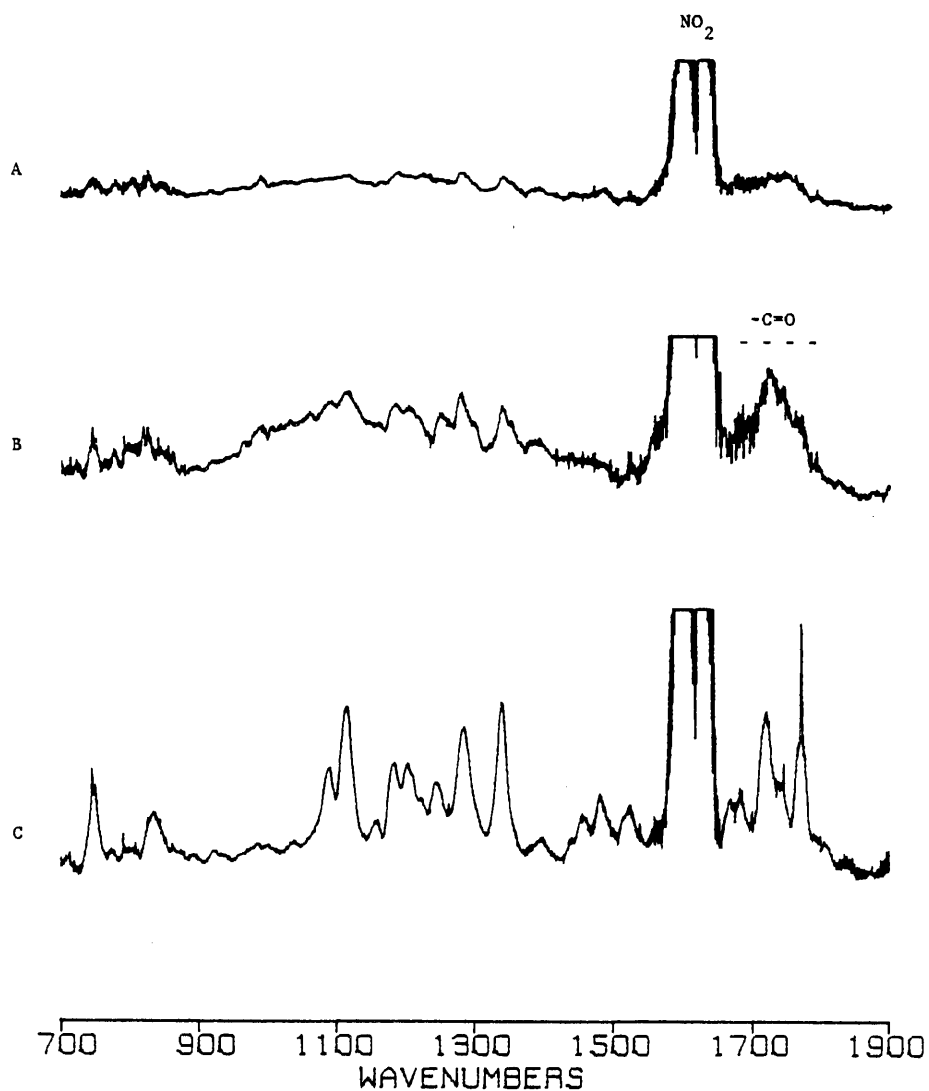
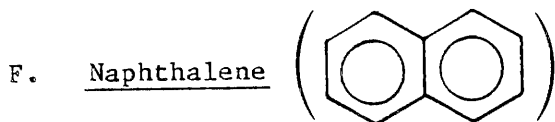


Figure IV-27. Product spectra from: (A) 2,3-dihydrobenzofuran-CH₃ONO-NO-air mixture after 17 min of irradiation; (B) same mixture after 62 min of irradiation; (C) irradiated 2,3-dihydrobenzofuran-Cl₂-NO-air mixture.

OH radical initiated and the Cl atom initiated reactions. Due to the obvious efficiency of the Cl atom initiated process, a more exhaustive study of certain atmospheric oxidation products of 1,4-benzodioxan and related compounds may indeed be better studied by this procedure.

The product spectra from the 2,3-dihydrobenzofuran-CH₃ONO-NO-air irradiation are given in Figure IV-27A for 17 min of irradiation, with a 1.2 ppm (2.9×10^{13} molecule cm⁻³) reactant loss and in Figure IV-27B for 62 min of irradiation, with 3.3 ppm (7.9×10^{13} molecule cm⁻³) reactant loss. The generally strong signatures of an aromatic nitro group, as seen in the case of 1,4-benzodioxan, is not visible in the product spectra of 2,3-dihydrobenzofuran. The most conspicuous functional group absorption is that due to the carbonyl group, suggesting that a significant extent of the reaction involves OH attack on the saturated ring. The absorption bands in Figures IV-27A and IV-27B are generally weak and broad, but the discernible structures below 1400 cm⁻¹ bear correspondence to those of Figure IV-27C, which is the product spectrum from an irradiated 2,3-dihydrobenzofuran-Cl₂-NO-air mixture after 17 min of irradiation, with 3.4 ppm (8.2×10^{13} molecule cm⁻³) of the organic reactant consumed.

The FT-IR spectroscopic data could not provide confirmation of the presence of phenolic products since the characteristic free OH absorption at ~ 3600 cm⁻¹ was beyond the sensitivity of the HgCdTe detector used. Thus, the FT-IR data could only provide supporting evidence to the GC-MS results for an aromatic nitro product from 1,4-benzodioxan. The present lack of mutual verification between the GC-MS and FT-IR product data may have stemmed from the difference in the sampling methods employed for the separate experiments analyzed. The preferential collection of certain products on the PUF plugs is a possible cause since the above irradiations were attended by considerable formation of aerosol matter.



Previous studies have shown that naphthalene, the simplest polycyclic aromatic hydrocarbon (PAH), reacts with OH radicals and with N₂O₅ (Atkinson 1986, Pitts et al. 1985), and the nitronaphthalene products from the N₂O₅ reaction have been measured (Pitts et al. 1985). While the OH radical reaction rate constant is reliably known to be 2.2×10^{-11} cm³

molecule⁻¹ s⁻¹ at 298 K (Atkinson 1986), the N₂O₅ rate constant of $\sim(2-3) \times 10^{-17}$ cm³ molecule⁻¹ s⁻¹ was obtained from a computer fit to the measured naphthalene and N₂O₅ time-concentration profiles of a single experiment carried out with similar initial concentrations of naphthalene and N₂O₅ (Pitts et al. 1985).

In order to obtain a more accurate rate constant for this N₂O₅ reaction with naphthalene, we measured the N₂O₅ decay rates as a function of the naphthalene concentration, in the presence of (generally) excess naphthalene in the 5800-liter evacuable chamber, using long pathlength FT-IR absorption spectroscopy to monitor naphthalene, N₂O₅ and NO₂. The experimental technique used has been described in Section III above.

The experimental conditions employed and the N₂O₅ decay rates determined for the reaction of N₂O₅ with naphthalene are given in Table IV-18. The maximum consumption of naphthalene during these experiments was 28%, with a typical consumption of $\sim 10\%$. The average naphthalene concentrations during each experiment are given in Table IV-18. While for several experiments the naphthalene concentration was similar to the initial N₂O₅ concentrations, the N₂O₅ decays were always exponential within the experimental uncertainties. The observed N₂O₅ decay rates are plotted against the average naphthalene concentrations in Figure IV-28. It can be seen from Table IV-18 and Figure IV-28 that the N₂O₅ decay rates for the experiments in which the $\text{NO}_2 / \text{N}_2\text{O}_5$ concentration ratio was < 1 were significantly higher than the decay rates for conditions where this concentration ratio was > 1 . Consistent with this observation, the addition of excess NO₂ is expected to decrease the importance of any secondary reactions involving NO₃ radicals and/or reactive reaction products, since the presence of NO₂ lowers the NO₃ radical concentrations in N₂O₅-NO₂-air mixtures and NO₂ may scavenge any radical reaction products.

Accordingly, a least squares analysis of the data obtained under conditions where $[\text{NO}_2]_{\text{avg}} / [\text{N}_2\text{O}_5]_{\text{initial}} > 1$ was carried out, using equation (VIII), to yield the rate constant

$$k(\text{N}_2\text{O}_5 + \text{naphthalene}) = (1.4 \pm 0.2) \times 10^{-17} \text{ cm}^3 \text{ molecule}^{-1} \text{ s}^{-1}$$

Table IV-18. Experimental Conditions Employed and N_2O_5 Decay Rates Observed for the Gas-Phase Reaction of N_2O_5 with Naphthalene at 298 ± 2 K

EC Run No.	10^{-13} x Concentration (molecule cm^{-3})			10^4 x N_2O_5 Decay Rate (s^{-1}) ^a
	Naphthalene (avg)	NO_2 (avg)	N_2O_5 (initial)	
1090	-	1.44	5.57	1.32 ± 0.03
1091	1.51	20.5	2.47	4.42 ± 0.05
1092	2.62	20.4	2.78	6.05 ± 0.17
1093	4.03	22.3	5.64	7.13 ± 0.20
1094	0.96	20.7	1.51	2.82 ± 0.10
1095	2.78	2.45	3.53	6.28 ± 0.15
1096	4.13	3.14	6.07	10.7 ± 0.23
1097	-	2.16	8.45	0.83 ± 0.05
1097 ^b	-	24.6	~5.95	0.88 ± 0.03
1098	-	1.85	5.98	0.88 ± 0.02
1099	4.15	20.8	1.42	6.47 ± 0.20
1100	7.34	21.8	2.90	12.1 ± 0.3
1101	8.69	22.9	4.37	11.9 ± 0.3
1102	11.4	23.6	5.69	12.7 ± 0.3
1103	5.62	3.24	1.46	9.93 ± 0.20
1105	14.3	5.45	4.82	22.8 ± 0.6
1106	9.89	5.33	4.39	18.0 ± 0.4
1107	-	3.82	5.71	0.78 ± 0.03
1203	-	4.10	15.6	1.73 ± 0.03
1204	7.08	3.02	5.86	17.6 ± 1.4
1205	7.44	22.4	3.72	12.1 ± 0.2
1206	7.20	1.97	3.86	23.0 ± 0.7
1207	7.90	0.98	1.73	20.3 ± 0.8
1208	7.90	3.46	1.73	15.2 ± 0.9

^aIndicated error limits are two least-squares standard deviations.

^b NO_2 added during background N_2O_5 decay experiment.

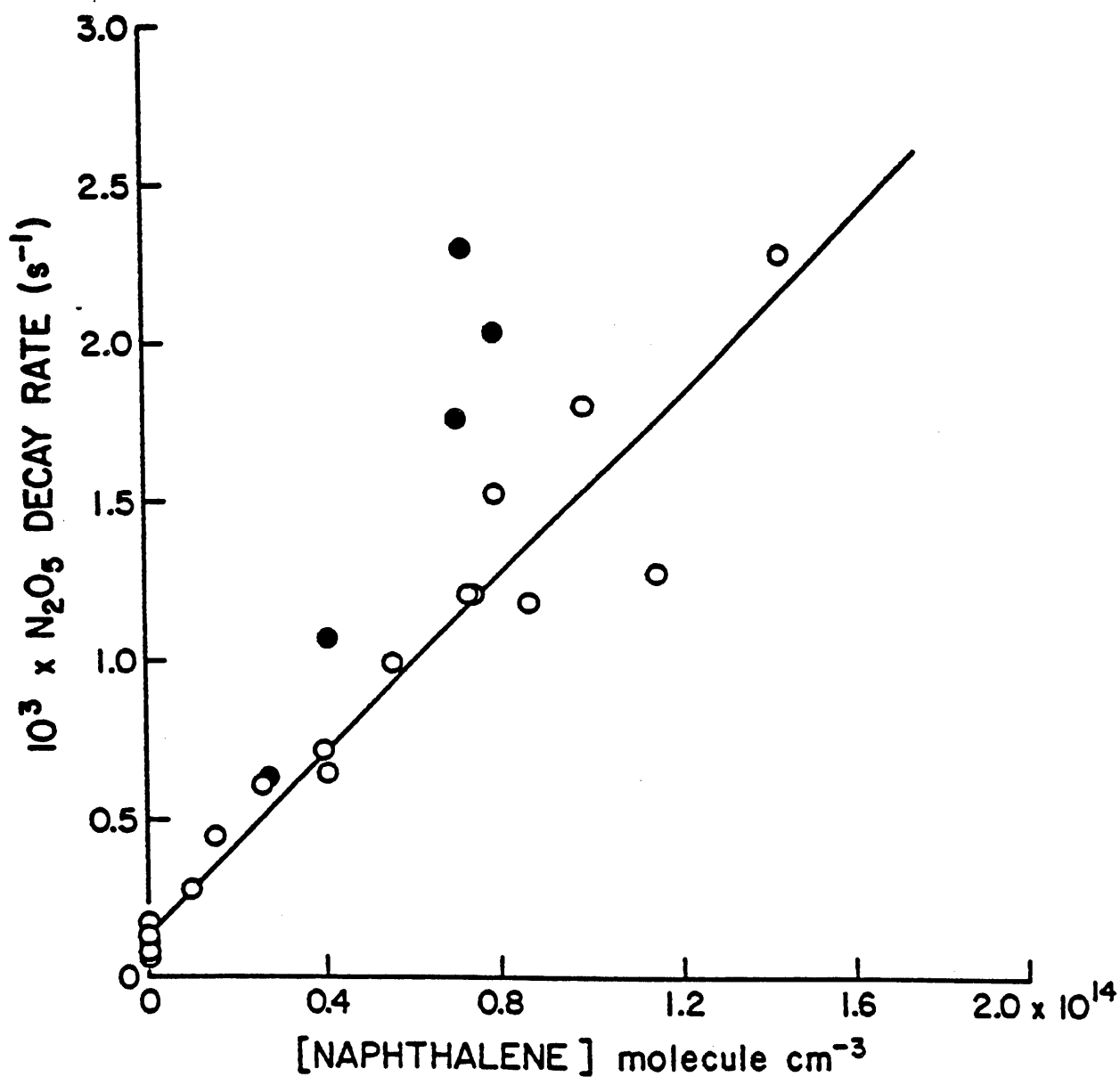
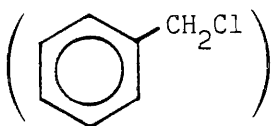


Figure IV-28. Plot of the N_2O_5 decay rates against the average naphthalene concentrations (● - $[\text{NO}_2]_{\text{av}}/[\text{N}_2\text{O}_5]_{\text{initial}} < 1$; ○ - $[\text{NO}_2]_{\text{av}}/[\text{N}_2\text{O}_5]_{\text{initial}} > 1$).

at 298 ± 2 K, where the indicated error limit is two least-squares standard deviations of the slope of the plot in Figure IV-28 combined with an estimated 10% maximum uncertainty in the naphthalene concentration calibration.

The rate constant measured here for the gas-phase reaction of N_2O_5 with naphthalene of $(1.4 \pm 0.2) \times 10^{-17} \text{ cm}^3 \text{ molecule}^{-1} \text{ s}^{-1}$ supercedes that of $\sim(2-3) \times 10^{-17} \text{ cm}^3 \text{ molecule}^{-1} \text{ s}^{-1}$ reported previously (Pitts et al. 1985) from a computer fit of the time-concentration profiles of N_2O_5 and naphthalene for a single N_2O_5 -naphthalene-air reactant mixture without initially added NO_2 . The lower rate constant determined in this study is consistent with our previous data, since it is apparent that secondary reactions occur in the absence of added NO_2 , leading to enhanced decays of N_2O_5 . This more accurate rate constant leads to a calculated atmospheric lifetime of naphthalene due to N_2O_5 reaction of ~ 80 days, using an estimated ambient N_2O_5 concentration of $2 \times 10^{10} \text{ molecule cm}^{-3}$ during 12-hr nighttime periods (Atkinson et al. 1986b). This calculated lifetime can be compared to that of ~ 1.1 day due to the OH radical reaction, showing that with respect to the atmospheric removal of naphthalene, the N_2O_5 reaction is of minor importance. However, both the N_2O_5 and the OH radical reactions must be considered with regard to the formation of nitronaphthalenes.

G. Benzyl Chloride



When this program was initiated, only an upper limit to the rate constant of $<4 \times 10^{-20} \text{ cm}^3 \text{ molecule}^{-1} \text{ s}^{-1}$ at room temperature for the O_3 reaction with benzyl chloride was available (Atkinson et al. 1982b). Thus, we determined the rate constants at room temperature for both the NO_3 and OH radical reactions, and also reinvestigated the kinetics of the O_3 reaction. The data obtained showed that reaction with the OH radical will be the dominant atmospheric removal route, and hence an attempt was made to study the products of the OH radical-initiated reaction. These studies are described below.

1. Kinetics of the O_3 Reaction

Ozone decays were monitored in the presence and absence of benzyl chloride, as described in Section III above. In the presence of $2.5 \times$

10^{14} molecule cm^{-3} of benzyl chloride, calculated from the amount introduced into the reaction chamber, the O_3 decay rate of $1.3 \times 10^{-5} \text{ s}^{-1}$ was indistinguishable from the background O_3 decay rates of $\sim(1.3-3.3) \times 10^{-5} \text{ s}^{-1}$ observed during our present study. Assuming that this entire O_3 decay rate was due to reaction with benzyl chloride leads to the upper limit to the rate constant of

$$k(\text{O}_3 + \text{benzyl chloride}) < 6 \times 10^{-20} \text{ cm}^3 \text{ molecule}^{-1} \text{ s}^{-1}$$

at $297 \pm 2 \text{ K}$, totally consistent with our previous data (Atkinson et al. 1982b).

2. Kinetics of the NO_3 Radical Reaction

The experimental technique used has been described in Section III above. Experiments were carried out in the 5800-liter evacuable chamber, with propene as the reference organic. Benzyl chloride and propene were monitored by GC-FID and, within the measurement uncertainties of $\leq 5\%$, no loss of benzyl chloride was observed during the reaction, while 60% of the propene was reacted. These data lead to an upper limit to the rate constant ratio of

$$k(\text{benzyl chloride})/k(\text{propene}) < 0.06$$

which, using a rate constant for the reaction of NO_3 radicals with propene of $(9.2 \pm 1.1) \times 10^{15} \text{ cm}^3 \text{ molecule}^{-1} \text{ s}^{-1}$ (Ravishankara and Mauldin 1985, Atkinson et al. 1987) yields

$$k(\text{NO}_3 + \text{benzyl chloride}) < 6 \times 10^{-16} \text{ cm}^3 \text{ molecule}^{-1} \text{ s}^{-1}$$

at $298 \pm 2 \text{ K}$.

3. Kinetics of the OH Radical Reaction

The experimental techniques used were similar to those described in Sections III and IV.B.3. Irradiations of $\text{CH}_3\text{ONO-NO-benzyl chloride-dimethyl ether-air}$ mixtures, with and without added ethane, were carried out in the 5800-liter evacuable chamber. Benzyl chloride and dimethyl ether were monitored during these irradiations by long pathlength FT-IR absorption spectroscopy. The experimental data obtained are plotted in accordance with equation (III) in Figure IV-29.

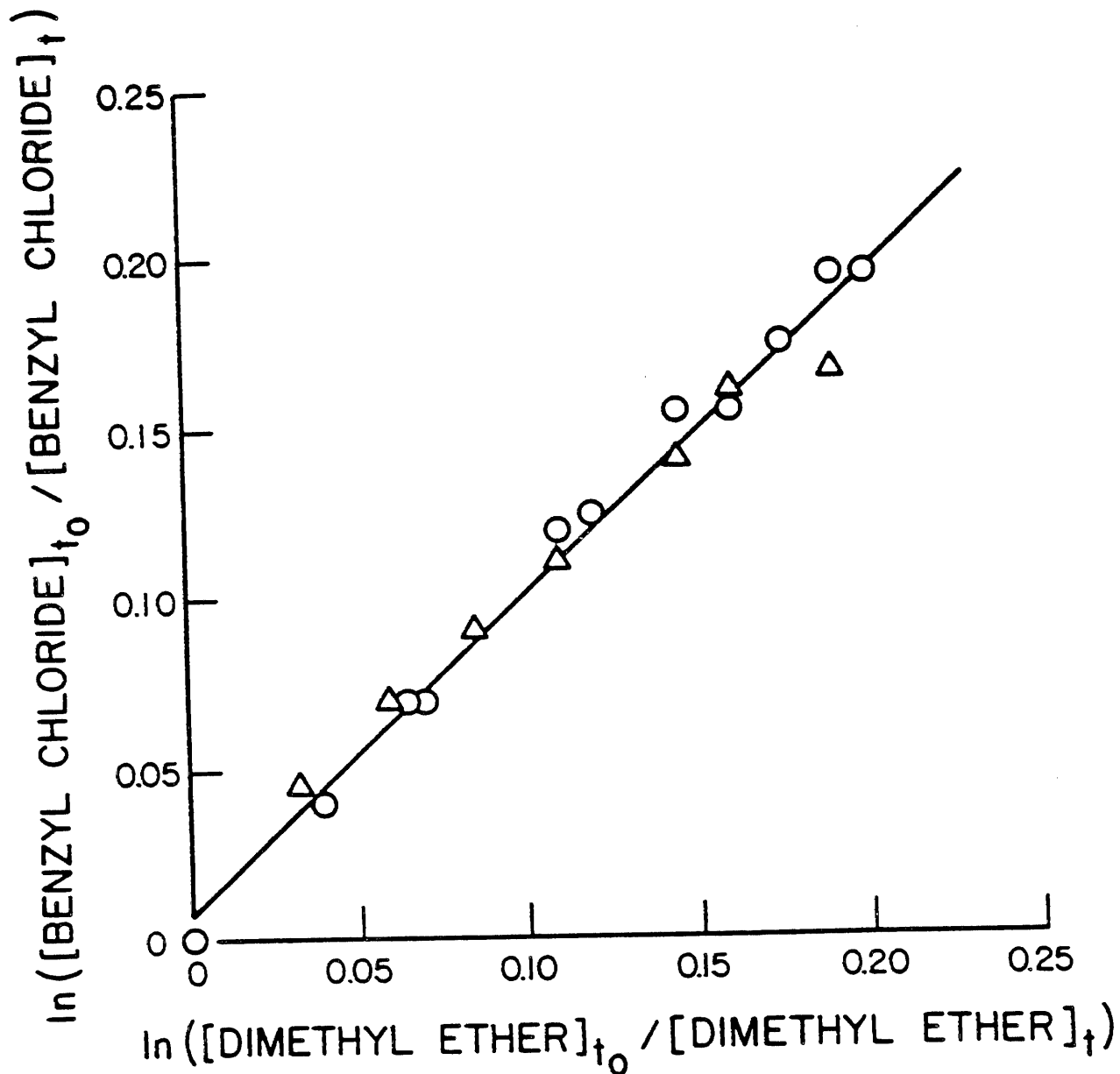


Figure IV-29. Plot of equation (III) for the reaction of OH radicals with benzyl chloride, with dimethyl ether as the reference compound. (O - in the absence of ethane; Δ - in the presence of 4.8×10^{14} molecule cm^{-3} of ethane.)

Within the experimental errors, the slope of the plot of the data obtained in the presence of C_2H_6 (0.879 ± 0.099) is indistinguishable from that in the absence of C_2H_6 (0.993 ± 0.053) [where the error limits are two least-squares standard deviations], as can be seen from Figure IV-29. Accordingly, we carried out a least-squares analysis of the complete data set, yielding the rate constant ratio

$$k(\text{benzyl chloride})/k(\text{dimethyl ether}) = 0.939 \pm 0.062$$

at 298 ± 2 K, where the error limits are again two least-squares standard deviations. Use of a rate constant for the reaction of OH radicals with dimethyl ether of $2.98 \times 10^{-12} \text{ cm}^3 \text{ molecule}^{-1} \text{ s}^{-1}$ (Atkinson 1986) leads to a rate constant of

$$k(\text{OH} + \text{benzyl chloride}) = (2.80 \pm 0.19) \times 10^{-12} \text{ cm}^3 \text{ molecule}^{-1} \text{ s}^{-1}$$

at 298 ± 2 K. This room temperature rate constant is in excellent agreement with that of $(2.95 \pm 0.15) \times 10^{-12} \text{ cm}^3 \text{ molecule}^{-1} \text{ s}^{-1}$ reported recently by Edney et al. (1986a). The study of Edney et al. (1986a) provides information that Cl atoms are generated from the OH radical reaction, and this indicates that the OH radical and Cl atom reactions with benzyl chloride and dimethyl ether both have similar rate constant ratios.

The kinetic data obtained here clearly show that only the OH radical reaction need be considered as an atmospheric removal process for benzyl chloride, with a lifetime of ~ 8 days being calculated for a daytime ambient OH radical concentration of $1 \times 10^6 \text{ molecule cm}^{-3}$.

4. Products of the OH Radical Reaction

The spectrum of benzyl chloride and the spectrum of the reactant mixture with CH_3ONO ($2.4 \times 10^{14} \text{ molecule cm}^{-3}$) and NO ($1.8 \times 10^{14} \text{ molecule cm}^{-3}$) are given in Figures IV-30A and IV-30B. The spectrum of this reactant mixture after 57 min of irradiation is presented in Figure IV-30C. Absorptions from the usual inorganic products (NO_2 , HNO_3 , $HONO$) and products due to methyl nitrite ($HCHO$, $HCOOH$, CH_3ONO_2) are highly conspicuous, but those from benzyl chloride itself are quite weak.

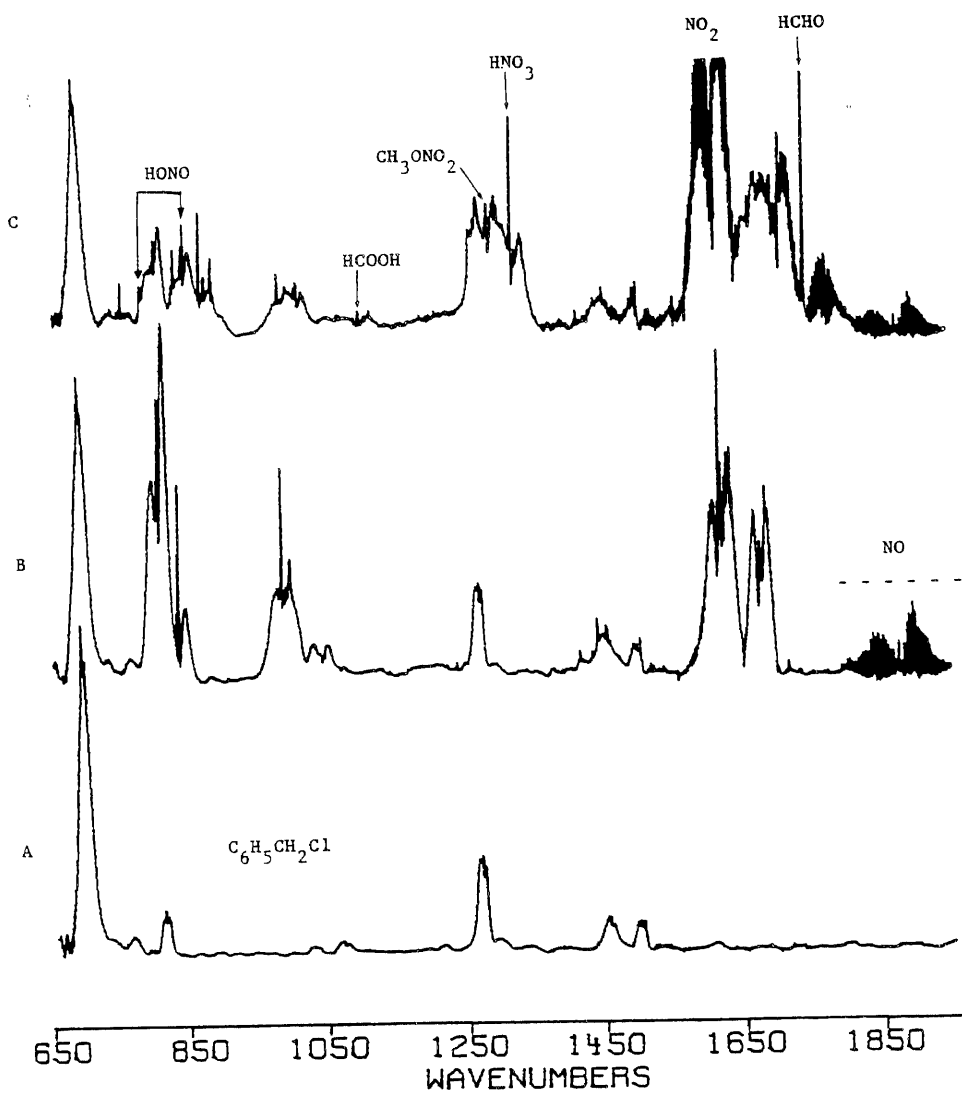
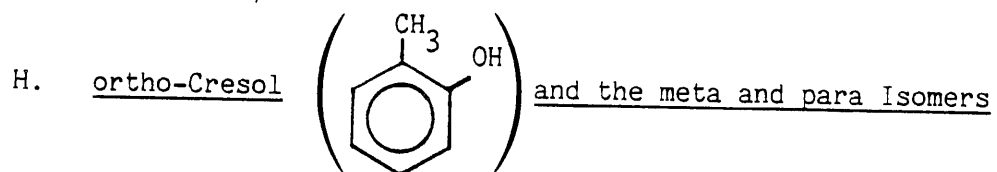


Figure IV-30. Infrared spectra of (A) benzyl chloride; (B) initial benzyl chloride- CH_3ONO - NO -air mixture, and (C) mixture after 57 min of irradiation.

The weak absorptions of the products derived from benzyl chloride are presented in the expanded plots of the residual spectra given in Figures IV-31A and IV-31B. They correspond, respectively, to irradiation times of 17 min and 57 min and amounts of benzyl chloride consumed of 3.4×10^{13} molecule cm^{-3} and 6.0×10^{13} molecule cm^{-3} , respectively. Due to the spurious spikes generated by the inexact cancellation of the strong NO_2 (and H_2O) absorptions, the segment $\sim 1570\text{--}1720 \text{ cm}^{-1}$ has been omitted from Figures IV-31A and IV-31B. By examining the time sequence of these residual spectra, absorptions due to probable products from benzyl chloride were identified. Thus, the presence of absorption bands at ~ 1555 and $\sim 1350 \text{ cm}^{-1}$ is consistent with a product (or products) that has a nitro group, most likely in the aromatic ring. The bands marked with asterisks in Figure IV-31 have been identified as belonging to peroxybenzoyl nitrate (PBzN) [Stephens 1969]. The absorption features of PBzN are more clearly depicted in Figure IV-31C, which is a spectrum of the products from a separate irradiation of a benzyl chloride- Cl_2 -NO-air mixture.

The exact identity of the NO_2 -substituted aromatic product(s), and hence its concentration, cannot be established with the present spectroscopic data. However, if it can be assumed that the absorptivities of the 1555 and 1350 cm^{-1} bands are in the range of those of nitrobenzene and nitroalkanes, then it can be estimated that the aromatic nitro product(s) accounts for only $\sim 15\text{--}25\%$ of the benzyl chloride lost. With the use of literature values for the infrared absorptivities of peroxybenzoyl nitrate (Stephens 1969), its yield is estimated to be no more than $\sim 5\text{--}10\%$.



The rate constants for the reactions of all three cresol isomers with OH and NO_3 radicals and with O_3 have previously been determined (Atkinson and Carter 1984, Atkinson et al. 1984c, Atkinson 1986), and these data show that under atmospheric conditions both the daytime O_3 and the nighttime NO_3 reactions must be considered as atmospheric removal processes. The OH radical reaction with o-cresol appears to proceed mainly ($92^{+4}_{-8}\%$ at 298 K) by OH radical addition to the aromatic ring, with

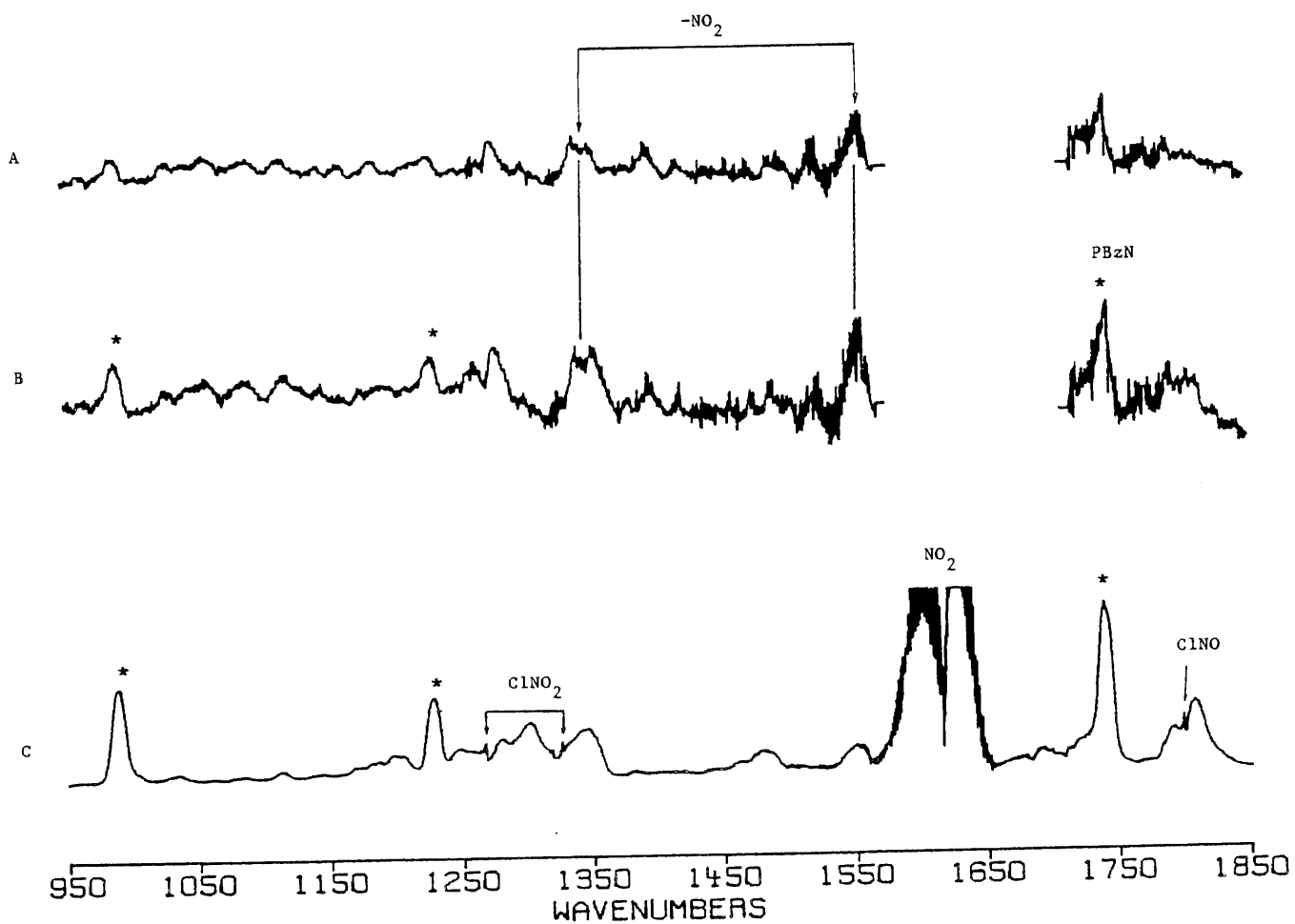
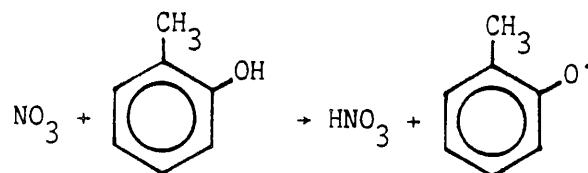


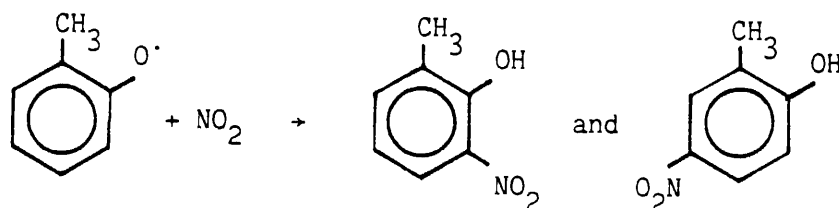
Figure IV-31. Residual spectra of products from (A) benzyl chloride- $\text{CH}_3\text{ONO}-\text{NO}$ -air mixture after 17 min of irradiation; (B) same mixture after 57 min of irradiation; (C) irradiated benzyl chloride- Cl_2-NO -air mixture.

the remainder proceeding by H-atom abstraction from the substituent -OH group, and the other two cresol isomers are expected to react totally analogously.

Based upon the kinetic data for the cresols and other aromatic compounds (Table IV-18), it appears that the NO_3 radical reaction occurs solely by H-atom abstraction from the substituent -OH group:



followed by reactions of the methylphenoxy radicals with NO_2 to yield hydroxynitrotoluenes.



To help elucidate this NO_3 radical reaction, we studied the products of the NO_3 radical reaction with o-cresol, as described below.

1. Products of the NO_3 Radical Reaction

To help elucidate this NO_3 radical reaction, we conducted a longpath FT-IR study of the products of the NO_3 radical reaction with the three cresol isomers. The reaction was carried out in the 5800 liter evacuable chamber by adding N_2O_5 ($\sim 1.4 \times 10^{14}$ molecule cm^{-3}), with rapid mixing, to the particular cresol isomer ($\sim 2.4 \times 10^{14}$ molecule cm^{-3}). These reactions went to completion within a few minutes, as evidenced by the lack of N_2O_5 absorptions in the product spectra.

The reference spectra of ortho-, meta-, and para-cresol in the vapor phase are given in Figure IV-32 for comparison purposes. The infrared signatures of the product(s) from each isomer (after subtraction of HNO_3 and NO_2 absorptions) are shown in Figure IV-33. A pair of bands at ~ 1540 and $\sim 1350 \text{ cm}^{-1}$ normally indicates NO_2 substitution in the aromatic ring, with expected shifts from these positions according to the inductive,

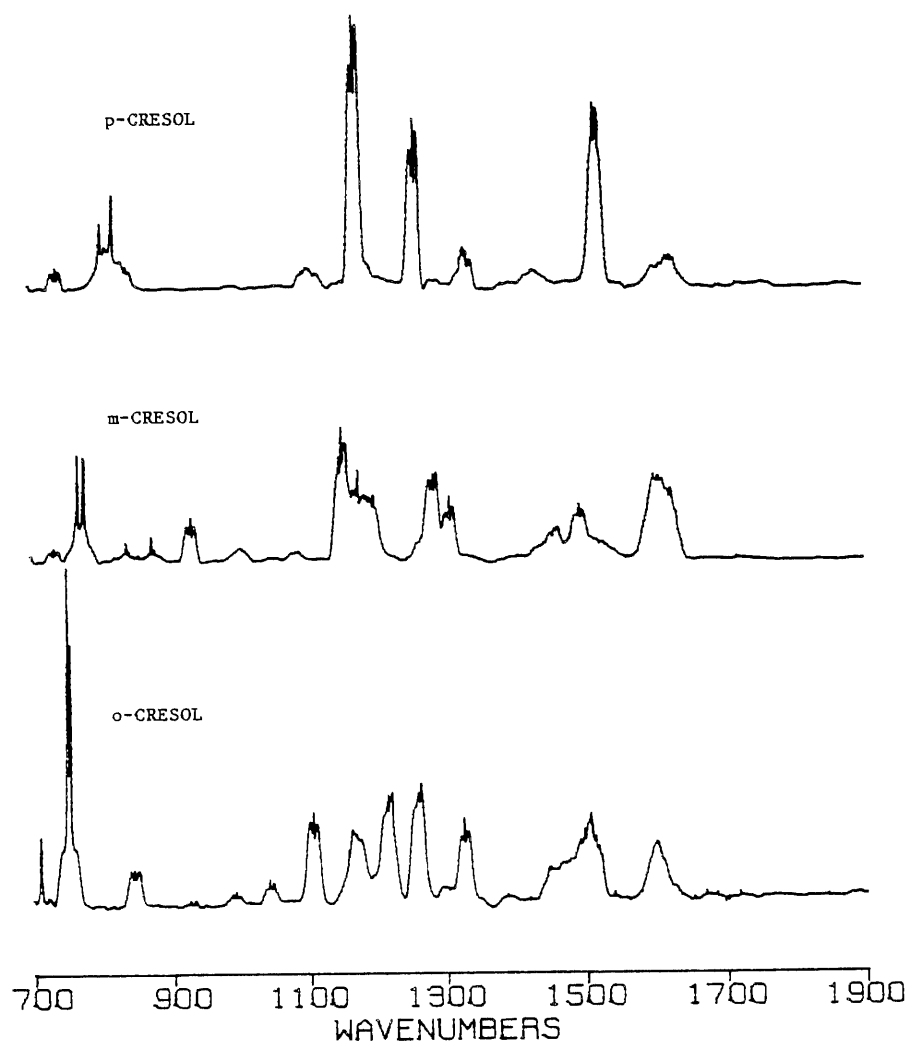


Figure IV-32. Infrared spectra of the cresol isomers.

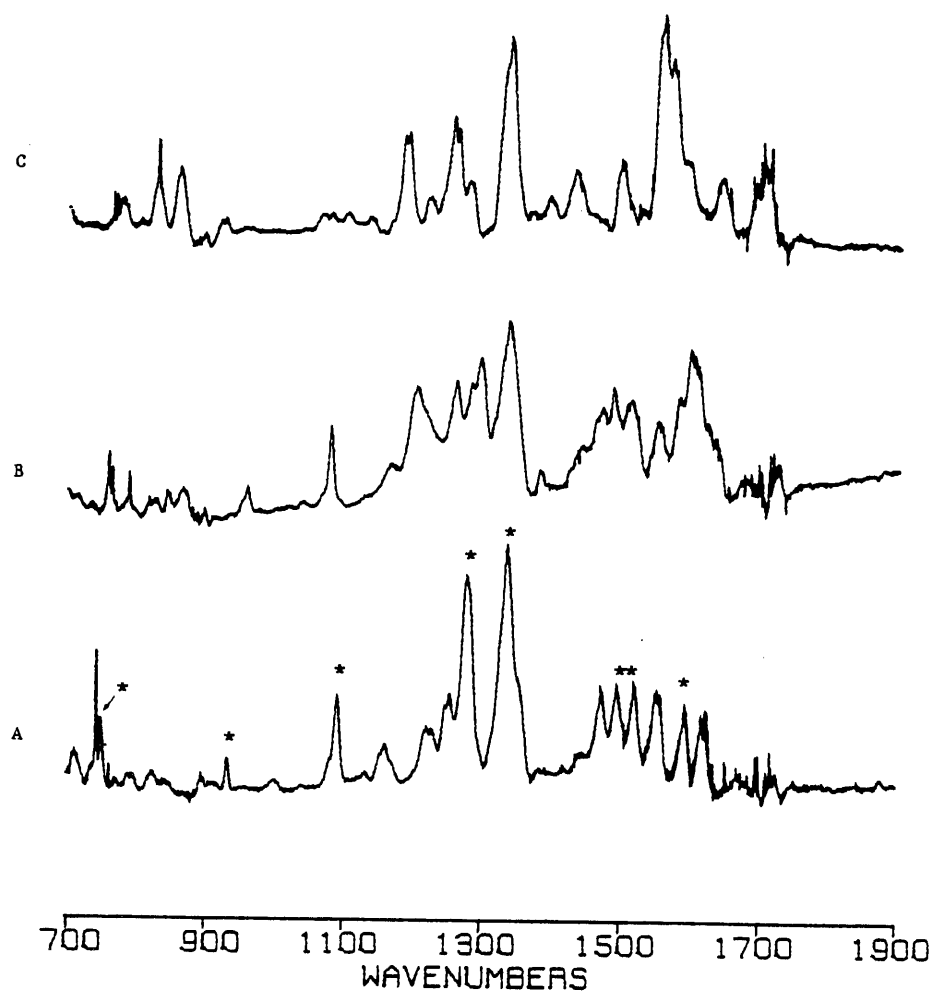
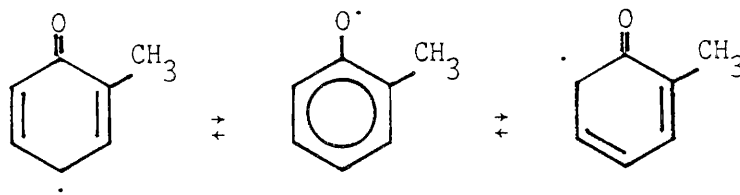


Figure IV-33. Product spectra from the mixture of N_2O_5 with (A) o-cresol, (B) m-cresol, and (C) p-cresol. Asterisks identify the bands of an o-cresol product which condensed at a faster rate than other components.

mesomeric, and steric influence of the other substituents. These characteristic bands are most conspicuous in the product spectrum of the para-isomer (Figure IV-33A), which appears to have a simpler spectrum in the $\sim 1500\text{--}1600\text{ cm}^{-1}$ range than those from the other two isomers. (This region is additionally complicated by the presence of two C=C stretching absorptions at ~ 1500 and $\sim 1600\text{ cm}^{-1}$). The more diffuse band structure in the $1500\text{--}1600\text{ cm}^{-1}$ range of the o-cresol and m-cresol product spectra is partly due to the presence of more than one methylnitrophenol isomers in each case. This was particularly evident in the case of the o-cresol products. When the reaction mixture was allowed to stand for ~ 15 min the difference in the spectra showed that one component was decaying faster than the other, presumably by deposition on the chamber walls. The absorption bands of the product that showed a faster loss rate are indicated by asterisks in Figure IV-33C. Thus, the above product spectra are consistent with the formation of isomeric methylnitrophenols from the reactions of the NO_3 radical with the cresol isomers.

In the case of the methylphenoxy radical formed during the initial attack of the NO_3 radical on o-cresol, resonance delocalization of the odd electron is expected to impart ortho and para directing influence on the subsequent NO_2 addition to the ring. [The detailed mechanism leading to the phenolic O-H bond formation is not yet clear (Niki et al. 1979).]

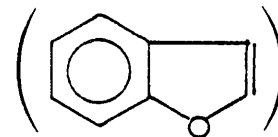


Indeed, the above-mentioned time dependence of the band intensities showed that only two product species are formed from o-cresol. Authentic samples are required to verify that they are in fact 2-methyl-2-nitrophenol and 2-methyl-4-nitrophenol.

I. Other Compounds Studied

In addition to the studies described above, we carried out additional kinetic studies for other compounds in order to aid in the interpretation of the data obtained. These additional studies are described below.

1. Kinetics of the Reaction of O₃ with 2,3-Benzofuran



The rate constant for this reaction was determined at 297 ± 2 K using the experimental techniques described in Section III. The concentrations of 2,3-benzofuran were calculated from the amount introduced into the reaction chamber and the chamber volume. The experimental data are given in Table IV-19, and a least-squares analysis of these data yields

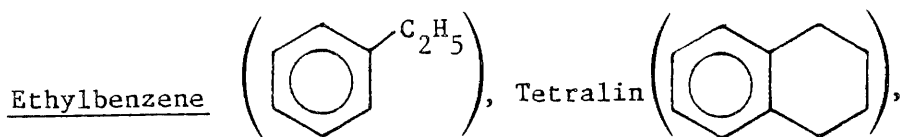
$$k(\text{O}_3 + 2,3\text{-benzofuran}) = (1.83 \pm 0.21) \times 10^{-18} \text{ cm}^3 \text{ molecule}^{-1} \text{ s}^{-1}$$

at 297 ± 2 K, where the indicated error limit represents two least-squares standard deviations combined with an estimated 10% uncertainty in the 2,3-benzofuran concentrations. The magnitude of this rate constant is consistent with the presence of a $>\text{C}=\text{C}<$ bond in the furan moiety of this molecule (see also 2,3-dihydrobenzofuran, Section IV.E.1 above).

Table IV-19. Experimental Data for the Gas-Phase Reaction of O₃ with 2,3-Benzofuran at 297 ± 2 K

$10^{-14} \times 2,3\text{-Benzofuran}$ Concentration (molecule cm^{-3})	$10^3 \times \text{O}_3$ Decay Rate (s^{-1})
2.61	0.475
5.21	0.992
7.62	1.46
10.0	1.81
-	0.017

2. Kinetics of the Reactions of NO₃ Radicals with



Acetylene (CH₃CH), Propyne (CH₃C≡CH) and Crotonaldehyde (CH₃CH=CHCHO)

Rate constants for the gas-phase reactions of the NO₃ radical with these organic compounds were determined as described in Section III above. Experiments were carried out in either a 2500-liter all-Teflon chamber (acetylene and propyne) or in the 5800-liter evacuable chamber. Ethylbenzene, tetralin, acetylene and propyne were monitored by GC-FID, while crotonaldehyde was monitored by long pathlength FT-IR absorption spectroscopy. Ethene or propene were used as the reference organic.

A representative plot of equation (VII) is shown in Figure IV-34 for crotonaldehyde, and the rate constant ratios and rate constants determined are given in Table IV-20.

3. Kinetics of the Reactions of OH Radicals with cis- and trans-1,3-Dichloropropene and 3-Chloro-2-chloromethyl-1-propene

Since the present study showed that the production of Cl atoms from the initial reaction of OH radicals with the chloroethenes could lead to erroneous OH radical reaction rate constants as measured using relative rate techniques, rate constants were remeasured for cis- and trans-1,3-dichloropropene and 3-chloro-2-chloromethyl-1-propene in the presence of ethane as a Cl atom scavenger. The reactions were carried out with gas chromatographic analysis as described above (Section III) and previously (Tuazon et al. 1984), except that a 6400-liter all-Teflon environmental chamber was used.

The data obtained are plotted in accordance with equation (III) in Figures IV-35 and IV-36, using n-octane as the reference organic for the experiments involving cis- and trans-1,3-dichloropropene and isoprene (2-methyl-1,3-butadiene) as the reference organic for the experiments involving 3-chloro-2-chloromethyl-1-propene. The rate constant ratios obtained were: $k(\text{cis-1,3-dichloropropene})/k(\text{n-octane}) = 0.969 \pm 0.046$; $k(\text{trans-1,3-dichloropropene})/k(\text{n-octane}) = 1.65 \pm 0.09$; and $k(3\text{-chloro-2-chloromethyl-1-propene})/k(\text{isoprene}) = 0.332 \pm 0.029$, where the indicated errors are two least-squares standard deviations. These rate constant

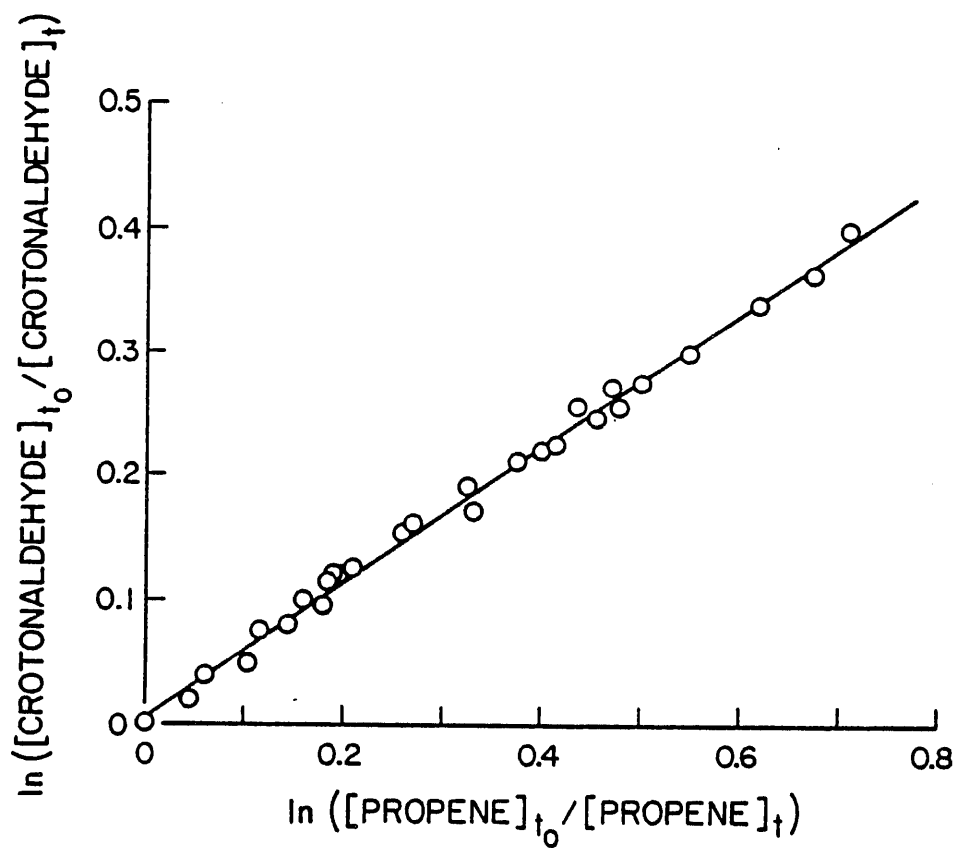


Figure IV-34. Plot of equation (VII) for the reaction of NO_3 radicals with crotonaldehyde, with propene as the reference organic.

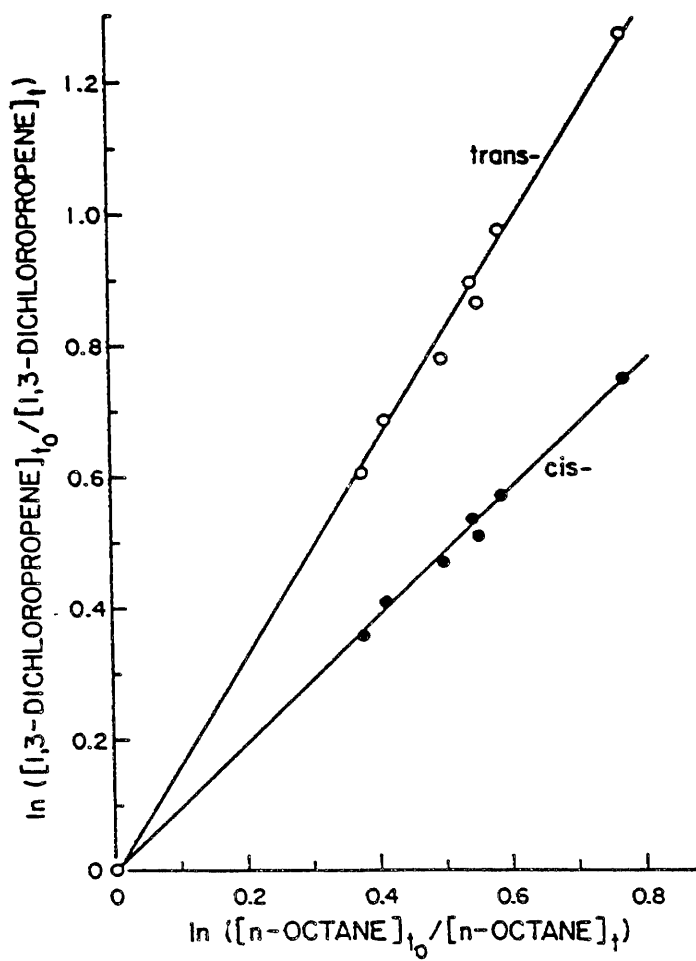


Figure IV-35. Plots of equation (III) for the reaction of OH radicals with cis- and trans-1,3-dichloropropene, with n-octane as the reference organic, in the presence of ethane.

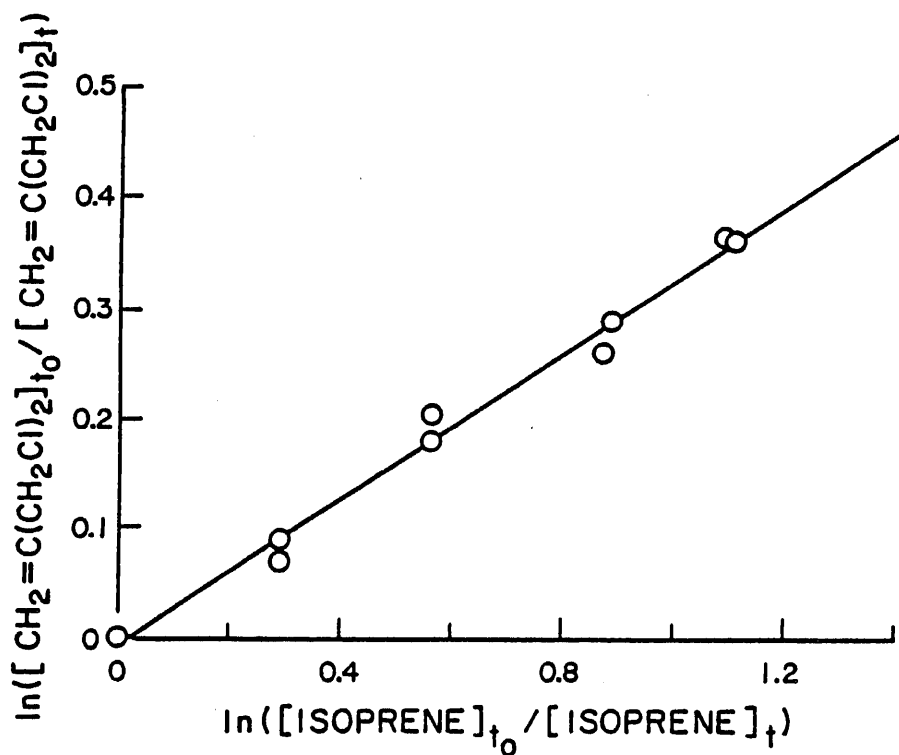
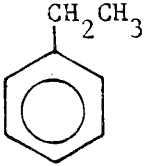
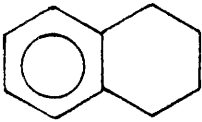


Figure IV-36. Plot of equation (III) for the reaction of OH radicals with 3-chloro-2-chloromethyl-1-propene, with isoprene (2-methyl-1,3-butadiene) as the reference organic, in the presence of ethane.

Table IV-20. Rate Constant Ratios and Rate Constants for Gas-Phase Reactions of the NO_3 Radical with a Series of Organics at 298 ± 2 K

Organic	Structure	Rate Constant Ratio ^a		$k(\text{cm}^3 \text{ molecule}^{-1} \text{ s}^{-1})$
		Relative to $k(\text{ethene}) = 1.00$	Relative to $k(\text{propene}) = 1.00$	
Acetylene	$\text{CH}\equiv\text{CH}$	≤ 0.14		$\leq 3.8 \times 10^{-17}$
Propyne	$\text{CH}_3\text{C}\equiv\text{CH}$	0.85 ± 0.07		$(2.0 \pm 0.4) \times 10^{-16}$
Crotonaldehyde	$\text{CH}_3\text{CH}=\text{CHCHO}$		0.542 ± 0.017	$(5.0 \pm 0.7) \times 10^{-15}$
Ethylbenzene			≤ 0.06	$\leq 6 \times 10^{-16}$
Tetralin			1.17 ± 0.24	$(1.1 \pm 0.3) \times 10^{-14}$

^aIndicated errors are two least-squares standard deviations.

^bPlaced on an absolute basis by use of rate constants for the reactions of NO_3 radicals with ethene and propene of $(2.3 \pm 0.4) \times 10^{-16}$ and $(9.2 \pm 1.1) \times 10^{-15} \text{ cm}^3 \text{ molecule}^{-1} \text{ s}^{-1}$, respectively (Ravishankara and Mauldin 1985, Atkinson et al. 1987).

ratios may be compared to those obtained previously in the absence of ethane of 0.859 ± 0.013 , 1.45 ± 0.04 and 0.394 ± 0.053 , respectively (Tuazon et al. 1984). Repeat experiments for cis- and trans-1,3-dichloropropene in the absence of ethane gave results which agreed with our previous data to within 4%. Using rate constants for the reactions of the OH radical with n-octane and isoprene of 8.72×10^{-12} and $1.01 \times 10^{-10} \text{ cm}^3 \text{ molecule}^{-1} \text{ s}^{-1}$, respectively (Atkinson 1986), leads to OH radical rate constants at 298 ± 2 K of

$$k(\text{cis-1,3-dichloropropene}) = (8.45 \pm 0.41) \times 10^{-12} \text{ cm}^3 \text{ molecule}^{-1} \text{ s}^{-1},$$

$$k(\text{trans-1,3-dichloropropene}) = (1.44 \pm 0.08) \times 10^{-11} \text{ cm}^3 \text{ molecule}^{-1} \text{ s}^{-1},$$

$$k(3\text{-chloro-2-chloromethyl-1-propene}) = (3.35 \pm 0.30) \times 10^{-11} \\ \text{cm}^3 \text{ molecule}^{-1} \text{ s}^{-1}$$

These OH radical reaction rate constants for cis- and trans-1,3-dichloropropene are both ~13% higher than those reported previously (Tuazon et al. 1984), while that for 3-chloro-2-chloromethyl-1-propene is in agreement with our previous measurement within the combined experimental error limits.

V. ENVIRONMENTAL IMPLICATIONS

The atmospheric chemistry of the individual compounds studied has been dealt with in Section IV above, and the atmospheric lifetimes have been presented in that section. In this section, we summarize and tabulate these lifetimes and discuss them more fully, including their implications for the potential impacts of the compounds investigated. In particular, we examine which loss processes are important for each chemical on a 24-hr basis, and the implications concerning the radius of influence of the individual compounds in terms of their local, regional or global effects. In certain cases, we also consider the relative importance of physical versus chemical removal processes.

The rate constants for the gas-phase reactions of the organics studied with OH and NO₃ radicals and O₃, from which the atmospheric lifetimes are calculated, are listed in Table V-1. For those cases in which the rate constants were not determined in the present program but literature data are available, the latter are also given in Table V-1. These literature values are obtained from the reviews of Atkinson and Carter (1984) for the ozone reactions and Atkinson (1986) for the OH radical reactions.

As noted in Section II, the atmospheric lifetime, τ , of an organic compound due to gas-phase reaction with a reactive species X is given by

$$\tau = (k_x[X])^{-1} \quad (\text{XII})$$

where k_x is the rate constant for reaction with X and [X] is the atmospheric concentration of the species X. The overall lifetime in the atmosphere due to chemical reaction is then given by

$$1/\tau_{\text{overall}} = 1/\tau_{\text{OH}} + 1/\tau_{\text{O}_3} + 1/\tau_{\text{NO}_3} + \dots \quad (\text{XIII})$$

and

$$1/\tau_{\text{overall}} = k_{\text{OH}}[\text{OH}] + k_{\text{O}_3}[\text{O}_3] + k_{\text{NO}_3}[\text{NO}_3] + \dots \quad (\text{XIV})$$

For certain compounds, photolysis, reaction with N₂O₅, or a physical removal process such as rainout or dry deposition may also need to be considered. In such a case, appropriate additional terms would be added

Table V-1. Room Temperature Rate Constants for the Gas-Phase Reactions of OH and NO₃ Radicals and O₃ with the Compounds Investigated in this Study

Organic Compound	Rate Constant (cm ³ molecule ⁻¹ s ⁻¹)		
	OH	NO ₃	O ₃
Ethylene Oxide	7 x 10 ⁻¹⁴ ^a		
Vinyl Chloride	6.6 x 10 ⁻¹² ^a	4.8 x 10 ⁻¹⁶	2.5 x 10 ⁻¹⁹ ^b
1,1-Dichloroethene	8.1 x 10 ⁻¹²	1.4 x 10 ⁻¹⁵	3.7 x 10 ⁻²¹ ^b
<u>cis</u> -1,2-Dichloroethene	2.4 x 10 ⁻¹²	1.6 x 10 ⁻¹⁶	<5 x 10 ⁻²¹ ^b
<u>trans</u> -1,2-Dichloroethene	1.8 x 10 ⁻¹²	1.2 x 10 ⁻¹⁶	1.5 x 10 ⁻¹⁹ ^b
Trichloroethene	2.4 x 10 ⁻¹² ^a	3.2 x 10 ⁻¹⁶	<3 x 10 ⁻²⁰ ^b
Tetrachloroethene	1.7 x 10 ⁻¹³ ^a	<7 x 10 ⁻¹⁷	<2 x 10 ⁻²³ ^b
Acrolein	2.0 x 10 ⁻¹¹ ^a	1.2 x 10 ⁻¹⁵	2.8 x 10 ⁻¹⁹ ^b
Allyl Chloride	1.7 x 10 ⁻¹¹	6.0 x 10 ⁻¹⁶	1.6 x 10 ⁻¹⁸
Benzyl Chloride	2.8 x 10 ⁻¹²	<6 x 10 ⁻¹⁶	<4 x 10 ⁻²⁰ ^b
o-Cresol	4.0 x 10 ⁻¹¹ ^a	2.0 x 10 ⁻¹¹	2.6 x 10 ⁻¹⁹ ^b
m-Cresol	5.7 x 10 ⁻¹¹ ^a	1.5 x 10 ⁻¹¹	1.9 x 10 ⁻¹⁹ ^b
p-Cresol	4.4 x 10 ⁻¹¹ ^a	2.1 x 10 ⁻¹¹	4.7 x 10 ⁻¹⁹ ^b
Naphthalene	2.2 x 10 ⁻¹¹ ^a	c	<2 x 10 ⁻¹⁹ ^b
1,4-Benzodioxan	2.5 x 10 ⁻¹¹	5.8 x 10 ⁻¹⁶	<1.2 x 10 ⁻²⁰
2,3-Dihydrobenzofuran	3.7 x 10 ⁻¹¹	1.1 x 10 ⁻¹³	<1 x 10 ⁻¹⁹

^aFrom Atkinson (1986).

^bFrom Atkinson and Carter (1984).

^cNo reaction with NO₃ radicals observed, but reacts with N₂O₅ with a room temperature rate constant of 1.4 x 10⁻¹⁷ cm³ molecule⁻¹ s⁻¹ (Section IV).

to expressions (XIII) and (XIV) to allow the overall atmospheric lifetime to be calculated.

The choice of appropriate atmospheric concentrations for OH and NO₃ radicals and O₃ for use in calculating atmospheric lifetimes from equation (XIV) is somewhat dependent on whether a compound is expected to react primarily within polluted urban atmospheres (with potentially elevated levels of the three reactive species), or in cleaner atmospheres more characteristic of the global troposphere. It should also be recognized

that there is considerable uncertainty associated with the atmospheric concentrations of OH radicals (Hewitt and Harrison 1985), since to date this free radical species has not been widely measured in the troposphere. Similarly, a rather wide range of NO₃ radical concentrations [$\sim(2.4-240) \times 10^7$ molecule cm⁻³] has been observed in continental atmospheres (Platt et al. 1984, Atkinson et al. 1986b), and the use of a single average concentration is thus a compromise.

Because many of the compounds investigated in this program are longer-lived (i.e., lifetimes of days to weeks or months), we have chosen to employ ambient atmospheric concentrations appropriate to the cleaner, nonurban areas of the troposphere. Specifically, we have used values for O₃ of 7×10^{11} molecule cm⁻³ (30 ppb) (Singh et al. 1978, Oltmanns 1981) throughout a 24-hr period, for OH radicals of 1×10^6 molecule cm⁻³ during a 12-hr daytime period (Crutzen 1982) and for NO₃ radicals of 2.4×10^8 molecule cm⁻³ (10 ppt) during a 12-hr nighttime period (Platt et al. 1984, Atkinson et al. 1986b). Using these ambient concentrations of the OH and NO₃ radicals and of O₃ and the room temperature rate constants given in Table V-1, the individual atmospheric lifetimes due to the three potential reaction routes were calculated, and these are tabulated in Table V-2.

From the atmospheric lifetime data in Table V-2, it can be seen that, except for a few cases, the dominant reaction pathway for the compounds studied is daytime reaction with the OH radical. The only exceptions to this are the three cresol isomers and 2,3-dihydrobenzofuran, which also react rapidly with NO₃ radicals. These compounds can therefore undergo substantial atmospheric degradation at night with NO₃ radicals as well as with OH radicals during daylight hours. It is important to note, however, that dibenzofuran, and its chlorinated and brominated analogues, for which 2,3-dihydrobenzofuran served as a model compound, will not react with NO₃ radicals because of the structural effects discussed in Section IV.E.3. In this respect, 2,3-dihydrobenzofuran was not a completely faithful model compound since it undergoes an additional reaction pathway. However, the data obtained for 2,3-dihydrobenzofuran allows the atmospheric lifetimes for the dibenzofurans to be estimated, and thus it serves as an appropriate model compound for this purpose.

As can be seen from Table V-2, none of the compounds investigated react sufficiently fast with O₃ under atmospheric conditions for this

Table V-2. Calculated Atmospheric Lifetimes of Compounds Investigated for Reaction with OH and NO₃ Radicals and O₃

Organic Compound	Atmospheric Lifetimes ^a		
	OH	NO ₃	O ₃
Ethylene Oxide	330 days		
Vinyl Chloride	3.5 days	200 days	66 days
1,1-Dichloroethene	2.9 days	70 days	12 yr
<u>cis</u> -1,2-Dichloroethene	9.6 days	1.7 yr	>9 yr
<u>trans</u> -1,2-Dichloroethene	13 days	2.2 yr	110 days
Trichloroethene	9.6 days	300 days	>1.5 yr
Tetrachloroethene	140 days	3.8 yr	>2 x 10 ³ yr
Acrolein	1.2 days	80 days	60 days
Allyl Chloride	1.4 days	160 days	10 days
Benzyl Chloride	8.3 days	>160 days	>1.1 yr
o-Cresol	6.9 hr	3.5 min	64 days
m-Cresol	4.9 hr	4.6 min	87 days
p-Cresol	6.3 hr	3.3 min	35 days
Naphthalene	1.1 days	b	>80 days
1,4-Benzodioxan	11 hr	166 days	>3.8 yr
2,3-Dihydrobenzofuran	7.5 hr	11 hr	>165 days

^aFor concentrations of: O₃, 24-hr average of 7 x 10¹¹ molecule cm⁻³; OH, 12-hr daytime average of 1 x 10⁶ molecule cm⁻³; NO₃, 12-hr nighttime average of 2.4 x 10⁸ molecule cm⁻³.

^bReaction with 2 x 10¹⁰ molecule cm⁻³ of N₂O₅ during nighttime hours (Atkinson et al. 1986b) leads to a calculated lifetime of ~80 days for this process.

process to represent a significant degradation pathway. Similarly, although naphthalene reacts with a measurable rate with N₂O₅, its calculated atmospheric lifetime due to this reaction of ~80 days means that this reaction pathway will be of negligible importance as a naphthalene loss process, compared to the OH radical reaction.

From the data in Table V-2 it is possible to group the compounds studied into three categories, corresponding to very short atmospheric lifetimes (a few minutes to one day), moderately long lifetimes (a few

days), and long-lived species with lifetimes ranging from about one week to many years. Such a grouping is shown in Table V-3, with corresponding designations of local, regional and global ranges of transport. (Clearly any compound which can undergo global transport may also have local and regional impacts, and similarly any regionally distributed pollutant may also cause local effects.)

An important qualification for the grouping given in Table V-3 concerns the possible role of the products of the atmospheric reactions of compounds which have short or moderate lifetimes since such products may in turn have their own regional or global impacts. Thus, in the case of the chloroethenes with moderate lifetimes, certain of their atmospheric transformation products (e.g., phosgene) may be longer lived and of significant biological concern.

Table V-3. Ranges of Influence of Parent Compounds Based on Atmospheric Lifetimes

Atmospheric Lifetime	Range of Influence	Organic Compounds
Short (<1 day)	Local	Cresols 1,4-Benzodioxan 2,3-Dihydrobenzofuran
Moderate (~1-7 days)	Regional	Vinyl Chloride 1,1-Dichloroethene Acrolein Allyl chloride Naphthalene
Long (~1 week-1 yr)	Global	Benzyl chloride <u>cis</u> -1,2-Dichloroethene <u>trans</u> -1,2-Dichloroethene Trichloroethene Tetrachloroethene Ethylene oxide

With regard to the class of longer-lived organics, potential health effects due to toxicity are not the only impacts to be considered. Thus, these compounds may dry deposit in remote, supposedly pristine ecosystems and, in the case of certain of the chloroethenes (for example, tetrachloroethene), may reach the stratosphere with consequent effects on the stratospheric ozone layer.

VI. ESTIMATION OF GAS-PHASE HYDROXYL RADICAL RATE CONSTANTS FOR ORGANIC COMPOUNDS

As discussed earlier in this report, organic chemicals emitted into the troposphere are removed by chemical reaction with a number of reactive intermediate species, including OH, HO₂ and NO₃ radicals and O₃, and by photolysis and wet and dry deposition. For the majority of organic chemicals present in the troposphere, reaction with the OH radical during daylight hours is expected to be the dominant atmospheric removal process (Finlayson-Pitts and Pitts 1986, Atkinson 1986; see also Table V-2).

However, in order to allow the dominant tropospheric removal process(es) of organic compounds to be assessed and their atmospheric lifetimes calculated, it is necessary to know the reaction rate constants (over the temperature range appropriate for the troposphere) and the ambient atmospheric concentrations of the reactive intermediates.

While rate constants for the gas-phase reactions of large number (>400) of organic chemicals with the OH radical have been measured to date (Atkinson 1986), the inherent complexity and concurrent low volatility of many industrially and agriculturally-used organic chemicals makes such measurements difficult and time- and cost-consuming. With the increasingly large data base available, the development and use of estimation techniques for the reliable calculation of OH radical reaction rate constants for a wide number of classes of organic compounds has become feasible. Such estimation techniques can be classified into two general categories; those which rely solely on the structure of the organic chemical (structure-reactivity relationships or SAR's) and those which utilize a physical or chemical property such as the ionization potential or bond dissociation energy or correlations between gas- and solution-phase OH radical reaction rate constants.

The intrinsically simplest of these estimation techniques, which should be applicable to all organics, are those utilizing structure-reactivity relationships. Such relationships are of growing interest to regulatory agencies which must prepare risk assessments for organic chemicals emitted into the atmosphere. Our development of such an SAR is described and its use illustrated. The California Air Resources Board may wish to consider the application of this technique to the Tanner process

in those cases where it is appropriate, i.e., in the case of those compounds, under review as potential toxic air contaminants, for which it may not be possible to obtain experimental data concerning their atmospheric lifetimes and fates.

Formulation of the SAR

This estimation method utilizes the fact that several separate OH radical reaction pathways occur, and that they can be dealt with individually. As presently known, these processes involve (a) H-atom abstraction from C-H bonds in alkanes, carbonyls and other saturated organics, and from O-H bonds in alcohols and glycols, (b) OH radical addition to $>C=C<$ and $-C\equiv C-$ unsaturated bonds, (c) OH radical addition to aromatic rings, and (d) OH radical interaction with nitrogen-, sulfur- and phosphorus-containing groups.

The total OH radical reaction rate constant is then given by

$$\begin{aligned} k_{\text{total}} = & k(\text{H-atom abstraction from C-H and O-H bonds}) \\ & + k(\text{OH radical addition to } >C=C< \text{ and } -C\equiv C- \text{ bonds}) \\ & + k(\text{OH radical addition to aromatic rings}) \\ & + k(\text{OH radical interaction with N-, S- and P-} \\ & \quad \text{containing groups}) \end{aligned}$$

These separate processes are dealt with below.

A. H-Atom Abstraction from C-H and O-H Bonds

As discussed by Atkinson (1986, 1987), the calculation of overall H-atom abstraction rate constants is based upon the estimation of $-CH_3$, $-CH_2-$, $>CH-$ and $-OH$ group rate constants. The $-CH_3$, $-CH_2-$ and $>CH-$ group rate constants depend on the identity of the substituents around those groups, with

$$k(CH_3-X) = k_{\text{prim}}^0 F(X)$$

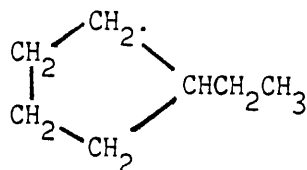
$$k(X-CH_2-Y) = k_{\text{sec}}^0 F(X) F(Y)$$

and

$$k(X-CH \begin{smallmatrix} Y \\ \diagdown \\ Z \end{smallmatrix}) = k_{\text{tert}}^0 F(X) F(Y) F(Z)$$

where k_{prim}° , k_{sec}° and k_{tert}° are the rate constants per $-\text{CH}_3$, $-\text{CH}_2-$ and $>\text{CH}-$ group for a "standard" substituent, X, Y and Z are the substituent groups, and $F(X)$, $F(Y)$ and $F(Z)$ are the corresponding substituent factors. The standard substituent group is chosen to be $X(=Y=Z) = -\text{CH}_3$, with $F(-\text{CH}_3) = 1.00$ by definition.

The group rate constants k_{prim}° , k_{sec}° , k_{tert}° and k_{OH} can be expressed in the temperature-dependent form $k = AT^2 e^{-E/T}$, and the A factors and values of E are given in Table VI-1. The effects of ring strain are taken into account by factors which account for the ring size; for example for ethylcyclopentane,



$$k = 2 k_{\text{sec}}^{\circ} [F(-\text{CH}_2-)]^2 + 2 k_{\text{sec}}^{\circ} F(-\text{CH}_2-) F(>\text{CH}-) + k_{\text{tert}}^{\circ} [F(-\text{CH}_2-)]^3 F_5 + k_{\text{sec}}^{\circ} F(>\text{CH}-) F(-\text{CH}_3) + k_{\text{prim}}^{\circ} F(-\text{CH}_2-)$$

where F_5 is the ring factor for a 5-membered ring (it is believed that only the groups involved in the ring are modified by the ring factor). For polycyclic systems the ring factors are multiplicative, as shown in Section VI-B below.

Table VI-1. Temperature Dependent Parameters, in the Form $k = AT^2 e^{-E/T}$, for CH_3- , $-\text{CH}_2-$, $>\text{CH}-$ and $-\text{OH}$ Group Rate Constants

	$10^{12} \times k (298 \text{ K})$ ($\text{cm}^3 \text{ molecule}^{-1} \text{ s}^{-1}$)	$10^{18} \times A$	E(K)
k_{prim}°	0.144	4.47	303
k_{sec}°	0.838	4.32	-233
k_{tert}°	1.83	1.89	-711
k_{OH}	0.036	1.89	460

The substituent factors $F(X)$, including factors F_{ring} , to take into account the ring strain per ring, are given in Table VI-2 for 298 K. With the assumption that the effects of a substituent group do not affect the A factor, then $F(X) = e^{E_X/T}$. Examples of the calculation of OH radical reaction rate constants for organic molecules of varying complexity are given below:

CH₃CHO

$$k = k_{\text{prim}}^{\circ} F(-\text{CHO}) + k_{\text{tert}}^{\circ} F(-\text{CH}_3) F(=\text{O})$$

CH₃CH₂COCH₃

$$k = k_{\text{prim}}^{\circ} F(-\text{CH}_2\text{C}(\text{O})-) + k_{\text{sec}}^{\circ} F(-\text{CH}_3) F(-\text{C}(\text{O})-) + k_{\text{prim}}^{\circ} F(-\text{C}(\text{O})-)$$

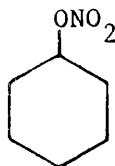
CH₃CH₂OCH₂CH₂OH

$$k = k_{\text{prim}}^{\circ} F(-\text{CH}_2-) + k_{\text{sec}}^{\circ} F(-\text{CH}_3) F(-\text{O}-) + k_{\text{sec}}^{\circ} F(-\text{O}-) F(-\text{CH}_2-) \\ + k_{\text{sec}}^{\circ} F(-\text{CH}_2-) F(-\text{OH}) + k_{\text{OH}}$$

CH₃C(O)OCH(CH₃)₂

$$k = k_{\text{prim}}^{\circ} F(-\text{C}(\text{O})\text{OR}) + k_{\text{tert}}^{\circ} [F(-\text{CH}_3)]^2 F(-\text{OC}(\text{O})\text{R}) + 2 k_{\text{prim}}^{\circ} F(>\text{CH}-)$$

Cyclohexyl nitrate



$$k = \left\{ 3 k_{\text{sec}}^{\circ} [F(-\text{CH}_2-)]^2 + 2 k_{\text{sec}}^{\circ} F(-\text{CH}_2-) F(>\text{CHONO}_2) \right. \\ \left. + k_{\text{tert}}^{\circ} F(-\text{CH}_2-)^2 F(-\text{ONO}_2) \right\} F_6$$

Table VI-2. Substituent Factors F(X) at 298 K

X	F(X) at 298 K
-CH ₃	1.00
$\left. \begin{array}{l} -\text{CH}_2- \\ >\text{CH}- \\ >\text{C}< \end{array} \right\}$	1.29
-F	0.099
-Cl	0.38
-Br	0.30
$\left. \begin{array}{l} -\text{CH}_2\text{Cl} \\ -\text{CHCl}_2 \\ -\text{CH}_2\text{Br} \end{array} \right\}$	0.57
-CCl ₃	0.090
-CH ₂ F	~0.85
-CHF ₂	~0.10
-CF ₂ Cl	~0.025
-CF ₃	0.075
=O	8.8
-CClO	~0.5
$\left. \begin{array}{l} -\text{CHO} \\ -\text{C(=O)}- \end{array} \right\}$	0.76
$\left. \begin{array}{l} -\text{CH}_2\text{C(=O)}- \\ >\text{CHC(=O)}- \\ ->\text{CC(=O)}- \end{array} \right\}$	4.4
-C ₆ H ₅	~1.0

(continued)

Table VI-2 (continued) - 2

X	F(X) at 298 K
$\begin{array}{l} >C=C< \\ -C\equiv C- \end{array} \left. \vphantom{\begin{array}{l} >C=C< \\ -C\equiv C- \end{array}} \right\}$	~1.0
-OH	3.4
-O-	6.1
-C(O)OR	0.0
-OC(O)R	1.5
$\begin{array}{l} -CH_2ONO_2 \\ >CHONO_2 \\ ->CONO_2 \end{array} \left. \vphantom{\begin{array}{l} -CH_2ONO_2 \\ >CHONO_2 \\ ->CONO_2 \end{array}} \right\}$	0.21
-ONO ₂	0.10
-CN	0.14
-CH ₂ CN	0.5
3-membered ring	0.017
4-membered ring	0.22
5-membered ring	0.80
6-membered ring	1.00
7-membered ring	~1.0

B. OH Radical Addition to $>C=C<$ and $-C\equiv C-$ Bonds

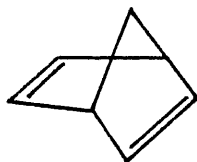
The estimation method used to calculate the rate constants for OH radical addition to $>C=C<$ and $-C\equiv C-$ bond systems is based upon the number of unconjugated double or triple bonds or conjugated double bond systems and the degree, identity and configuration of substitution around these double bonds. For example, for $CH_2=C(CH_3)CH_2CH=CH_2$ the rate constant is given by

$$k = k(CH_2=C<) + k(CH_2=CH-) + k_{sec}^0 F(>C=C<)^2$$

where $k(CH_2=C<)$ and $k(CH_2=CH-)$ are the rate constants for OH radical addition to 2-methylpropene and propene, respectively. For conjugated dialkenes, the $>C=C-C=C<$ structure is considered as a single unit, with the rate constant depending solely upon the number of alkyl substituents on this structural unit. The rate constants at 298 K for the various $>C=C<$, $-C\equiv C-$ and $>C=C-C=C<$ structural units are given in Table VI-3.

Hydrogen atom abstraction from vinyl hydrogens is generally negligible at temperatures ≤ 500 K (Atkinson 1986). Thus, the contribution of H-atom abstraction from C-H bonds on substituted alkyl groups to the overall room temperature rate constants is generally minor, but is taken into account, as shown above for $CH_2=C(CH_3)CH_2CH=CH_2$, with (Table VI-1) $F(>C=C<) = 1.0$.

There are no ring strain effects for OH radical addition to $>C=C<$ bonds (Atkinson 1986). As an example, for bicyclo[2.2.1]-2,5-heptadiene



$$k = 2 k(\text{cis-CH=CH-}) + \left\{ 2 k_{tert}^0 F(>C=C<)^2 F(-CH_2-) + k_{sec}^0 F(>CH-)^2 \right\} F_5^2 F_6$$

For alkenes containing substituent groups other than alkyl groups, substituent factors $C(X)$ are used. For example, for $CH_2=CXY$ the rate constant is given by

$$k = k(CH_2=C<) C(X) C(Y) +$$

$k(\text{H-abstraction from the X and Y substituent groups}).$

Table VI-3. Room Temperature Group Rate Constants for OH Radical Addition to $>C=C<$, $-C\equiv C-$, $>C=C=C<$ and $>C=C-C=C<$ Structural Units

Structure	$10^{11} \times k$ ($\text{cm}^3 \text{ molecule}^{-1} \text{ s}^{-1}$)
$\text{CH}_2=\text{CH}-$	2.63
$\text{CH}_2=\text{C}<$	5.14
cis- $\text{CH}=\text{CH}-$	5.61
trans- $\text{CH}=\text{CH}-$	6.37
$-\text{CH}=\text{C}<$	8.69
$>\text{C}=\text{C}<$	11.0
$\text{HC}\equiv\text{C}-$	0.64
$-\text{C}\equiv\text{C}-$	2.9
<u>$>\text{C}=\text{C}-\text{C}=\text{C}<$ unit</u>	
One-alkyl substituent	10.5
Two-alkyl substituents	13.5
Three-alkyl substituents	18.
Four-alkyl substituents	23.

The substituent factors $C(X)$ at room temperature are given in Table VI-4. A negative temperature dependence of the rate constants for these reactions equivalent to an Arrhenius activation energy of -1 kcal mol^{-1} is generally applicable for the calculation of OH radical addition rate constants at temperatures $\leq 500 \text{ K}$.

Table VI-4. Substituent Factors C(X) at 298 K

Substituent X	C(X)
-F	~0.4
-Cl	0.20
-Br	0.26
-CH ₂ Cl	0.76
-CN	0.15
-CHO	0.26
-COCH ₃	0.91
-OCH ₃	1.3
=O	1.0

C. OH Radical Addition to Aromatic Rings

As discussed previously by Zetzsch (1982) and Atkinson (1986, 1987) the correlation between the rate constant for OH radical addition to aromatic rings and the sum of the electrophilic substituent constants, $\Sigma\sigma^+$, of Brown and Okamoto (1958) provides a means of estimating the rate constants for OH radical addition to aromatic rings.

A least-squares correlation of the room temperature rate constants for OH radical addition to the aromatic ring and the $\Sigma\sigma^+$ values for 34 aromatic compounds yields

$$\begin{aligned} \log_{10} k(\text{OH radical addition to aromatic rings}) \\ = -11.69 - 1.35 \Sigma\sigma^+ \text{ cm}^3 \text{ molecule}^{-1} \text{ s}^{-1} \end{aligned} \quad (\text{XV})$$

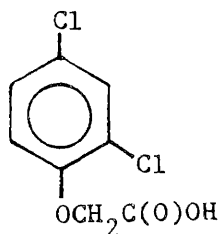
$\Sigma\sigma^+$ is calculated by assuming that (a) steric hindrance can be neglected and σ_{ortho}^+ is set equal to σ_{para}^+ ; (b) $\Sigma\sigma^+$ is the sum of all substituent constants of the substituents connected to the aromatic ring; (c) the OH radical adds to the position yielding the most negative value of $\Sigma\sigma^+$

(preferably to a free position); and (d) if all positions are occupied, the ipso position is treated as a meta position.

Of course, the contributions of H-atom abstraction from C-H and O-H bonds on alkyl, -OH and -CHO substituent groups and OH radical interaction with -NH₂ and -N(CH₃)₂ substituent groups (see below) must be taken into account, using (Table VI-2) F(aromatic ring) = 1.0. For example, for ethylbenzene, for which $\Sigma\sigma^+ = -0.295$,

$$k(\text{ethylbenzene}) = 10^{[-11.69 - 1.35(-0.295)]} + k_{\text{sec}}^{\circ} F(-\text{C}_6\text{H}_5) F(-\text{CH}_3) + k_{\text{prim}}^{\circ} F(-\text{CH}_2-)$$

As a further example, for 2,4-D



the values of σ_p^+ (Cl) and σ_m^+ (Cl) are 0.114 and 0.399, respectively. For the -OCH₂C(O)OH group the (perhaps gross) assumption is made that its effect is similar to a -OCH₃ group, with values of σ_p^+ and σ_m^+ of -0.778 and 0.047, respectively. The most negative value of $\Sigma\sigma^+ = +0.020$ occurs for OH radical addition at the position ortho to the -OCH₂C(O)OH group and meta to the two chlorines. This then yields $k = 1.9 \times 10^{-12} \text{ cm}^3 \text{ molecule}^{-1} \text{ s}^{-1}$ at 298 K.

This estimation method has also been extended to the polychloro-biphenyls, polychlorodibenzo-p-dioxins and polychloro-dibenzofurans and related compounds. In order to use equation (XV) to calculate rate constants for reaction of the OH radical with PCB's, rate constants for each ring must be estimated. This necessitates the prior estimation of the σ^+ values for the mono- and polychlorophenyl groups. Assuming that the value of σ^+ for the C₆H₄Cl substituent does not depend on the location of the Cl atom in the ring, then $\sigma^+(\text{C}_6\text{H}_4\text{Cl})$ can be obtained from the experimental data for the 2-, 3- and 4-chlorobiphenyls (Atkinson 1986).

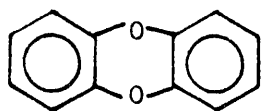
Assuming that the incremental changes in σ_p^+ and σ_m^+ remain constant for each additional Cl atom substituent on the phenyl group, values of σ_m^+ and σ_p^+ for the other polychlorophenyl groups can be derived, and these are given in Table VI-5. Hydroxyl radical rate constants can then be calculated for the di-, tri-, tetra- and pentachlorobiphenyls using equation (XV) and these σ^+ values.

Table VI-5. Estimated Electrophilic Substituent Constants σ_m^+ and σ_p^+ for $C_6H_{5-x}Cl_x$ Groups

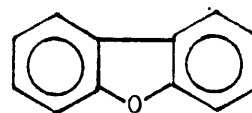
Substituent Group	σ_m^+	σ_p^+
C_6H_5	0.109 ^a	-0.179 ^a
C_6H_4Cl	0.25	0.02
$C_6H_3Cl_2$	0.39	0.22
$C_6H_2Cl_3$	0.53	0.42
C_6HCl_4	0.67	0.62
C_6Cl_5	0.81	0.82

^aFrom Brown and Okamoto (1958).

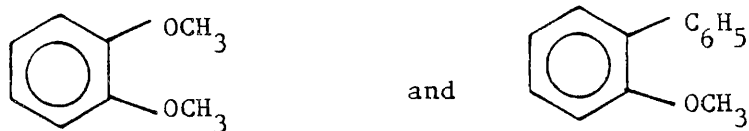
The room temperature rate constants for the polychlorodibenzo-p-dioxins and the polychlorodibenzofurans can be calculated by assuming that the structures



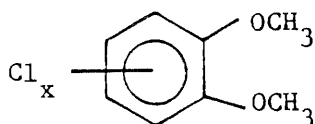
and



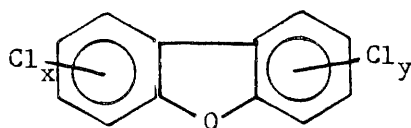
can be respectively represented as being built up of the two substructural units,



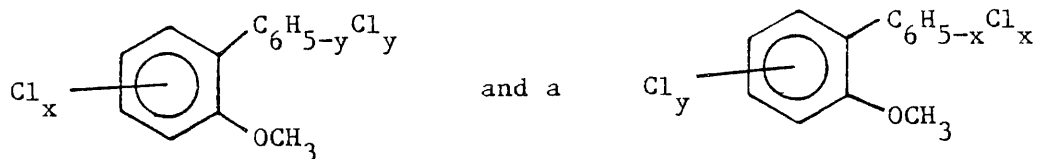
respectively. Room temperature rate constants for the PCDD's can be readily calculated using this approach, with each aromatic ring, represented as,



being dealt with independently. For the polychlorodibenzofurans the two aromatic rings cannot be viewed as being independent, and the general structural formula



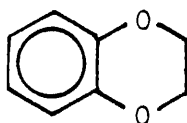
can be viewed as being comprised of a



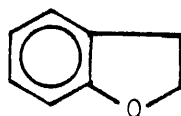
ring. Rate constants for each individual ring system can then be calculated, as for the PCBs, using the electrophilic substituent constants estimated for the $\text{C}_6\text{H}_5\text{Cl}_x$ groups. As an example, the room temperature OH radical reaction constants for dibenzo-p-dioxin, 2,3,7,8-tetrachlorodibenzo-p-dioxin, dibenzofuran and 2,3,7,8-tetrachlorodibenzofuran are calculated to be:

$$\begin{aligned}
 k(\text{dibenzo-p-dioxin}) &= 4.0 \times 10^{-11} \text{ cm}^3 \text{ molecule}^{-1} \text{ s}^{-1}, \\
 k(2,3,7,8\text{-tetrachlorodibenzo-p-dioxin}) &= 8.0 \times 10^{-12} \text{ cm}^3 \text{ molecule}^{-1} \text{ s}^{-1}, \\
 k(\text{dibenzofuran}) &= 3.3 \times 10^{-11} \text{ cm}^3 \text{ molecule}^{-1} \text{ s}^{-1}, \text{ and} \\
 k(2,3,7,8\text{-tetrachlorodibenzofuran}) &= 2.3 \times 10^{-12} \text{ cm}^3 \text{ molecule}^{-1} \text{ s}^{-1}.
 \end{aligned}$$

This general approach can be used for other non-fused polyaromatic systems. Thus, two similar, but simple, aromatic compounds for which experimental rate constant data are now available are 1,4-benzodioxan



and 2,3-dihydrobenzofuran



Using the approach described above, rate constants for these compounds can be calculated as follows:

$$\begin{aligned}
 k(1,4\text{-benzodioxan}) &= k \left(\text{OH radical addition to } \text{C}_6\text{H}_2(\text{OCH}_3)_2 \right) \\
 &\quad + 2 k_{\text{sec}}^{\text{O}} \text{F}(-\text{O}-) \text{F}(-\text{CH}_2-)
 \end{aligned}$$

and

$$\begin{aligned}
 k(2,3\text{-dihydrobenzofuran}) &= k \left(\text{OH radical addition to } \text{C}_6\text{H}_3(\text{CH}_3)(\text{OCH}_3) \right) \\
 &\quad + \left\{ k_{\text{sec}}^{\text{O}} \text{F}(-\text{C}_6\text{H}_5) \text{F}(-\text{CH}_2-) \right. \\
 &\quad \left. + k_{\text{sec}}^{\text{O}} \text{F}(-\text{O}-) \text{F}(-\text{CH}_2-) \right\} \text{F}_5
 \end{aligned}$$

The calculated rate constants at 298 K are then $3.3 \times 10^{-11} \text{ cm}^3 \text{ molecule}^{-1} \text{ s}^{-1}$ for 1,4-benzodioxan and $3.4 \times 10^{-11} \text{ cm}^3 \text{ molecule}^{-1} \text{ s}^{-1}$ for 2,3-dihydrobenzofuran. These values can be compared to our measured room temperature rate constants of $2.5 \times 10^{-11} \text{ cm}^3 \text{ molecule}^{-1} \text{ s}^{-1}$ for 1,4-dibenzodioxan and $3.7 \times 10^{-11} \text{ cm}^3 \text{ molecule}^{-1} \text{ s}^{-1}$ for 2,3-dihydrobenzofuran. Clearly, the calculated and experimental data are in excellent agreement, suggesting that the approach used in these calculations for the dibenzofurans and dibenzodioxins is valid.

A plot of the calculated versus experimental room temperature rate constants for ~270 organic compounds which react with the OH radical via H-atom abstraction from C-H and O-H bonds, OH radical addition to $>\text{C}=\text{C}<$ and $-\text{C}\equiv\text{C}-$ bonds and OH radical addition to non-fused aromatic rings (including aniline and N,N-dimethylaniline) is shown in Figure VI-1. Only for 16 of those compounds do the calculated and experimental room temperature rate constants disagree by more than a factor of two.

D. OH Radical Reaction with $-\text{NH}_2$, $>\text{NH}$, $>\text{N}-$, $-\text{SH}$ and $-\text{S}-$ Containing Compounds

Under atmospheric conditions, the gas-phase reactions of the OH radical with thiols (RSH), sulfides (RSR'), disulfides (RSSR') and amines (RNH_2 , $\text{RR}'\text{NH}$ and $\text{RR}'\text{R}''\text{N}$) proceed, at least in part, via initial OH radical addition to the S- and N-atoms (Atkinson 1986). The values of $F(-\text{S}-)$, $F(-\text{SH})$, $F(-\text{NH}_2)$, $F(-\text{NH}-)$, $F(-\text{N}<)$, $F(-\text{NNO})$, $F(-\text{NNO}_2)$, $k_{-\text{SH}}$, $k_{-\text{S}-}$, $k_{-\text{SS}-}$, $k_{-\text{NH}_2}$, $k_{>\text{NH}}$, $k_{>\text{N}-}$, $k_{>\text{NNO}}$ and $k_{>\text{NNO}_2}$ estimated from the available data are given in Table VI-6. It should be noted that the substituent factors $F(\text{X})$ given in Table VI-6 are applicable to H-atom abstraction from C-H bonds only, i.e., for CH_xNH_y compounds. A comparison of the calculated and experimental room temperature rate constants for the amines and related compounds is given in Figure VI-2 and again the calculated and experimental data agree to within a factor of 2 (which may not be surprising since essentially the entire data set was used to derive the necessary parameters).

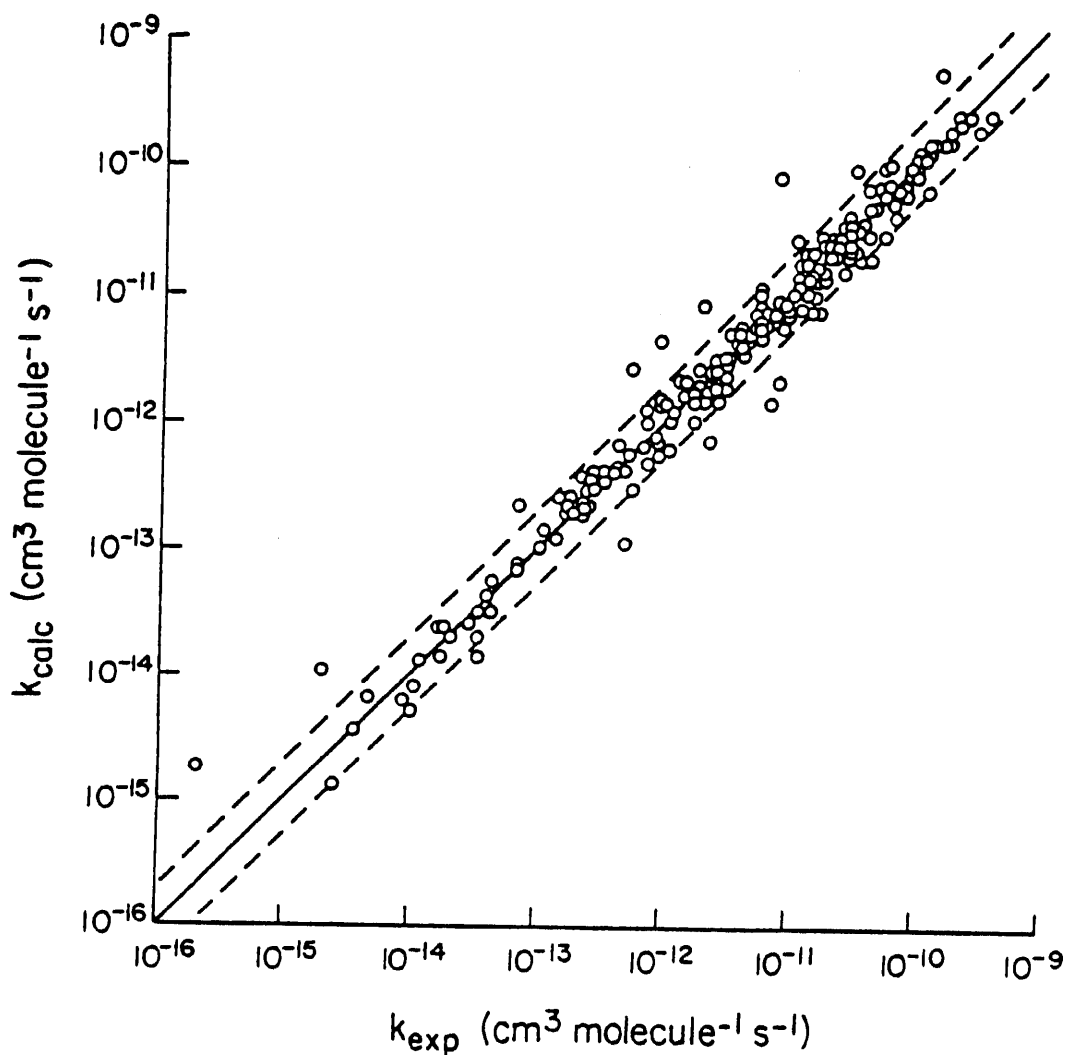


Figure VI-1. Plot of calculated versus experimentally measured room temperature rate constants for gas-phase reaction of the OH radical with alkanes, haloalkanes, alkenes, alkynes, haloalkenes, oxygen-containing organics and aromatic compounds (total ~270 compounds). The solid line indicates perfect agreement; the dashed lines disagreement by a factor of 2.

Table VI-6. Substituent Factors F(X) for H-Atom Abstraction from C-H Bonds and Group Rate Constants at 298 K for OH Radical Reaction with Thiols, Sulfides, Disulfides, Amines and Related Organics

Substituent Group X	F(X)
$\left. \begin{array}{l} -\text{SH} \\ -\text{S}- \\ -\text{SS}- \end{array} \right\}$	9.0
$\left. \begin{array}{l} -\text{NH}_2 \\ -\text{NH}- \\ -\text{N}< \\ -\text{NNO} \\ -\text{NNO}_2 \end{array} \right\}$	10
Group	$10^{12} \times k \text{ (cm}^3 \text{ molecule}^{-1} \text{ s}^{-1}\text{)}$
-SH	31
-S-	2.0 ^a
-SS-	~200
-NH ₂	20
>NH	60
>N-	60
$\left. \begin{array}{l} >\text{NNO} \\ >\text{NNO}_2 \end{array} \right\}$	0

^aApplicable only for 760 torr total pressure of air and 298 K.

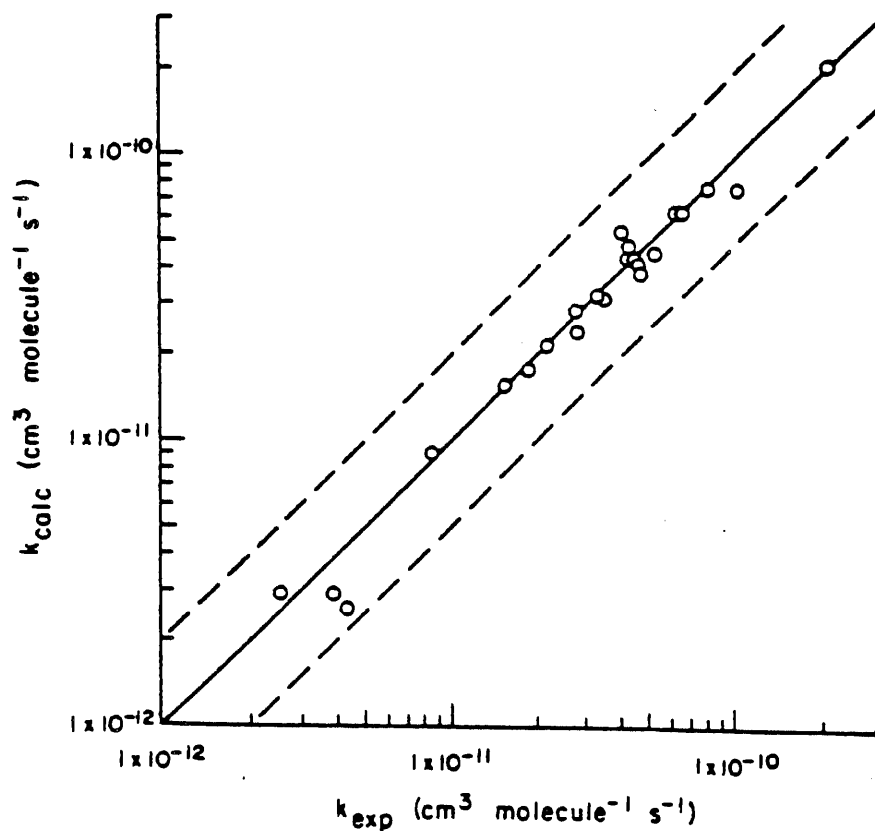
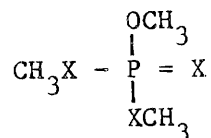


Figure VI-2. Plots of calculated versus experimentally measured room temperature rate constants for the gas phase reaction of the OH radical with S- and N-containing aliphatic compounds. The solid line indicates perfect agreement; the dashed lines disagreement by a factor of 2.

E. Phosphorus-Containing Organics

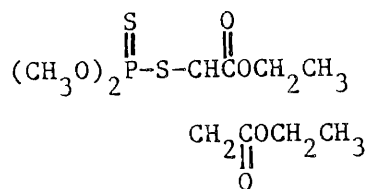
A large number of phosphorus-containing organic compounds are used in industrial and agricultural operations. However, for these compounds, kinetic data are presently available for only five compounds of the general structure



where X = O and/or S. The experimental data show that $k(\text{P}=\text{O}) \sim \text{zero}$; $k(\text{P}=\text{S}) = 5.5 \times 10^{-11} \text{ cm}^3 \text{ molecule}^{-1} \text{ s}^{-1}$; and $F(-\text{OP}-) = F(-\text{SP}-) = 20$ (which can be compared to $F(-\text{O}-) = 6.1$, indicating that the $-\text{OCH}_3$ and $-\text{SCH}_3$ groups bonded to a P atom are more reactive than the $-\text{OCH}_3$ groups in the aliphatic ethers).

Comparison of the calculated and measured room temperature rate constants for these five phosphorus-containing compounds is given in Table VI-7. The agreement is seen to be excellent, and the data show that the inclusion of a $\text{P}=\text{S}$ system leads to a high reactivity, with a calculated atmospheric lifetime of ~ 4 hrs for a daytime OH radical concentration of $1 \times 10^6 \text{ molecule cm}^{-3}$.

As an example, the rate constant for Malathion



is calculated as

$$\begin{aligned} k &= 2 k_{\text{prim}}^{\text{O}} F(-\text{CH}_2-) + 2 k_{\text{sec}}^{\text{O}} F(-\text{CH}_3) F(-\text{OC}(\text{O})\text{R}) \\ &\quad + k_{\text{sec}}^{\text{O}} F(>\text{CH}-) F(-\text{C}(\text{O})\text{OR}) + k_{\text{tert}}^{\text{O}} F(-\text{SP}-) F(-\text{CH}_2-) F(-\text{C}(\text{O})\text{OR}) \\ &\quad + k_{-\text{P}=\text{S}} + 2 k_{\text{prim}}^{\text{O}} F(-\text{OP}-) \\ &= 6.4 \times 10^{-11} \text{ cm}^3 \text{ molecule}^{-1} \text{ s}^{-1} \text{ at } 298 \text{ K.} \end{aligned}$$

Table VI-7. Comparison of Experimental and Calculated Room Temperature Rate Constants for Reactions of OH Radicals with P-Containing Organics

Compound	$10^{12} \times k \text{ (cm}^3 \text{ molecule}^{-1} \text{ s}^{-1}\text{)}$	
	Calculated	Observed ^a
$(\text{CH}_3\text{O})_3\text{PO}$	8.6	7.4
$(\text{CH}_3\text{O})_2\text{P(O)SCH}_3$	8.6	9.2
$(\text{CH}_3\text{S})_2\text{P(O)OCH}_3$	8.6	9.5
$(\text{CH}_3\text{O})_3\text{P(S)}$	64	70
$(\text{CH}_3\text{O})_2\text{P(S)SCH}_3$	64	56

^aFrom Goodman et al. (1987).

F. Conclusions

A technique for the calculation of rate constants for the reaction of OH radicals with organic compounds under atmospheric conditions has been developed and tested against the available data base. Only for 18 out of a total of ~300 organic compounds do the calculated and experimental room temperature OH radical reaction rate constants disagree by more than a factor of 2. While essentially the entire kinetic data base available has been used in the development of this estimation procedure, it is expected that OH radical reaction rate constants can be calculated with similar accuracy levels for organic chemicals for which experimental data do not exist.

While the rate constants for the reactions of organic compounds with the OH radical can often be measured to an accuracy of 25% or better, and can be often estimated to within a factor of 2, the calculated atmospheric lifetimes are much more uncertain due to the large uncertainties in our knowledge of the ambient atmospheric concentrations of the OH radical. Thus, the ambient atmospheric OH radical concentrations at any given time and/or place must be judged to be uncertain to a factor of at least 5, and more likely 10 (Hewitt and Harrison 1985). The diurnally and annually

averaged tropospheric OH radical concentrations appear to be better known, to within possibly a factor of <2 (Crutzen 1982), being calculated to be $\sim 5 \times 10^5$ and $\sim 6 \times 10^5$ molecule cm^{-3} in the northern and southern hemisphere, respectively.

It is evident that further experimental work is necessary to provide kinetic and mechanistic information for several classes of organic compounds, especially those containing N, S and P heteroatoms and for compounds containing multiple non-alkyl substituent groups.

VII. REFERENCES

- Atkinson, R., Carter, W. P. L., Winer, A. M. and Pitts, J. N., Jr. (1981): An experimental protocol for the determination of OH radical rate constants with organics using methyl nitrite photolysis as an OH radical source. *J. Air Pollut. Control Assoc.*, 31, 1090-1092.
- Atkinson, R., Aschmann, S. M., Winer, A. M. and Pitts, J. N., Jr. (1982a): Rate constants for the reactions of OH radicals with a series of alkanes and alkenes at 299 ± 2 K. *Int. J. Chem. Kinet.*, 14, 507-516.
- Atkinson, R., Aschmann, S. M., Fitz, D. R., Winer, A. M. and Pitts, J. N., Jr. (1982b): Rate constants for the gas-phase reactions of O_3 with selected organics at 296 K. *Int. J. Chem. Kinet.*, 14, 13-18.³
- Atkinson, R., Aschmann, S. M., Carter, W. P. L., Winer, A. M. and Pitts, J. N., Jr. (1982c): Alkyl nitrate formation from the NO_x -air photooxidations of C_2 - C_8 n-alkanes. *J. Phys. Chem.*, 86, 4563-4569.
- Atkinson, R. and Carter, W. P. L. (1984): Kinetics and mechanisms of the gas-phase reactions of ozone with organic compounds under atmospheric conditions. *Chem. Rev.*, 84, 437-470.
- Atkinson, R. and Lloyd, A. C. (1984): Evaluation of kinetic and mechanistic data for modeling of photochemical smog. *J. Phys. Chem. Ref. Data*, 13, 315-444.
- Atkinson, R., Plum, C. N., Carter, W. P. L., Winer, A. M. and Pitts, J. N., Jr. (1984a): Rate constants for the gas-phase reactions of NO_3 radicals with a series of organics in air at 298 ± 1 K. *J. Phys. Chem.*, 88, 1210-1215.
- Atkinson, R., Pitts, J. N., Jr. and Aschmann, S. M. (1984b): Tropospheric reactions of dimethyl sulfide with NO_3 and OH radicals. *J. Phys. Chem.*, 88, 1584-1587.
- Atkinson, R., Carter, W. P. L., Plum, C. N., Winer, A. M. and Pitts, J. N., Jr. (1984c): Kinetics of the gas phase reactions of NO_3 radicals with a series of aromatics at 296 ± 2 K. *Int. J. Chem. Kinet.*, 16, 887-898.
- Atkinson, R. and Aschmann, S. M. (1985): Kinetics of the gas phase reactions of Cl atoms with a series of organics at 296 ± 2 K and atmospheric pressure. *Int. J. Chem. Kinet.*, 17, 33-41.
- Atkinson, R. (1986): Kinetics and mechanisms of the gas phase reactions of the hydroxyl radical with organic compounds under atmospheric conditions. *Chem. Rev.*, 86, 69-201.
- Atkinson, R., Tuazon, E. C., Mac Leod, H., Aschmann, S. M. and Winer, A. M. (1986a): The gas-phase reaction of chlorine nitrate with water vapor. *Geophys. Res. Lett.*, 13, 117-120.

- Atkinson, R., Winer, A. M. and Pitts, J. N., Jr. (1986b): Estimation of nighttime N_2O_5 concentrations from ambient NO_2 and NO_3 radical concentrations and the role of N_2O_5 in nighttime chemistry. *Atmos. Environ.*, 20, 331-339.
- Atkinson, R. (1987): A structure-activity relationship for the estimation of rate constants for the gas-phase reactions of OH radicals with organic compounds. *Int. J. Chem. Kinet.*, in press.
- Atkinson, R., Aschmann, S. M. and Pitts, J. N., Jr. (1987): unpublished data.
- Ayscough, P. B., Dainton, F. S. and Fleischfresser, B. E. (1966): Photochlorination studies. Part 10 - Excited chloroalkyl radicals in photochlorination of chloroethylenes. *Trans Faraday Soc.*, 62, 1846-1858.
- Brown, H. C. and Okamoto, Y. (1958): Electrophilic substituent constants. *J. Am. Chem. Soc.*, 80, 4979-4987.
- Carter, W. P. L., Winer, A. M. and Pitts, J. N., Jr. (1981): Major atmospheric sink for phenol and the cresols. Reaction with the nitrate radical. *Environ. Sci. Technol.*, 15, 829-831.
- Crutzen, P. J. (1982): The global distribution of hydroxyl. In: Atmospheric Chemistry, E. D. Goldberg (Ed.), Springer-Verlag, New York, pp. 313-328.
- Davis, D. D., Braun, W. and Bass, A. M. (1970): Reactions of $\text{Cl } ^2\text{P}_{3/2}$: Absolute rate constants for reaction with H_2 , CH_4 , C_2H_6 , CH_2Cl_2 , C_2Cl_4 , and $\text{C-C}_6\text{H}_{12}$. *Int. J. Chem. Kinet.*, 2, 101-114.
- Doyle, G. J., Bekowies, P. J., Winer, A. M. and Pitts, J. N., Jr. (1977): Charcoal-adsorption air purification system for chamber studies investigating atmospheric photochemistry. *Environ. Sci. Technol.*, 11, 45-51.
- Edney, E. O., Kleindienst, T. E. and Corse, E. W. (1986a): Room temperature rate constants for the reaction of OH with selected chlorinated and oxygenated hydrocarbons. *Int. J. Chem. Kinet.*, 18, 1355-1371.
- Edney, E. O., Shepson, P. B., Kleindienst, T. E. and Corse, E. W. (1986b): The photooxidation of allyl chloride. *Int. J. Chem. Kinet.*, 18, 597-608.
- Finlayson-Pitts, B. J. and Pitts, J. N., Jr. (1986): Atmospheric Chemistry: Fundamentals and Experimental Techniques. Wiley, NY.
- Gilbert, D., Goyer, M., Lyman, W., Magil, G., Walker, P., Wallace, D., Wechsler, A. and Yee, J. (1980): An exposure and risk assessment for tetrachloroethylene. EPA-440/4-85-015, July.

- Goodman, M. A., Aschmann, S. M., Atkinson, R. and Winer, A. M. (1987): Kinetics of the atmospherically important gas-phase reactions of a series of trimethyl phosphorothioates. *Arch. Environ. Contamin. Toxicol.*, in press.
- Graham, R. A. and Johnston, H. S. (1978): The photochemistry of NO_2 and the kinetics of the $\text{N}_2\text{O}_5\text{-O}_3$ system. *J. Phys. Chem.*, 82, 254-268.
- Hatakeyama, S., Honda, S., Washida, N. and Akimoto, H. (1985): Rate constants and mechanism for reactions of ketenes with OH radicals in air at 299 ± 2 K. *Bull. Chem. Soc. Jpn*, 58, 2157-2162.
- Knox, J. H. and Riddick, J. (1966): Activated chloroethyl radicals in the chlorination of 1,2-dichloroethylenes. *Trans. Faraday Soc.*, 62, 1190-1205.
- Lewis, R. S., Sander, S. P., Wagner, S. and Watson, R. T. (1980): Temperature-dependent rate constants for the reaction of ground-state chlorine with simple alkanes. *J. Phys. Chem.*, 84, 2009-2015.
- Manning, R. G. and Kurylo, M. J. (1977): Flash photolysis resonance fluorescence investigation of the temperature dependencies of the reactions of $\text{Cl}(^2\text{P})$ atoms with CH_4 , CH_3Cl , CH_3F , $\text{CH}_3\text{F}^\dagger$, and C_2H_6 . *J. Phys. Chem.*, 81, 291-296.
- Michael, J. V., Nava, D. F., Payne, W. A. and Stief, L. J. (1979): Rate constants for the reaction of atomic chlorine with methanol and dimethyl ether from 200 to 500 K. *J. Chem. Phys.*, 70, 3652-3656.
- Niki, H., Maker, P. D., Savage, C. M. and Breitenbach, L. P. (1978): FTIR spectroscopic observation of peroxyalkylnitrates formed via $\text{ROO} + \text{NO}_2 \rightarrow \text{ROONO}_2$. *Chem. Phys. Lett.*, 55, 289-292.
- Niki, H., Maker, P. D., Savage, C. M. and Breitenbach, L. P. (1980): An FTIR study of the Cl atom-initiated oxidation of CH_2Cl_2 and CH_3Cl . *Int. J. Chem. Kinet.*, 12, 1001-1012.
- Niki, H., Maker, P. D., Savage, C. M. and Breitenbach, L. P. (1985) An FTIR spectroscopic study of the reactions $\text{Br} + \text{CH}_3\text{CHO} \rightarrow \text{HBr} + \text{CH}_3\text{CO}$ and $\text{CH}_3\text{C(O)OO} + \text{NO}_2 \rightleftharpoons \text{CH}_3\text{C(O)OONO}_2$ (PAN). *Int. J. Chem. Kinet.*, 17, 525-534.
- Oltmans, S. J. (1981): Surface ozone measurements in clean air. *J. Geophys. Res.*, 86, 1174-1180.
- Pitts, J. N., Jr., Atkinson, R., Sweetman, J. A. and Zielinska, B. (1985): The gas-phase reaction of naphthalene with N_2O_5 to form nitronaphthalenes. *Atmos. Environ.*, 19, 701-705.
- Platt, U. F., Winer, A. M., Biermann, H. W., Atkinson, R. and Pitts, J. N., Jr. (1984): Measurement of nitrate radical concentrations in continental air. *Environ. Sci. Technol.*, 18, 365-369.
- Pouchert, C. J. (1975): The Aldrich Library of Infrared Spectra. Aldrich Chemical Co., Milwaukee, WI, 2nd ed, pp. 375-384.

- Ravishankara, A. R. and Mauldin, R. L., III (1985): Absolute rate coefficient for the reaction of NO_3 with trans-2-butene. J. Phys. Chem., 89, 3144-3147.
- Ray, G. W., Keyser, L. F. and Watson, R. T. (1980): Kinetics study of the $\text{Cl}(\text{}^2\text{P}) + \text{Cl}_2\text{O} \rightarrow \text{Cl}_2 + \text{ClO}$ reaction at 298 K. J. Phys. Chem., 84, 1674-1681.
- Sanhueza, E., Hisatsune, I. C. and Heicklen, J. (1976): Oxidation of haloethylenes. Chem. Rev., 76, 801-826.
- SCAQMD (1983): Emissions of potentially hazardous substances in the South Coast Air Basin. Report, South Coast Air Quality Management District, CA, September.
- SCAQMD (1985): Emissions of potentially toxic/hazardous air contaminants in the South Coast Air Basin. Report, 1984 update, South Coast Air Quality Management District, September.
- Singh, H. B., Ludwig, F. L. and Johnson, W. B. (1978): Tropospheric ozone: concentrations and variabilities in clean remote atmospheres. Atmos. Environ., 12, 2185-2196.
- Slagle, I. R., Park, J.-Y., Heaven, M. C. and Gutman, D. (1984): Kinetics of polyatomic free radicals produced by laser photolysis. 3. Reaction of vinyl radicals with molecular oxygen. J. Am. Chem. Soc., 106, 4356-4361.
- Stephens, E. R. (1969) The formation, reactions and properties of peroxyacyl nitrates (PANs) in photochemical air pollution. Adv. Environ. Sci., 1, 119-146.
- Terry Dana, M., Lee, R. N. and Hales, J. M. (1985): Hazardous air pollutants: wet removal rates and mechanisms. EPA-600/3-84-113, January.
- Thomas, R., Byrne, M., Gilbert, D., Goyer, M. and Moss, K. (1981): An exposure and risk assessment for trichloroethylene. EPA-440/4-85-019, March.
- Tuazon, E. C., Atkinson, R., Winer, A. M. and Pitts, J. N., Jr. (1984): A study of the atmospheric reactions of 1,3-dichloropropene and other selected organochlorine compounds. Arch. Environ. Contam. Toxicol., 13, 691-700.
- Winer, A. M., Graham, R. A., Doyle, G. J., Bekowies, P. J., McAfee, J. M. and Pitts, J. N., Jr. (1980): An evacuable environmental chamber and solar simulator facility for the study of atmospheric photochemistry. Environ. Sci. Technol., 10, 461-511.
- Zetsch, C. (1982): Predicting the rate of OH-addition to aromatics using σ^+ -electrophilic substituent constants for mono- and polysubstituted benzene. 15th Int. Conf. Photochem., Stanford, CA, June 27-July 1.

VIII. PUBLISHED SCIENTIFIC PAPERS RESULTING WHOLLY
OR IN PART FROM THIS PROGRAM

1. Estimation of OH radical reaction rate constants and atmospheric lifetimes for polychlorobiphenyls, dibenzo-p-dioxans, and dibenzofurans
Environ. Sci. Technol., 21, 305-307 (1987)
R. Atkinson
2. Kinetics of the gas-phase reactions of NO₃ radicals with a series of alkynes, haloalkenes, and α,β -unsaturated aldehydes
Int. J. Chem. Kinet., 19, 299-307 (1987)
R. Atkinson, S. M. Aschmann and M. A. Goodman
3. Kinetics and products of the gas-phase reactions of OH radicals and N₂O₅ with naphthalene and biphenyl
Environ. Sci. Technol., 21, 1014-1022 (1987)
R. Atkinson, J. Arey, B. Zielinska and S. M. Aschmann
4. Kinetics of the gas-phase reactions of Cl atoms with chloroethenes at 298 \pm 2 K and atmospheric pressure
Int. J. Chem. Kinet., 19, 1095-1105 (1987)
R. Atkinson and S. M. Aschmann
5. Kinetics of the reactions of NO₃ radicals with a series of aromatic compounds
Environ. Sci. Technol., 21, 1123-1126 (1987)
R. Atkinson, S. M. Aschmann and A. M. Winer
6. Estimation of gas-phase hydroxyl radical rate constants for organic compounds
Environ. Toxicol. Chem., in press
R. Atkinson
7. Atmospheric reactions of chloroethenes with the OH radical
Environ. Sci. Technol., in press
E. C. Tuazon, R. Atkinson, S. M. Aschmann, M. A. Goodman and A. M. Winer

